Chameleon Fields and Compact Objects

Jan Øye Lindroos

Thesis submitted for the degree of
Master in Physics

Department of Physics
University of Oslo

June 2009

Acknowledgment

Finishing this thesis would not have been possible without the help and encouragement of many. In particular my sincere gratitude goes to:

- My supervisor **Øystein Elgarøy** and **David F. Mota** for shearing their expertise and for giving valuable advice and encouragement.

- My fellow students at the institute of theoretical astrophysics and the institute of physics for making this a pleasant experience, and for many interesting discussions and helpful advice. In particular I mention **Hans A. Winther** and **Johannes Rekkedal**, who were both so kind as to read through the thesis.

- **Mom** and **dad** for their love and support over the years, and mom for reading through the thesis and helping me with the grammar.

THANK YOU!

Notation

- **Units**

  We use units where

  $$\hbar \equiv c \equiv 1 \quad , \quad M_{Pl} \equiv \frac{1}{\sqrt{8\pi G}}$$

  so that all quantities are expressed in the same units. The conversion factors are given by

  $$\text{length} = c \cdot \text{time} \quad , \quad \text{energy} = c^2 \cdot \text{mass} = \frac{\hbar c}{\text{length}}$$

- **Derivatives**

  We will use the following notation for different derivatives

  $$\begin{aligned} &\text{Total derivatives:} \quad \frac{df}{dq} \quad , \quad f' = \frac{df}{dx} \quad , \quad \dot{f} = \frac{df}{dt} \\ &\text{Partial derivatives:} \quad \frac{\partial f}{\partial q} = \partial_q f = f_{,q} \quad , \quad \nabla = \sum_{x_i = x,y,z} \frac{\partial}{\partial x_i} \vec{e}_{x_i} \\ &\text{Covariant derivatives:} \quad \nabla_\mu f = f_{;\mu} \end{aligned}$$

- **Summation convention**

  We use Einsteins summation convention where equal upper and lower indices are summed over

  $$A^\mu B_\mu \equiv g_{\mu\nu} A^\mu B^\nu \equiv \sum_{\mu,\nu=0}^{3} g_{\mu\nu} A^\mu B^\nu$$

- **Vectors and Tensors**

  We usually write vectors and tensors in component form, with spacetime indices denoted by greek letters $\mu.\nu, \alpha, \beta, \ldots$ and all other indices by latin letters $i, j, k, l, \ldots$. We sometimes also use full vectors, and in this case we denote the full four vector by ordinary letters A while all other vectors are denoted by $\vec{A}$

  $$A = A^\mu e_\mu \quad , \quad \vec{A} = A^i \vec{e}_i$$

- **Metric**

  A general spacetime metric is denoted by $g_{\mu\nu}$, and the special case of the Minkowski metric by $\eta_{\mu\nu}$. We use the metric signature

  $$\text{sign}\,(g_{\mu\nu}) = (-1, 1, 1, 1)$$

  and denote the determinant of the metric by $g \equiv \det g_{\mu\nu}$, or in the Minkowski case $\eta \equiv \det \eta_{\mu\nu}$.

Contents

Chapter 1

Introduction

Topic

Over the last decade, growing observational data seems to indicate that the expansion of the universe is accelerating. What causes this acceleration is still an open question but one of the simplest and most widely studied explanation is that the acceleration is due to some new form of energy with the peculiar property of negative pressure, known as *Dark Energy*. The current observational constraints on such models are very loose, which have led to a plethora of different models for dark energy, the simplest one being that the acceleration is due to a constant vacuum energy or cosmological constant Λ. However this explanation gives rise to several problems. On problem is that particle physics gives estimates of the energy density of vacuum much larger then what is required from cosmology and as of yet we know of no natural way of removing this discrepancy. Another problem, known as the coincidence problem, is why the energy density of vacuum is of the same order of magnitude today as the density of matter. If the vacuum energy is constant it would mean that it would have to be miniscule compared to the density of matter in the far past, and that the energy density of matter will be negligible compared to the density of vacuum in the future. Many see it as an unlikely coincidence that we live in an era where they are approximately equal.

This is an important motivation for another dark energy model known as Quintessence, where dark energy is dynamic and is allowed to vary in time. In Quintessence, dark energy is modeled by a scalar field Φ and by allowing the field to have a suitable self interaction through a potential $V(\Phi)$, the evolution of dark energy mimics the behavior of the dominant energy component in the past, and the small dark energy density today is explained in the same way as the small matter density, namely as a consequence of the universe being old. Unfortunately this causes other problems. First of all we have no good explanation for why dark energy has come to dominate the evolution today and to obtain this feature, the self interaction potential has to be tuned. In particular the mass of the associated particle would have to have a very small mass. Secondly it seems unlikely that the Quintessence field does not interact with other forms of energy, and as the force mediated by the field is inversely proportional to the mass, this would lead to a new long ranged force, tightly constrained by experiments.

A proposed solution to this problem is *chameleon dark energy*, where the scalar field couples to matter in such a way that the mass of the associated particle depends on the local density. In high density regions such as here on earth and in the solar system, the mass of the field is large and as such the fifth force range is suppressed, while in low density regions the mass of the Chameleon is small, allowing cosmic acceleration. The reason for this is that the mass of the field is related to the curvature of the potential, and when the scalar field couples to matter, the effective potential seen by the field will be matter dependent $V_{eff}(\Phi, \rho_m)$ and larger matter densities yields larger potential curvature and a larger chameleon mass. Scalar fields similar to the chameleon field arise from proposed theories of quantum gravity, and these fields generally couple to matter with the strength of gravity. For such strong couplings the mass suppression is not enough for the theory to be in accordance with current experimental bounds, but in Chameleon theories there is also

an additional suppression from what is known as the *thin shell mechanism*. The force from the chameleon is proportional to the gradient of the field $\nabla\Phi$ and some objects, such as the sun and the earth, yield a profile for Φ where the field is approximately constant throughout most of the object, staying close to the minimum of the effective potential V_{eff}, before it rapidly moves towards the minimum of the potential in the background in a small shell at the surface of the object known as the thin shell. This behavior leads to a suppression factor of the chameleon gradient and force outside the object, proportional to the size of the shell, and as such makes the chameleon model consistent with experimental bounds even for large matter couplings. In this thesis we will study these chameleon models.

Main Goal

The thin shell mechanism was originally shown to appear in a highly idealized situation where one looked at the non-relativistic spherical symmetric objects with constant densities, and though it might work as a good approximation in some situations, it is not very realistic. The goal of this thesis as originally formulated, was to study how the conclusions from the idealized situation is altered by taking into account a gradually changing density profile and general relativistic effects. The approach to reaching this goal was to look at the specific example of a neutron star where we generalize the relativistic equations of hydrostatic equilibrium to include the chameleon, using a polytropic equation of state suitable for neutron stars, and study both how the inclusion of the chameleon alters the standard results for neutron stars, such as the maximum mass and the mass-radius relation, and also see how the resulting matter density profile affects the chameleon profile and whether or not the results from the non relativistic, constant density approximation still hold. Reaching this main goal can be done through two partial goals, one analytic and one numerical

- **Analytic Partial Goal:**

  Derive the relevant equations to be solved numerically. This can be done by generalizing the chameleon equations of motion to include relativistic effects, and generalizing the hydrostatic equilibrium equations to include the chameleon.

- **Numerical Partial Goal:**

  Solve the equations numerically and see if the properties of neutron stars are altered, and if taking into account relativistic effects and a continuous density profile affects the chameleon profile.

We managed to reach the first of these partial goals, and found the appropriate equations to be solved. Unfortunately we were unable to reach the second goal, because we encountered severe stability issues. We used Matlab's built in ODE suite to solve the equations derived and obtained reasonable numerical solutions to the equations. However we did not manage to obtain physically reasonable solutions, because this required fine tuning of the initial value of Φ at the center of the star beyond the capabilities of Matlab and this made it hard to come to any definitive conclusions regarding whether or not the chameleon model is viable in more realistic scenarios.

Thesis Structure

We have split this thesis into four parts. The first part introduces the theoretical framework for chameleon theory, while the second part is devoted to the accelerating universe, and dark energy in general. We then move on to a more detailed description of the chameleon dark energy model in part three, before we end the thesis by giving our attempt at reaching the main goal given above. We give a more detailed description of what is contained in the different parts below

- **Part I: Preliminaries**

  In this part we review the theoretical framework of this thesis, which is General relativity as a classical field theory. We therefor start by giving a short introduction to the methods and results of classical

field theory in chapter 2, before we look at the theory of general relativity in chapter 3. At the end of chapter 3 we give the equations for hydrostatic equilibrium in GR in section 3.5, and numerical solutions to the equations in section 3.6, which forms the basis for the numerics in chapter 8.

- **Part II: Dark Energy**

  In this part we give a brief review of the cosmic acceleration and dark energy. In chapter 4 we start by giving a brief introduction to the basic concepts needed to understand the observational evidence for dark energy before we give look at our universe and what observations tells us. In chapter 5 we look at different dark energy models, where we place emphasis on vacuum energy, quintessence and scalar tensor theory from which the chameleon model originates.

- **Part III: Chameleon Fields**

  In this part of the thesis we discuss the theoretical foundation for chameleon models and derive results relevant for finding the coupled TOV equations. In particular we derive the general relativistic equations of motion in section 6.1 and the energy density and pressure of the free chameleon in section 6.2, both of which will be used in chapter 8.

- **Part IV: Chameleons and Compact Objects**

  We end the thesis by giving our attempt at reaching the goal stated above. In chapter 7 we redo both the analytic and numerical work in the original paper by Khoury & Weltman, and try to build our intuition for the solutions to the equation of motion. The numerics serves as the basis for the numerical treatment of the equations of motion in the general relativistic approach of chapter 8, and also shows the sensitivity to variations in initial conditions, preventing us from reaching the numerical partial goal. In chapter 8, we start by giving a very brief review of a recent study on the general relativistic effects on the chameleon profile in section 8.1 before we continue by giving our approach in section 8.2. Here we start by setting up the equation to be solved numerically and show how these compare to what is given in section 8.1. This completes the analytic partial goal. We then show the numerical results we are able to produce and try to justify them using the intuition built in chapter 7. We conclude the thesis with chapter 9 where we give some suggestions to what we could have done differently in order to complete the main goal and how the work done in this thesis might be built upon.

We also include two appendices, where we calculate the Tensor components used in the thesis in appendix A and give Matlab codes used for the numerics in appendix B. With these introductory remarks out of the way, we give you our work.

Part I

Preliminaries

Chapter 2

Field Theory

This chapter is mainly based on [1], [2] and [3]. A field is a physical quantity that is defined everywhere in spacetime. The simplest form is a scalar field with a number associated with each point in spacetime. These numbers can be either complex or real and Newton's gravitational potential field Φ is an example of a real scalar field while complex scalar fields are used to describe charged spin zero particles in quantum field theory(QFT). We also have vector fields like the electromagnetic potential field A^μ , tensor fields like the metric tensor field $g_{\mu\nu}$ and even spinor fields used to describe spin 1/2 particles in QFT. A more abstract way of looking at a field is as a dynamical system of infinitely many degrees of freedom and as such the dynamics of the field is usually written in terms of a Lagrangian density which through Hamilton's principle gives us field equations.

2.1 Hamilton's Principle and Equations of Motion for Discrete Systems

The description of classical particle mechanics was originally derived from Newton's famous second law which states that in inertial reference frames the force on a particle is equal to the change in its momentum

$$F = \frac{dp}{dt} = m\frac{dv}{dt}$$

However the same dynamics is also derivable from more abstract and general principles that yield the same results for Newtonian systems, but remains valid in the post-Newtonian theories of quantum mechanics and relativity. Hamilton's principle is one such principle which is a principle concerning the global behavior of a dynamical system. Here the dynamics of the system is contained in the Lagrangian L given by the kinetic energy K minus the potential energy V of the system

$$L(q_i, \dot{q}_i, t) = K(q_i, \dot{q}_i, t) - V(q_i, \dot{q}_i, t) \tag{2.1}$$

where K and V are functions of the degrees of freedom of the system q_i , i.e the variables needed to completely specify its state at a particular time, and their time derivatives $\dot{q}_i$ together with any explicit time dependence describing the systems rate of change. Now if we think of $q(t) = \{q_1(t), q_2(t), \ldots, q_N(t)\}$ as a path through an N dimensional space , we can derive the equations of motion for the system by using *Hamilton's principle* which states that of all continuous paths connecting an initial state given by $q(t_i)$ and a final state given by $q(t_f)$, the physical path is the one for which the line integral

$$S = \int_{t_i}^{t_f} L(q, \dot{q}, t)dt$$

called the action, has a stationary value. For such a path any infinitesimal variation away from it, $q(t) \rightarrow q(t) + \epsilon$ which leaves the initial and final states unchanged, also leaves the action unchanged. Written explicitly this corresponds to

$$q \to q + \epsilon \;\Rightarrow\; S \to S + \delta S \quad , \quad \delta S = \int_{t_i}^{t_f} \delta L dt = 0$$

The equations of motion can now be found by writing the variation δL in terms of the variation of the path ϵ_i and its time derivative $\dot{\epsilon}_i$

$$\begin{aligned} \delta L &= \frac{\partial L}{\partial q_i}\epsilon_i + \frac{\partial L}{\partial \dot{q}_i}\dot{\epsilon}_i \\ &= \left[\frac{\partial L}{\partial q_i} - \frac{d}{dt}\left(\frac{\partial L}{\partial \dot{q}_i}\right)\right]\epsilon_i - \frac{d}{dt}\left(\frac{\partial L}{\partial \dot{q}_i}\epsilon_i\right) \end{aligned} \tag{2.2}$$

and integrating over time

$$\delta S = \int_{t_i}^{t_f} \left[\frac{\partial L}{\partial q_i} - \frac{d}{dt}\left(\frac{\partial L}{\partial \dot{q}_i}\right)\right]\epsilon_i dt + \left[\frac{\partial L}{\partial \dot{q}_i}\epsilon_i\right]_{t_i}^{t_f} = 0$$

The last term vanishes since we are keeping the endpoints fixed $\epsilon_i(t_i) = \epsilon_i(t_f) = 0$, and since the first integral should vanish for arbitrary variations ϵ_i we see that

$$\frac{\partial L}{\partial q_i} - \frac{d}{dt}\left(\frac{\partial L}{\partial \dot{q}_i}\right) = 0 \tag{2.3}$$

These are the equations of motion for a system described by the Lagrangian L , called the Euler-Lagrange equations. We see that multiplying the Lagrangian by a constant doesn't change the equations of motion, so there is no unique Lagrangian for a certain dynamical problem. The Euler-Lagrange equations can also be derived from Newton's second law by using a local principle known as D'Alembert's principle and we can go the other way by looking at a particle with position $x(t)$, moving in a potential $V(x)$. This gives the Lagrangian

$$L = \frac{1}{2}m\dot{x}^2 - V(x)$$

and plugging this into equation (2.3) we get

$$m\ddot{x} = -\frac{dV(x)}{dx} = F$$

which is Newton's second law for conservative forces. Another important formulation of mechanics much used in quantum and statistical mechanics is the Hamiltonian formulation obtained by applying a Legendre transform on the Lagrangian. This formulation contains no new physics but provides new powerful methods of studying physical systems. In the Hamiltonian formulation a system of N degrees of freedom is described by $2N$ first order equations rather than the N second order Euler-Lagrange equations. These equations are obtained by defining the generalized momentum p_i associated with a degree of freedom q_i

$$p_i \equiv \frac{\partial L}{\partial \dot{q}_i}$$

This quantity is conserved if the Lagrangian is independent of the coordinate q_i as can be seen from equation (2.3) which tells us that

$$\dot{p}_i \equiv \frac{\partial L}{\partial q_i}$$

now by writing the differential of the Lagrangian in terms of p_i and $\dot{p}_i$

$$\begin{aligned} dL &= \frac{\partial L}{\partial q_i}dq_i + \frac{\partial L}{\partial \dot{q}_i}dq_i + \frac{\partial L}{\partial t}dt \\ &= \dot{p}_i dq_i + p_i dq_i + \frac{\partial L}{\partial t}dt \end{aligned}$$

the Hamiltonian $H(q,p,t)$ is generated by the Legendre transform

$$H(q,p,t) = \dot{q}_i p_i - L(q,\dot{q},t)$$

which gives the differential

$$\begin{aligned} dH &= \frac{\partial H}{\partial p_i}dp_i + \frac{\partial H}{\partial q_i}dq_i + \frac{\partial H}{\partial t}dt \\ &= \dot{q}_i dp_i - \dot{p}_i dq_i - \frac{\partial L}{\partial t}dt \end{aligned}$$

Comparing the two ways of writing the differential we obtain the $2N+1$ equations. These are the $2N$ first order Hamiltonian equations of motion

$$\frac{\partial H}{\partial p_i} = \dot{q}_i \tag{2.4}$$

$$-\frac{\partial H}{\partial q_i} = \dot{p}_i \tag{2.5}$$

together with an equation relating the explicit time dependence of the Hamiltonian H and the Lagrangian L .

$$\frac{\partial H}{\partial t} = -\frac{\partial L}{\partial t}$$

A more detailed description of Legendre transformations and the Hamiltonian equations of motion are given in [1, chap. 8].

2.2 Generalization to Fields

As was mentioned in the beginning of this section a Lagrangian formulation for fields can be found by looking at discrete system of N degrees of freedom and taking the limit $N \to \infty$

$$\lim_{N\longrightarrow\infty} \{q_1(t), q_2(t), \ldots, q_N(t)\} = \Phi(x,t)$$

To show how this comes about we consider an example, which will give us the Lagrangian for a massless scalar field. We look at a one dimensional system of N point particles connected by springs with equilibrium length Δx and denote the displacement from equilibrium of particle i by Φ_i , as shown in figure 2.1.

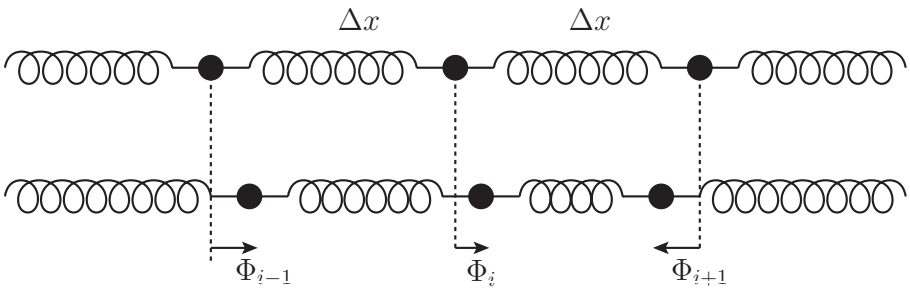

Figure 2.1: A discrete system of particles separated by a distance Δx in equilibrium and with the displacement from equilibrium given by Φ

The kinetic energy K of this system is then given by

$$K_i = \frac{1}{2} m \dot{\Phi}_i^2$$

while the potential energy stored in the spring connecting particle i with particle $i+1$ is given by Hooke's law

$$V_i = \frac{1}{2} k \left(\Phi_{i+1} - \Phi_i\right)^2$$

Summing over all particles and springs we obtain the full Lagrangian, which for later convenience is rewritten in terms of Δx

$$L = \frac{1}{2} \sum_i \left[\frac{m}{\Delta x} \left(\frac{d\Phi_i}{dt} \right)^2 - k \Delta x \left(\frac{(\Phi_{i+1} - \Phi_i)}{\Delta x} \right)^2 \right] \Delta x$$

Now, by taking the limit $\Delta x \to 0$ so that the number of particles per unit length goes to infinity, we have a particle at each coordinate x so rather than denoting the different displacements by a label i, we denote them by their spatial coordinate. We thus change $\Phi_i(t)$ to $\Phi(x,t)$, switch the sum into an integral and recognizing that the potential term is just the derivative of Φ with respect to x giving

$$L = \int \frac{1}{2} \left[\alpha \left(\frac{\partial \Phi(x,t)}{\partial t} \right)^2 - \beta \left(\frac{\partial \Phi(x,t)}{\partial x} \right)^2 \right] dx = \int \mathcal{L} dx$$

where $\alpha = m/dx$ and $\beta = kdx$ and the total derivatives have been replaced by partial derivatives reflecting the fact that we are considering explicit dependencies. The integrand is called a Lagrangian density $\mathcal{L}$ and is the same to field theory as the Lagrangian L is to particle mechanics. In the special case where $\alpha = \beta$ we have the Lagrangian density for a massless scalar field in one spatial dimension

$$\mathcal{L} = \frac{1}{2} \left[\left(\frac{\partial \Phi(x,t)}{\partial t} \right)^2 - \left(\frac{\partial \Phi(x,t)}{\partial x} \right)^2 \right]$$

We could have obtained a more general scalar field Lagrangian density by considering a three dimensional system of point particles connected by springs, who's dynamics also depended on a local potential depending only on the displacement of the particle itself $V(\Phi_i)$. Taking the continuous limit this would have given us the more general Lagrangian density

$$\mathcal{L} = -\frac{1}{2} \partial_\mu \Phi \partial^\mu \Phi - V(\Phi) \tag{2.6}$$

where we have introduced the relativistically covariant notation $\partial_\mu \Phi \partial^\mu \Phi = -(\partial_t \Phi)^2 + (\nabla \Phi)^2$. For continuous systems arising from discrete mechanical ones in the limit $N \to \infty$, the equations of motion in terms of the Lagrangian density can always be found by applying equation 2.3 to the discrete Lagrangian L

and taking the continuous limit, but fields often appear in physics in their own right without any underlying mechanical description and for this reason it is useful to write the equations of motion directly in terms of $\mathcal{L}$. This can be done by applying Hamilton's principle directly to $\mathcal{L}$ rather then L . Since $\mathcal{L}$ also depends on Φ' we get a spatial derivative term along with the time derivative term. Generalizing to three spatial dimensions and allowing several different fields, $\Phi_i = \Phi_i(x^\mu)$, we find

$$\begin{aligned} L &= \int \mathcal{L} d^3\mathbf{x} \\ \Rightarrow \quad \delta S &= \int \delta L dt = \int \delta \mathcal{L} d^4x = 0 \end{aligned}$$

and again writing the variation $\delta\mathcal{L}$ in terms of the variation in $\Phi_i = \Phi_i(x^\mu) + \epsilon_i(x^\mu)$

$$\begin{aligned} \delta\mathcal{L} &= \frac{\partial \mathcal{L}}{\partial \Phi_i}\epsilon_i + \frac{\partial \mathcal{L}}{\partial\left(\partial_\mu \Phi_i\right)}\partial_\mu \epsilon_i \\ &= \left[\frac{\partial \mathcal{L}}{\partial \Phi_i} - \partial_\mu \frac{\partial \mathcal{L}}{\partial\left(\partial_\mu \Phi_i\right)}\right]\epsilon_i + \partial_\mu\left[\frac{\partial \mathcal{L}}{\partial\left(\partial_\mu \Phi_i\right)}\epsilon_i\right] \end{aligned}$$

yielding a variation δS

$$\delta S = \int \left[\frac{\partial \mathcal{L}}{\partial \Phi_i} - \partial_\mu\left(\frac{\partial \mathcal{L}}{\partial(\partial_\mu \Phi_i)}\right)\right]\epsilon_i d^4x + \int \partial_\mu\left(\frac{\partial \mathcal{L}}{\partial(\partial_\mu \Phi_i)}\epsilon_i\right) d^4x = 0$$

The second term again vanishes if we apply the four dimensional version of the divergence theorem

$$\int_V \partial_\mu f(x^\mu) dV = \int_S n \cdot f(x^\mu) dS$$

and demand $\epsilon_i = 0$ at the surface. We are thus left with

$$\delta S = \int \left[\frac{\partial \mathcal{L}}{\partial \Phi_i} - \partial_\mu\left(\frac{\partial \mathcal{L}}{\partial(\partial_\mu \Phi_i)}\right)\right]\epsilon_i d^4x$$

and since the variation ϵ_i is arbitrary we get the covariant Euler-Lagrange equations for fields

$$\frac{\partial \mathcal{L}}{\partial \Phi_i} - \partial_\mu\left(\frac{\partial \mathcal{L}}{\partial(\partial_\mu \Phi_i)}\right) = 0 \tag{2.7}$$

This equation is called covariant because the form of the equation is independent of any specific choice of coordinates t, x, y, z , and since the principle of relativity states that the laws of physics should be independent of choice of reference frames, the field description provides a natural framework for relativistic theories. We can also find an analogous quantity to the Hamiltonian $H(p, q)$ by defining a canonical momentum density

$$\pi_i \equiv \lim_{\Delta x \to 0} \frac{p_i}{\Delta x} = \frac{\partial \mathcal{L}}{\partial \dot{\Phi}_i} \tag{2.8}$$

and defining the Hamiltonian density $\mathcal{H}(\dot{\phi}, \pi)$ to be

$$\mathcal{H} = \pi_i \dot{\Phi}_i - \mathcal{L} \quad , \quad H = \int \mathcal{H} d^3\mathbf{x} \tag{2.9}$$

where $\mathcal{H}$ is related to H in a similar manner as $\mathcal{L}$ is related to L . In the Hamiltonian formulation the spacetime coordinates are no longer treated symmetrically and time is given a special role. For this reason the Lagrangian formulation is a more powerful tool for describing relativistic field theories. The derivation of the equations of motion in terms of the Hamiltonian density is somewhat tedious and since they are of little relevance to this thesis we're just going to state them for completeness. Written in terms of functional derivatives they take on the same form as in the discrete case

$$\frac{\delta \mathcal{H}}{\delta \pi_i} = \dot{\Phi}_i \tag{2.10}$$

$$-\frac{\delta \mathcal{H}}{\delta \Phi_i} = \dot{\pi}_i \tag{2.11}$$

where the functional derivative is given by

$$\frac{\delta}{\delta \Phi} = \frac{\partial}{\partial \Phi} - \nabla \frac{\partial}{\partial \nabla \Phi}$$

2.3 Symmetries and Conservation Laws

There is a deep connection between conservation laws such as the conservation of energy and momentum, and the symmetries of the Lagrangian density $\mathcal{L}$. For example, if $\mathcal{L}$ is invariant under time translations, energy is conserved, if $\mathcal{L}$ is invariant under space translation, linear momentum is conserved, and if $\mathcal{L}$ is invariant under rotations, angular momentum is conserved. The formal statement is due to Emmy Noether through what is widely known as Noether's theorem. Noether's theorem states that for any field theory derivable from a Lagrangian density $\mathcal{L}$, it is possible to construct conserved quantities from the invariance of $\mathcal{L}$ under symmetry transformations. This is shown by first assuming a transformation

$$\Phi \;\rightarrow\; \Phi' = \Phi + \delta\Phi \tag{2.12}$$

Now the change in $\mathcal{L}$ caused by a change in Φ can be rewritten by using the covariant Euler-Lagrange equation 2.7

$$\delta\mathcal{L} = \frac{\partial \mathcal{L}}{\partial \Phi}\delta\Phi + \frac{\partial \mathcal{L}}{\partial\left(\partial_\mu \Phi\right)}\delta\left(\partial_\mu \Phi\right) \quad , \quad \frac{\partial \mathcal{L}}{\partial \Phi} = \partial_\mu\left(\frac{\partial \mathcal{L}}{\partial(\partial_\mu \Phi)}\right)$$

$$\Rightarrow\; \delta\mathcal{L} = \partial_\mu\left(\frac{\partial \mathcal{L}}{\partial(\partial_\mu \Phi)}\right)\delta\Phi + \frac{\partial \mathcal{L}}{\partial\left(\partial_\mu \Phi\right)}\partial_\mu\left(\delta\Phi\right) = \partial_\mu\left(\frac{\partial \mathcal{L}}{\partial(\partial_\mu \Phi)}\delta\phi\right) \tag{2.13}$$

where we simplify the notation by defining $\mathcal{N}^\mu$ and its spatial integral N^μ

$$\mathcal{N}^\mu = \frac{\partial \mathcal{L}}{\partial(\partial_\mu \Phi)}\delta\Phi \quad , \quad N^\mu = \int \mathcal{N}^\mu d^3\mathbf{x}$$

so that

$$\delta\mathcal{L} = \partial_\mu \mathcal{N}^\mu$$

Now if the transformation $\Phi \rightarrow \Phi + \delta\Phi$ is a symmetry of $\mathcal{L}$, the change $\delta\mathcal{L}$ vanishes so

$$\delta\mathcal{L} = \partial_\mu \mathcal{N}^\mu = \frac{\partial \mathcal{N}^0}{\partial t} + \nabla \cdot \boldsymbol{\mathcal{N}} = 0 \;\Rightarrow\; \frac{\partial \mathcal{N}^0}{\partial t} = -\nabla \cdot \boldsymbol{\mathcal{N}}$$

Finally we take the derivative of N^0 with respect to time, and as long as the change in Φ vanishes at infinity we can use the divergence theorem to obtain

$$\frac{\partial N^0}{\partial t} = \int \frac{\partial \mathcal{N}^0}{\partial t} d^3\mathbf{x} = -\int \nabla \cdot \boldsymbol{\mathcal{N}} d^3\mathbf{x} = -\int \boldsymbol{\mathcal{N}} \cdot \mathbf{n}\, dS = 0$$

Since the time derivative is seen to vanish, N^0 must be a conserved quantity

$$N^0 = \int \mathcal{N}^0 d^3\mathbf{x} = \text{Constant} \tag{2.14}$$

and $\mathcal{N}^0$ is called a conserved current. As examples we have already mentioned the invariance under spacetime translations and rotations which yields conservation of energy and momenta, and other examples are the conservation of charge which follows from global gauge invariance of the Dirac Lagrangian $\mathcal{L}_D$ describing the interaction between electrons and the electromagnetic field. It is also possible to use Noether's Theorem to define the stress energy tensor, which is a covariant way of describing the energy and momentum of a system, but in this thesis we will use the definition from Einstein's field equations which we come back to in the next section.

2.4 Quantum Field Theory

We conclude this section with a brief description of one of the most important applications of field theory in modern physics, namely quantum field theory. In quantum field theory both particles and forces are described by quantized fields. We will give an example by looking at the simple case of a real free scalar field and apply the canonical quantization scheme (as opposed to the path integral quantization). In quantum field theory such a field is described by the Klein-Gordon Lagrangian density

$$\mathcal{L}_{KG} = -\frac{1}{2}\partial_\mu \Phi \partial^\mu \Phi - \frac{1}{2}m^2\Phi^2$$

yielding the canonical momenta

$$\pi = \frac{\partial \mathcal{L}}{\partial \dot{\Phi}} = \dot{\Phi}$$

and through equation 2.7, the equation of motion, called the Klein-Gordon equation

$$\partial_\mu \partial^\mu \Phi - m^2 \Phi = 0$$

The general solution to this equation is a superposition of positive and negative frequency plane wave solutions with wave number $\mathbf{k}$ and frequency ω

$$\Phi(x^\mu) = \sum_{\mathbf{k}} a_{\mathbf{k}} e^{ik_\mu x^\mu} + a^*_{\mathbf{k}} e^{-ik_\mu x^\mu} \quad , \quad k^\mu = (\omega, \mathbf{k}) \quad , \quad \omega^2 = \mathbf{k}^2 + m^2$$

where our demand that Φ is real means that the coefficients of the negative frequency solution, $a^*_{\mathbf{k}}$, must be the complex conjugate of the positive frequency coefficients $a_{\mathbf{k}}$. Now these fields are quantized in a manner analogous to what is done in non-relativistic quantum mechanics, where the position and momentum (x, p) are promoted to operators $(\hat{x}, \hat{p})$ obeying the commutation relation

$$[\hat{x}, \hat{p}] = i$$

In quantum field theory the field Φ and the canonical momentum π become operators obeying the equal time commutation relation

$$\left[\hat{\Phi}(t, \mathbf{x}), \hat{\pi}(t, \mathbf{x}')\right] = i\delta^3(\mathbf{x}' - \mathbf{x})$$

where δ is the three dimensional delta function. In field theory we also need to state that Φ and π commutes with itself, which is implicit in QM, because there is only one single coordinate and momentum. Since the field is now an operator, the coefficients $(a_{\mathbf{k}}, a^*_{\mathbf{k}})$ also become operators $\left(\hat{a}_{\mathbf{k}}, \hat{a}^\dagger_{\mathbf{k}}\right)$ obeying the commutation relation

$$\left[\hat{a}_{\mathbf{k}}, \hat{a}^\dagger_{\mathbf{k'}}\right] = \delta^3(\mathbf{k} - \mathbf{k}')$$

where all other combinations again commutes. The operators $\hat{a}^\dagger_{\mathbf{k}}$ and $\hat{a}_{\mathbf{k}}$ are called creation and annihilation operators respectively and play a similar role in QFT as the ladder operators $\hat{a}^\dagger$ and $\hat{a}$ used to raise or lower the energy of the harmonic oscillator in QM. In fact the free quantum field can be viewed as an infinite collection of harmonic oscillators of different frequencies where the creation and annihilation

operators are used to raise or lower the energy of these oscillators corresponding to creating or destroying particles. In the case of the real scalar field the excitations in the field corresponds to neutral spin zero particles. Although the equations of motion can be solved for free fields, they are not very interesting in themselves and to get physically interesting answers we have to look at the interactions between the different fields. This makes things much more complicated and as of today we have no exact solutions for interacting fields in more than two dimensions, and we have to rely on approximate solutions based on perturbation theory to get physical answers from QFT. Today all particles and forces are believed to arise from quantum fields and their interactions, and all but one of these forces have been unified in what is called the standard model of particle physics where the interactions between the different fields arise from gauge symmetry, see [2] or [3] for more details. The only exception is gravity and as of yet we have no satisfying quantum theory of gravity.

Chapter 3

General Relativity

This chapter is mainly based on [4],[5],[6] and [7]. General relativity is Einstein's theory of gravity, where gravitation is a manifestation of the curvature of spacetime. The curvature is described by a tensor field $g_{\mu\nu}$, called the metric, and as such GR can be viewed as a field theory. GR is built mainly on two principles which we will briefly state below, see [1, chap. 7.11] for more details

- **Principle of General Covariance**

  The principle of general covariance is a generalization of the principle of special covariance which is one of the fundamental building blocks of special relativity. While the special principle states that the laws of nature should be the same for all inertial observers, the general principle of covariance states that the laws of nature should be the same for all observers.

- **Principle of Equivalence**

  The principle of equivalence states that there is no way to distinguish between the effects of uniform acceleration and a uniform gravitational field. Similarly there is no way to distinguish between a freely falling reference frame in a uniform gravitational field and an inertial frame in the absence of gravity. In other words freely falling reference frames are inertial and the presence of gravitational forces are due to deviations from inertial motion, just as inertial forces are due to acceleration.

The first principle helps us to choose the appropriate mathematical objects to describe physical quantities, namely tensors, while the second principle suggests that gravity is related to the geometry of spacetime itself, and as such helps us to choose the appropriate mathematical framework which is differential geometry, where spacetime is considered to be a differentiable manifold, see [4] for details. Since general relativity can be viewed as a generalization of special relativity and many of the important concepts of GR also occur in the more familiar theory of SR, we will start with a brief review of this subject.

3.1 Special Relativity

Special relativity is based on the special principle of covariance, which states that the laws of nature should be the same in any non-accelerating reference frame, together with the assumption that the speed of light c is independent of the relative velocity of the light source compared to the observer. This naturally leads to a world view where space and time no longer are independent absolute concepts, but come together to form spacetime where what is time and what is space depends on the observer. In fact the relationship between the spacetime coordinates of two observers moving relative to each other, is closely analogous to the relationship between the spatial coordinates of two coordinate systems related by a rotation.

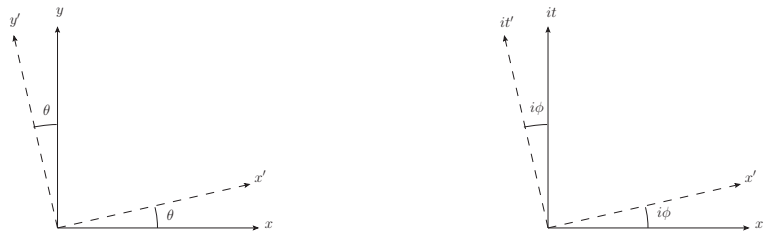

Figure 3.1: the transformation of spacetime coordinates under a boost is closely analogous to the transformations of spatial coordinates under rotation

The rotations in figure 3.1 give the coordinate transformations

$$\begin{array}{ll} x' = x\cos\theta + y\sin\theta & t' = t\cos i\phi + ix\sin i\phi = t\cosh\theta - x\sinh\phi \\ y' = -x\sin\theta + y\cos\theta \quad , & x' = it\sin i\phi + x\cos i\phi = -t\sinh\phi + x\cosh\phi \end{array} \tag{3.1}$$

where we see that the spacetime transformations give the famous Lorentz transformation under a boost along x, where the rapidity ϕ is related to the relative velocity v of the two frames by

$$v = \tanh\phi$$

Although the components of a spatial three vector A^i depends on the coordinates used, the vector itself has an existence independent of any choice of coordinates, so quantities related to the vector as a whole, like the inner product $\vec{A}\cdot\vec{A}$ is the same in all frames. The same applies to the spacetime transformations where we have Lorentzian four vectors with coordinate dependent components A^μ, but a coordinate independent inner product $A\cdot A$

$$A\cdot A = \eta_{\mu\nu}A^\mu A^\nu = -\left(A^0\right)^2 + \vec{A}\cdot\vec{A} \tag{3.2}$$

where $\eta_{\mu\nu}$ is the metric associated with flat spacetime in Cartesian coordinates, known as the *Minkowski metric*

$$(\eta_{\mu\nu}) = \begin{pmatrix} -1 & 0 & 0 & 0 \\ 0 & 1 & 0 & 0 \\ 0 & 0 & 1 & 0 \\ 0 & 0 & 0 & 1 \end{pmatrix} \tag{3.3}$$

The metric can be viewed as the inner product of the basis vectors $g_{\mu\nu} = e_\mu \cdot e_\nu$, and tells us how the components of four vectors and more generally tensors, are related in different coordinate systems and more importantly contains the information about the structure of spacetime itself. More generally the metric is usually denoted by $g_{\mu\nu}$ and an example of a non-Minkowskian metric in flat spacetime is the metric associated with polar coordinates where the metric is given by

$$(g_{\mu\nu}) = \begin{pmatrix} -1 & 0 & 0 & 0 \\ 0 & 1 & 0 & 0 \\ 0 & 0 & r^2 & 0 \\ 0 & 0 & 0 & r^2\sin^2\theta \end{pmatrix} \tag{3.4}$$

Another way of expressing the information content in the metric is through the invariant line element ds^2, which gives the infinitesimal distance between two points or events in spacetime. For Cartesian coordinates in flat spacetime the line element is given by

$$ds^2 = \eta_{\mu\nu}dx^\mu dx^\nu = -dt^2 + dx^2 + dy^2 + dz^2 \tag{3.5}$$

The line element can be used to quantify the paths taken by observers through spacetime. In particular there always exist frames associated with massive objects where the objects are at rest and in these frames

the line element ds^2 along their paths are given only in terms of the change in time. This leads us to define the proper time τ via

$$ds^2 = -d\tau^2$$

The proper time is the time elapsed along a path as measured by an observer following this world line. Paths where $ds^2 < 0$, are called timelike and spacetime points connected by such paths are causally connected. Paths with $ds^2 = 0$ are called lightlike, reflecting the fact that light follows such world lines, while paths with $ds^2 > 0$ are called spacelike and points connected by only such paths can never be in causal contact. Just as observers moving with constant velocity follows the shortest possible path through space in Newtonian mechanics (i.e they move in straight lines), inertial observers follows the shortest possible path through spacetime, in the sense that an inertial path connecting two spacetime points give the shortest spatial distance and longest time as measured along the path (minimizes proper length and maximizes proper time). For timelike paths it is usual to parametrize the path by the proper time $x^\mu(\tau)$, and with this parametrization the relativistic equation of motion for an inertial object is given by

$$\frac{d^2x^2}{d\tau^2} = 0$$

where the tangent vector of the path $U^\mu = dx^\mu/d\tau$ is called the four-velocity, indicating that the four velocity is constant along inertial paths. As with all four vectors we have an invariant inner product $U \cdot U$, which in this case is given by

$$U \cdot U = \eta_{\mu\nu} U^\mu U^\nu = -1$$

since $dx^0 = d\tau$ and $d\vec{x} = 0$ in the rest frame. The four-momentum of a particle with rest mass m is then given by $p^\mu = mU^\mu$, where p^0 is the energy and $\vec{p} = \gamma m\vec{v}$ is the relativistic three-momentum of the particle. From this it follows that in the rest frame $p^0 = E = m$, which when c is reinserted, yields Einsteins famous mass-energy relation $E = mc^2$. We see from the four-momentum that neither energy nor momentum are conserved quantities when going from one inertial frame to another, but rather energy momentum on the whole given by the inner product of the four-momentum

$$p \cdot p = E^2 - p^2 = m^2 \tag{3.6}$$

this is sufficient for the relativistic description of single particles but often we are more interested in systems with many degrees of freedom, and such systems are most easily described as a fluid characterized by macroscopic quantities such as density, pressure, viscosity and so on. A relativistic description of such a fluid is most easily done by defining an energy-momentum tensor $T^{\mu\nu}$ defined as the flux of four-momentum p^μ through a surface of constant x^μ . This tensor is symmetric and in the rest frame of the fluid the diagonal elements describe the energy density and pressure, while the off diagonal elements describes the momentum density and flux of the fluid. When matter is described in this way the conservation of Stress-Energy tensor is given by the simple law

$$\partial_\mu T^{\mu\nu} = 0 \tag{3.7}$$

Fluids in general can be complicated to handle and for this reason we often approximate matter as a perfect fluid which has no shear forces, viscosity or heat conduction. In this case we have a general expression for the Stress-Energy tensor in terms of the pressure p , density ρ and four velocity U^μ of the fluid in any inertial frame, given by

$$T^{\mu\nu} = (\rho + p)\, U^\mu U^\nu + p\eta^{\mu\nu} \tag{3.8}$$

For a more detailed discussion on relativistic fluid mechanics we recommend the excellent treatment in [6].

3.2 Tensors

General relativity is built upon a generalization of the special principle of relativity, naturally called the general principle of relativity, which states that the laws of nature should be the same in *all* reference frames. This means that the laws of nature should be formulated in a coordinate independent way and this is where tensors come in handy. Tensors can be viewed as a generalization of Lorentz scalars with no spacetime indices and four vectors with one spacetime index to a larger class of objects with an arbitrary number of spacetime indices that can be either upper indices as in the four vector A^μ, or lower indices as in the dual vector A_μ. Tensors can be defined by their transformation law under coordinate transformations given by

$$T^{\mu'\cdots\nu'}{}_{\alpha'\cdots\beta'} = \frac{\partial x^{\mu'}}{\partial x^\mu}\cdots\frac{\partial x^{\nu'}}{\partial x^\nu}\frac{\partial x^\alpha}{\partial x^{\alpha'}}\cdots\frac{\partial x^\beta}{\partial x^{\beta'}}T^{\mu\cdots\nu}{}_{\alpha\cdots\beta} \tag{3.9}$$

and since the transformation law is independent of what kind of tensor is being transformed, any law of nature written in terms of tensors will look the same after a coordinate transformation, thus satisfying the general principle of relativity. If a tensor has n upper indices and m lower indices it is called a (n,m)-tensor which can be contracted to form a $(n-1,m-1)$-tensor by summing over one upper and one lower index

$$S^{\mu\cdots}{}_{\alpha\cdots} = T^{\mu\lambda\cdots}{}_{\alpha\lambda\cdots}$$

and for a two index tensor this is usually called taking the trace. A tensor is said to be symmetric in the indices α and β if the tensor components $T^{\alpha\beta}$ are equal to the components with β and α interchanged, $T^{\alpha\beta} = T^{\beta\alpha}$. Similarly a tensor is said to be antisymmetric in the indices α and β if the magnitudes of the components stay the same but the sign changes $T^{\alpha\beta} = -T^{\beta\alpha}$. The most important tensor in GR is the metric tensor $g_{\mu\nu}$ which is a two index symmetric tensor. Other than describing the geometry of spacetime, the metric can also be used to manipulate other tensors. For example the generalization of the inner product of four vectors given in equation 3.2 is given by

$$A\cdot A = g_{\mu\nu}A^\mu A^\nu$$

This suggests that we can construct a $(0,1)$-tensor A_ν by contracting the $(1,0)$-tensor A^μ with the metric

$$A_\nu = g_{\mu\nu}A^\mu$$

known as a dual vector or one form, so that the inner product is given by the contraction of a four vector with its dual vector $A\cdot A = A_\nu A^\nu$. If we also define an inverse metric by

$$g^{\mu\lambda}g_{\lambda\nu} = \delta^\mu_{\ \nu}$$

where $\delta^\mu_{\ \nu}$ is the four dimensional Kronecker delta[1], we can construct a $(1,0)$-tensor A^μ from a $(0,1)$-tensor A_ν

$$A^\nu = g^{\mu\nu}A_\mu$$

This procedure is known as raising and lowering indices, and applies to all tensors. We also have another concept closely related to tensors, known as tensor densities which are important when we construct an invariant action integral S in curved spacetime. These quantities transform in a similar manner as tensors except that in addition the tensor density gets multiplied by a power of the Jacobian determinant, see [8].

$$D^{\mu'\cdots\nu'}{}_{\alpha'\cdots\beta'} = \left|\frac{\partial x'}{\partial x}\right|^w \frac{\partial x^{\mu'}}{\partial x^\mu}\cdots\frac{\partial x^{\nu'}}{\partial x^\nu}\frac{\partial x^\alpha}{\partial x^{\alpha'}}\cdots\frac{\partial x^\beta}{\partial x^{\beta'}}T^{\mu\cdots\nu}{}_{\alpha\cdots\beta} \tag{3.10}$$

where w is called the weight of the tensor density. The determinant of the metric denoted by $g = \det(g_{\mu\nu})$ and the four dimensional volume element $d^4x = dx^0dx^1dx^2dx^3$ are examples of tensor densities with no

[1] In matrix notation this would be written $\mathbf{g}\mathbf{g}^{-1} = \mathbf{I}$

indices, and weight $w = -2$ and $w = 1$ respectively, and as such are sometimes called scalar densities. The transformation properties of the two scalar densities are

$$g' = \left|\frac{\partial x'}{\partial x}\right|^{-2} g \tag{3.11}$$

$$d^4x' = \left|\frac{\partial x'}{\partial x}\right| d^4x \tag{3.12}$$

which means that we can define an invariant spacetime volume element dV by multiplying dx^4 by $\sqrt{-g}$, where the minus sign is due to the fact that the determinant of metrics with signature $(-,+,+,+)$ will be negative

$$dV \equiv \sqrt{-g}d^4x \quad \Rightarrow \quad dV' = \sqrt{-g'}d^4x' = \left|\frac{\partial x'}{\partial x}\right|^{1-1} \sqrt{-g}d^4x = dV$$

Finally we also need to consider derivatives of tensors. If we start by looking at a four vector we know that in Cartesian coordinates in flat spacetime the partial derivative of a four vector is found by taking the derivative of its components so we can write

$$\frac{\partial A}{\partial x^\nu} = \frac{\partial A^\mu}{\partial x^\nu}\vec{e}_\mu = A_{,\mu}\vec{e}_\mu$$

so here the derivative of a four vector written in terms of its components is just $A_{,\mu}$. However this is due to the fact that in Cartesian coordinates the basis vectors are fixed, but in general the basis vectors can depend on the coordinates, as is the case with polar coordinates. The more general case can be written

$$\frac{\partial A}{\partial x^\nu} = \frac{\partial A^\mu}{\partial x^\nu}\vec{e}_\mu + A^\alpha\frac{\partial \vec{e}_\alpha}{\partial x^\nu} = \left(A^\mu{}_{,\nu} + A^\alpha\Gamma^\mu{}_{\alpha\nu}\right)\vec{e}_\mu \quad , \quad \frac{\partial \vec{e}_\alpha}{\partial x^\nu} = \Gamma^\mu{}_{\alpha\nu}\vec{e}_\mu$$

where we have written the change in the basis vector as a linear combination of the original basis vectors. We thus introduce the more general concept of a covariant derivative Δ_ν of the components of a tensor A^μ

$$\nabla_\nu A^\mu = A^\mu_{;\nu} = A^\mu{}_{,\nu} + A^\alpha\Gamma^\mu{}_{\alpha\nu} \tag{3.13}$$

The coefficients $\Gamma^\mu{}_{\alpha\nu}$ are known as Christoffel symbols and can be related to the metric through the relation $g_{\mu\nu} = \vec{e}_\mu \cdot \vec{e}_\nu$. This involves some tensor algebra, using the relations we have defined so far so it might be instructive to give a brief description. The first step is to take the ordinary partial derivative of the metric and express it in terms of the basis vectors and their derivatives, which in turn can be written in terms of Christoffel symbols and the metric.

$$g_{\mu\nu,\sigma} = \partial_\sigma\left(\vec{e}_\mu \cdot \vec{e}_\nu\right) = \vec{e}_\nu \cdot \partial_\sigma\vec{e}_\mu + \vec{e}_\mu \cdot \partial_\sigma\vec{e}_\nu = \Gamma^\lambda{}_{\mu\sigma}g_{\lambda\nu} + \Gamma^\lambda{}_{\nu\sigma}g_{\lambda\mu}$$

Next we combine several metric derivatives so that the combination can be written in terms of only one combination of Christoffel symbols and the metric

$$g_{\mu\sigma,\nu} + g_{\sigma\nu,\mu} - g_{\mu\nu,\sigma} = 2\Gamma^\lambda{}_{\mu\nu}g_{\sigma\lambda}$$

Finally we can multiply by $1/2g^{\sigma\alpha}$ on both sides and use the definition of the inverse metric to get a single Christoffel symbol on the right hand side

$$\Gamma^\lambda{}_{\mu\nu}g_{\sigma\lambda}g^{\sigma\alpha} = \Gamma^\lambda{}_{\mu\nu}\delta^\alpha_\lambda = \Gamma^\alpha{}_{\mu\nu}$$

yielding the relation

$$\Gamma^\alpha{}_{\mu\nu} = \frac{1}{2}g^{\sigma\alpha}\left(g_{\mu\sigma,\nu} + g_{\sigma\nu,\mu} - g_{\mu\nu,\sigma}\right) \tag{3.14}$$

From the symmetry of the metric we see that the Christoffel symbols are symmetric in their lower indices $\Gamma^{\alpha}{}_{\mu\nu} = \Gamma^{\alpha}{}_{\nu\mu}$. The procedure of writing derivatives of tensor components in a covariant way can be generalized to tensors of arbitrary rank and the general expression is given by

$$\begin{aligned}\nabla_\sigma T^{\mu\cdots\nu}{}_{\alpha\cdots\beta} &= \partial_\sigma T^{\mu\cdots\nu}{}_{\alpha\cdots\beta} \\ &+ \Gamma^{\mu}{}_{\sigma\lambda} T^{\lambda\cdots\nu}{}_{\alpha\cdots\beta} + \cdots + \Gamma^{\nu}{}_{\sigma\lambda} T^{\mu\cdots\lambda}{}_{\alpha\cdots\beta} \\ &- \Gamma^{\lambda}{}_{\sigma\alpha} T^{\mu\cdots\nu}{}_{\lambda\cdots\beta} - \cdots - \Gamma^{\lambda}{}_{\sigma\beta} T^{\mu\cdots\nu}{}_{\alpha\cdots\lambda}\end{aligned} \tag{3.15}$$

A nice feature of the covariant derivative given here is that the covariant derivative of the metric $g_{\mu\nu}$ and its inverse $g^{\mu\nu}$ are always zero

$$g_{\mu\nu;\sigma} = 0 \quad , \quad g^{\mu\nu}{}_{;\sigma} = 0$$

The covariant derivative also gives a simple method for generalizing laws valid in flat spacetime to curved spacetime: Write the law in tensor form , replace $\eta_{\mu\nu}$ by $g_{\mu\nu}$ and replace the partial derivatives by covariant ones. As examples we take three equations that will be important to us later, namely the covariant Euler-Lagrange equations, the conservation of energy and momentum and the stress energy tensor of a perfect fluid in special relativity given by equations 2.7, 3.7 and 3.8. Following the recipe given above the curved spacetime generalization are given by

$$\frac{\partial \mathcal{L}}{\partial \Phi_i} - \nabla_\mu \left(\frac{\partial \mathcal{L}}{\partial (\nabla_\mu \Phi_i)} \right) = 0 \tag{3.16}$$

$$\nabla_\mu T^{\mu\nu} = T^{\mu\nu}{}_{;\mu} = 0 \tag{3.17}$$

$$T^{\mu\nu} = (\rho + p) U^\mu U^\nu + p g^{\mu\nu} \tag{3.18}$$

With the basics of flat spacetime and tensors out of the way we are prepared to go to curved spacetime.

3.3 Curvature

The principle of equivalence tells us that all objects, regardless of composition, are affected by gravity in the same way, and that freely falling objects are inertial. This seems to suggest that gravity is a property of spacetime itself, rather than a force, and by allowing spacetime to curve, the shortest possible paths through spacetime are no longer straight but curved, in accordance with the paths taken by observers moving in a gravitational field. To see this we can apply the recipe for generalizing laws to curved spacetime to the equation of motion for inertial objects. First we use $\frac{d}{d\tau} = \frac{dx^\nu}{d\tau}\partial_\nu = U^\nu \partial_\nu$ to rewrite

$$\frac{d^2 x^\mu}{d\tau^2} = U^\nu U^\mu{}_{,\nu} = 0$$

to obtain a tensorial equation and change the ordinary derivative with covariant ones giving

$$U^\nu U^\mu{}_{;\nu} = U^\nu U^\mu{}_{,\nu} + \Gamma^\mu_{\alpha\nu} U^\nu U^\alpha = 0$$

or more conventionally written in terms of the proper time

$$\frac{d^2 x^\mu}{d\tau^2} + \Gamma^\mu_{\alpha\nu} \frac{dx^\nu}{d\tau} \frac{dx^\alpha}{d\tau} = 0 \tag{3.19}$$

This equation is known as *the geodesic equation* and describes the paths taken by freely falling objects in curved spacetime, called geodesics. Newtonian gravity is approximately correct for small velocities, $U^0 >> U^i$, $\tau \approx t$, and weak static gravitational fields where the metric is time independent and nearly flat, $g_{\mu\nu} \approx \eta_{\mu\nu} + h_{\mu\nu}(x^i)$. Using equation 3.14 to calculate the Christoffel symbols and keeping only first order terms in h , the geodesic equation yields

$$\frac{d^2x^i}{dt^2} \approx \frac{1}{2}\partial_i h_{00}$$

in this limit. Reminding ourselves that in Newtonian gravity the gravitational acceleration is given by the gradient of the gravitational potential, $\vec{a} = -\nabla\Phi$, we see that the curvature description coincides with the Newtonian one, if we set $h_{00} = -2\Phi$, suggesting that gravity really can be viewed as an effect of objects following geodesics in curved spacetime.

It might not be completely clear what we mean by curvature, since we are used to think of curvature as a property of lines and surfaces embedded in some higher dimensional space. For example we usually use a two dimensional figure to visualize a curved line and a three dimensional one to visualize curved surfaces, but in the context of four dimensional spacetime it seems rather contrived to introduce a fifth dimension just so that spacetime has something to curve relative to. However curvature can have an existence independent of any embedding, and such curvature is known as intrinsic. This form of curvature not only changes how the surface, or submanifold, relates to the manifold in which it lives, but also changes the internal structure. While extrinsic curvature tells us how surfaces curve with respect to the space in which it lives, intrinsic curvature changes the geometry of the surface itself and can therefore be detected by geometrical surveys on the surface alone. As an example we consider the surface of a sphere and the surface of a cylinder, see figure 3.2

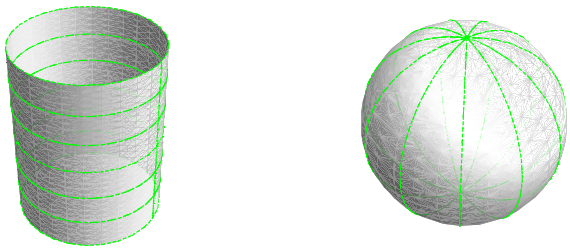

Figure 3.2: Two manifestly different curved surfaces: The cylinder is only extrinsically curved so it is impossible to say anything about the curvature from the surface alone, and on the left we have a sphere with intrinsic curvature, meaning information about the curvature is contained in the surface.

In the case of the cylinder one can easily imagine cutting it open along the side and spreading it out into a flat surface. This tells us that the laws of geometry we use on flat surfaces also apply to the cylinder. By looking at the sphere however we see that this is not possible without stretching or tearing the surface and if by ”straight” lines we mean the shortest distance between two points, we see that straight lines, initially parallel at the equator, will meet at the poles. This means that Euclid’s postulate that parallel straight lines never meet, no longer holds, making the geometry non-Euclidean. The deviation from Euclidean geometry can be quantified by looking at how vectors behave on the surface and to explain this we have to consider how vectors, and more generally tensors are related at different points in a curved space. Consider someone starting out at the south pole of the earth pointing straight ahead and then moving to the north pole without ever moving his hand. From our perspective here on earth we would say he is still pointing in the same direction, but as seen from outer space he is actually pointing in the opposite direction to where he was pointing initially. This is due to the fact that vectors, in general are elements of tangent spaces defined at each point on the surface, so in the example of the earth, the vector represented by the pointing finger hasn’t really changed, its only the tangent space that has a different orientation as seen from outer space. So far the discussion also applies to any curved surface, but for intrinsically curved surfaces something strange happens if we choose to transport the vector back to its initial position by another route. Sticking

to our example of the pointing finger, we let the person pointing travel back to the south pole sideways. When arriving back at the south pole the person will discover that now the finger is pointing in a different direction, perpendicular to the initial one, and this effect is due to the intrinsic curvature of the surface and allows him to deduce that the earth is curved without ever considering anything other then the surface itself. This whole procedure is known as a parallel transport of vectors and is illustrated in figure 3.3a.

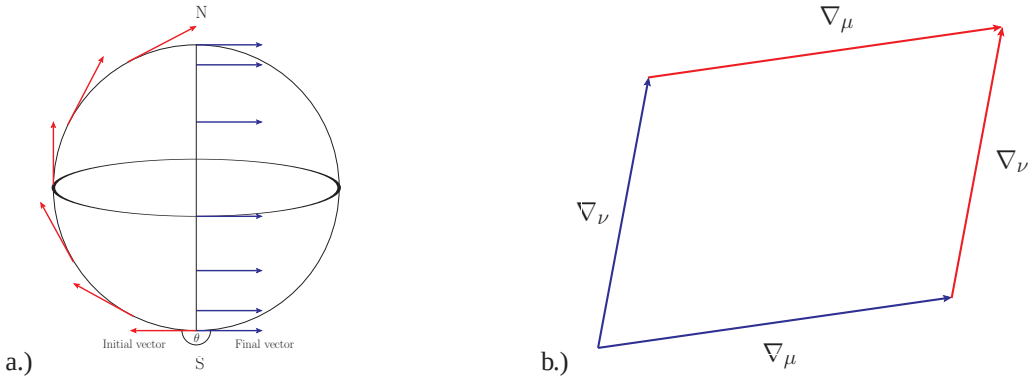

Figure 3.3: a.) Parallel transport of a vector on a sphere. Due to the intrinsic curvature the direction of the vector has changed when arriving back at the original position. b.) The Commutator of two covariant derivatives

This way of thinking also applies to curved spacetime and gives us a way of considering its curvature without relying on any embedding in a higher dimensional manifold. Mathematically, the parallel transport of a vector A along a path parametrized by some invariant quantity λ means that the derivative of the vector with respect to λ vanishes

$$\frac{dA}{d\lambda} = \frac{dx^\mu}{d\lambda}\frac{dA}{dx^\mu} = 0$$

which, by using equation 3.13, yields the component equation

$$\frac{dA^\mu}{d\lambda} + \Gamma^\mu_{\alpha\nu}\frac{dx^\nu}{d\lambda}A^\alpha = 0 \tag{3.20}$$

known as the equation of parallel transport. The intrinsic curvature of spacetime can be quantified by looking at how four-vectors change when they are parallel transported around an infinitesimal closed loop in spacetime. One could of course carefully do this parallel transportation by going through the loop and taking the difference between the initial and final vector, see [6, chap. 6.5], but the easiest way to express this mathematically is by calculating the commutator of covariant derivatives in different directions $[\nabla_\mu, \nabla_\nu]$, which basically is the same thing, see figure 3.3b and [4, chap. 3.6]. Applied to an arbitrary four vector A one finds that the commutator yields

$$[\nabla_\mu, \nabla_\nu]\, A^\alpha = R^\alpha_{\beta\mu\nu}A^\beta \tag{3.21}$$

where $R^\alpha_{\beta\mu\nu}$ is known as the Riemann tensor or simply the curvature tensor, and is given in terms of the Christoffel symbols an their derivatives

$$R^\alpha_{\beta\mu\nu} = \partial_\beta\Gamma^\alpha_{\mu\nu} - \partial_\nu\Gamma^\alpha_{\mu\beta} + \Gamma^\alpha_{\lambda\beta}\Gamma^\lambda_{\mu\nu} - \Gamma^\alpha_{\lambda\nu}\Gamma^\lambda_{\mu\beta} \tag{3.22}$$

This tensor contains the information of the curvature of the manifold and the manifold is flat if and only if all the components of the Riemann tensor vanishes. This tensor has $4^4 = 256$ components but only twenty of these are independent because many of the components are related by identities. We state them here without the proofs, which are found in the references given at the start of this chapter

- $R_{\alpha\beta\mu\nu} = -R_{\beta\alpha\mu\nu} = R_{\beta\alpha\nu\mu} - R_{\mu\nu\beta\alpha}$

- $R_{\alpha\beta\mu\nu} + R_{\alpha\nu\beta\mu} + R_{\alpha\mu\nu\beta} = 0$
- $R_{\alpha\beta\mu\nu;\lambda} + R_{\alpha\beta\lambda\mu;\nu} + R_{\alpha\beta\nu\lambda;\mu} = 0$

where the last identity is known as the Bianchi identity and was an important tool for Einstein in helping him obtain a divergence free curvature part for his field equations. From the Riemann tensor we can now construct several other tensors by using the methods of symmetrization and contraction described in section 3.2, but we will focus on the tensors which will be important to us when deriving Einsteins field equations, namely the Ricci tensor $R_{\mu\nu}$ and the Ricci scalar R. The Ricci tensor is found by contracting the upper index with the second lower index

$$R_{\mu\nu} = R^{\lambda}{}_{\mu\lambda\nu} \tag{3.23}$$

The symmetry relations of the Riemann tensor ensures both that this is the only independent contraction, and that the Ricci tensor is symmetric $R_{\mu\nu} = R_{\nu\mu}$. Another contraction yields the Ricci scalar

$$R = R^{\lambda}{}_{\lambda} \tag{3.24}$$

With Curvature quantified in terms of Riemann tensor $R^{\alpha}{}_{\beta\mu\nu}$, Ricci tensor $R_{\mu\nu}$ and Ricci scalar R, we are ready to relate curvature to matter and obtain the relativistic analogue of Newtons law of gravity, namely Einstein field equations.

3.4 Einstein's Field Equations

Although Einstein himself used more heuristic arguments in deriving his field equations, the same equations are derivable by treating $g_{\mu\nu}$ as a tensor field and applying Hamilton's principle as described in the first section. To derive the field equations in this way we need as a starting point a Lagrangian density $\mathcal{L}$ which is an invariant Lorentz scalar. Since curvature is related to the second derivative of the metric a Lagrangian density suitable to describe gravity must at least involve the second derivative of the metric. Hilbert found that the simplest possible choice is the Ricci scalar R and proposed that the Lagrangian density governing gravity is given by $\mathcal{L}_G = \kappa R$. Using this choice of a Lagrangian density we can construct an invariant action integral S by integrating over the invariant volume $dV = \sqrt{-g}d^4x$, yielding the Einstein-Hilbert action

$$S_G = \int \kappa R\sqrt{-g}d^4x \tag{3.25}$$

where κ is some constant which will be determined later. We choose to include $\sqrt{-g}$ in the density giving the Lagrangian density $\mathcal{L}_G$ for the free metric field

$$\mathcal{L}_G = \kappa\sqrt{-g}R \tag{3.26}$$

Including the matter Lagrangian density $\mathcal{L}_m$ where $\sqrt{-g}$ is contained in $\mathcal{L}_m$, we obtain the full Lagrangian and action

$$\mathcal{L} = \mathcal{L}_G + \mathcal{L}_m$$
$$S = \int \mathcal{L}d^4x$$

In the field theory section we derived a set of Euler-Lagrange equations for fields. However there we assumed the Lagrangian to be a function of the field and its first derivatives and since the gravitational Lagrangian depends on the second derivative of the metric field, these equations will not apply here, and we are forced to apply the variational methods directly. For convenience we choose to vary the Lagrangian in terms of the inverse metric $g^{\mu\nu}$. Using differentiation by parts the variation in $\mathcal{L}_G$ gives

$$\delta\mathcal{L}_G = \kappa\left(\sqrt{-g}\delta R + R\delta\sqrt{-g}\right)$$

where we start by looking at the variation in the Ricci scalar

- Variation in the Ricci Scalar δR

  The variation of the Ricci scalar δR can again be split into two parts giving

  $$\delta R = \delta(R_{\mu\nu}g^{\mu\nu}) = R_{\mu\nu}\delta g^{\mu\nu} + \delta R_{\mu\nu}g^{\mu\nu}$$

  Now as always we want to factor out the dependence on the variation in the inverse metric $\delta g^{\mu\nu}$ so the first term in the variation δR is already on the desired form. The variation of the Ricci tensor $\delta R_{\mu\nu}$ gives

  $$\begin{aligned}\delta R_{\mu\nu} &= \delta\Big(\partial_\alpha\Gamma^\alpha_{\mu\nu} - \partial_\nu\Gamma^\alpha_{\mu\alpha} + \Gamma^\alpha_{\lambda\alpha}\Gamma^\lambda_{\mu\nu} - \Gamma^\alpha_{\lambda\nu}\Gamma^\lambda_{\mu\alpha}\Big)\\ &= \partial_\alpha\delta\Gamma^\alpha_{\mu\nu} - \partial_\nu\delta\Gamma^\alpha_{\mu\alpha} + \Gamma^\lambda_{\mu\nu}\delta\Gamma^\alpha_{\lambda\alpha} + \Gamma^\alpha_{\alpha\lambda}\delta\Gamma^\lambda_{\mu\nu} - \Gamma^\lambda_{\alpha\mu}\delta\Gamma^\alpha_{\lambda\nu} - \Gamma^\lambda_{\alpha\nu}\delta\Gamma^\alpha_{\mu\lambda}\end{aligned}$$

  Even though the Christoffel symbols themselves are not tensors, the variation $\delta\Gamma$ is. We see that the variation $\delta R_{\mu\nu}$ only includes terms $\partial\delta\Gamma$ and $\Gamma\delta\Gamma$ which suggest that it might be possible to simplify $\delta R_{\mu\nu}$ by expressing it in terms of the covariant derivative of the variation of the connection coefficients $\nabla\delta\Gamma$ given by

  $$\nabla_\beta\delta\Gamma^\alpha{}_{\mu\nu} = \partial_\beta\delta\Gamma^\alpha{}_{\mu\nu} + \Gamma^\alpha{}_{\lambda\nu}\delta\Gamma^\lambda{}_{\mu\beta} - \Gamma^\lambda{}_{\beta\nu}\delta\Gamma^\alpha{}_{\lambda\nu} - \Gamma^\lambda{}_{\beta\nu}\delta\Gamma^\alpha{}_{\mu\lambda}$$

  Using this expression together with the symmetry $\Gamma^\alpha{}_{\mu\nu} = \Gamma^\alpha{}_{\nu\mu}$ we find that $\delta R_{\mu\nu}$ can be expressed as

  $$\delta R_{\mu\nu} = \nabla_\alpha\delta\Gamma^\alpha{}_{\mu\nu} - \nabla_\nu\delta\Gamma^\alpha{}_{\mu\alpha}$$

  yielding the full variation δR

  $$\delta R = R_{\mu\nu}\delta g^{\mu\nu} + \nabla_\alpha\delta\Gamma^\alpha{}_{\mu\nu} - \nabla_\nu\delta\Gamma^\alpha{}_{\mu\alpha} \tag{3.27}$$

- Variation in the Tensor Density $\delta\sqrt{-g}$

  First of all we write the variation $\delta\sqrt{-g}$ in terms of the variation in g

  $$\delta\sqrt{-g} = -\frac{1}{2\sqrt{-g}}\delta g \quad , \quad \delta g = \frac{\partial g}{\partial g^{\mu\nu}}\delta g^{\mu\nu}$$

  Dropping the summation convention for the moment and writing out sums explicitly, the determinant of the metric written can be written as the sum over α of the components of the metric $g_{\alpha\beta}$ times the determinant of its respective cofactor matrix $|C_{\alpha\beta}|$, where β is completely arbitrary.

  $$g = \sum_\alpha g_{\alpha\beta}(-1)^{(\alpha+\beta)}|C_{\alpha\beta}|$$

  Since β is arbitrary we are free to choose $\beta = \mu$ and by applying rules for matrix differentiation from [9, section. 2.2] we find

  $$\begin{aligned}\frac{\partial g}{\partial g^{\mu\nu}} &= \sum_\alpha \frac{\partial g_{\alpha\mu}}{\partial g^{\mu\nu}}(-1)^{(\alpha+\mu)}|C_{\alpha\mu}| \quad , \quad \frac{\partial g_{\alpha\mu}}{\partial g^{\mu\nu}} = -g_{\alpha\mu}g_{\mu\nu}\\ &= -g_{\mu\nu}\sum_\alpha g_{\alpha\mu}(-1)^{(\alpha+\mu)}|C_{\alpha\mu}|\\ &= -g_{\mu\nu}g\end{aligned}$$

Plugging this result into the variation $\delta\sqrt{-g}$ we get the full variation

$$\delta\sqrt{-g} = \frac{g}{2\sqrt{-g}} g_{\mu\nu}\delta g^{\mu\nu} = -\frac{\sqrt{-g}}{2} g_{\mu\nu}\delta g^{\mu\nu} \tag{3.28}$$

We can now combine the variation in the two terms to get the full variation in the gravitational part $\delta\mathcal{L}_G$

$$\delta\mathcal{L}_G = \sqrt{-g}\kappa\left(R_{\mu\nu} - \frac{1}{2}Rg_{\mu\nu}\right)\delta g^{\mu\nu} + \sqrt{-g}\kappa\left(\nabla_\alpha \delta\Gamma^\alpha{}_{\mu\nu} - \nabla_\nu \delta\Gamma^\alpha{}_{\mu\alpha}\right)$$

Finally we plug this into the the variation of the action δS

$$\begin{aligned}\delta S = &\int d^4x\sqrt{-g}\left[\kappa\left(R_{\mu\nu} - \frac{1}{2}Rg_{\mu\nu}\right) + \frac{1}{\sqrt{-g}}\frac{\partial\mathcal{L}_m}{\partial g^{\mu\nu}}\right]\delta g^{\mu\nu} \\ &+ \int d^4x\sqrt{-g}\kappa\left(\nabla_\alpha \delta\Gamma^\alpha{}_{\mu\nu} - \nabla_\nu \delta\Gamma^\alpha{}_{\mu\alpha}\right) = 0\end{aligned}$$

The last term vanishes if Γ is kept fixed at the boundary[2]and the remaining part of the integral should vanish for arbitrary variations $\delta g^{\mu\nu}$ which finally gives us the equations of motion for the gravitational field

$$R_{\mu\nu} - \frac{1}{2}Rg_{\mu\nu} = -\frac{1}{\kappa\sqrt{-g}}\frac{\partial\mathcal{L}_m}{\partial g^{\mu\nu}}$$

We now define the stress energy tensor as the source of gravity given by the right hand side of the above equation. To make this definition reduce to the one from Noether's theorem, in situations where it works well, it is conventional to define it as

$$T_{\mu\nu} \equiv -\frac{2}{\sqrt{-g}}\frac{\partial\mathcal{L}_m}{\partial g^{\mu\nu}} \tag{3.29}$$

This tensor is manifestly divergence-free and symmetric, in contrast to the definition from Noethers theorem, which is divergence-free but not necessarily symmetric (see [7] for details). We thus have

$$R_{\mu\nu} - \frac{1}{2}Rg_{\mu\nu} = \frac{1}{2\kappa}T_{\mu\nu}$$

where the left-hand side is known as the Einstein tensor $E_{\mu\nu}$. The final step is to determine the constant κ , and this can be done by demanding equivalence between the Newtonian theory and the weak field limit of Einsteins theory. As a first step we rewrite Einsteins field equations by recognizing that contracting the two indices in the equations, yields the relation $R = -T/(2\kappa)$ so we can rewrite

$$R_{\mu\nu} = \frac{1}{2\kappa}\left(T_{\mu\nu} - \frac{1}{2}g_{\mu\nu}T\right)$$

In the Newtonian limit the pressure of matter is negligible compared to the energy density, $T_{00} >> T_{ii}$, which means that the trace $T \approx -T_{tt} \approx -\rho$ to lowest order, where ρ is the matter density. This means that the time component of the equations yields

$$R_{00} = \frac{1}{2\kappa}\rho\left(1 + \frac{1}{2}g_{00}\right)$$

In the curvature section we found that the perturbation to the time component of the weak field metric $g_{00} \approx \eta_{00} - 2\Phi \approx -1$, where the last approximation stems from the fact that $\Phi << 1$, and Φ will only come into play through the Ricci tensor which involves derivatives of Φ . We thus have

[2]Usually we only need to demand that the variations in the field vanishes, but since $\delta\Gamma$ contains derivatives of the metric we must also require these to vanish. This issue is dealt with in [7]

$$R_{00} \approx \frac{1}{4\kappa}\rho$$

Finally, using the fact that the Christoffel symbols Γ are small, since they vanish for flat spacetime, and $R_{\mu\nu}$ only contains Γ only in the form Γ^2, the time component of the Ricci scalar in the static weak field limit reduces to

$$R_{00} = R^i{}_{0i0} = \Gamma^i{}_{00,i} \quad , \quad \Gamma^i{}_{00} = -\frac{1}{2}g^{ii}g_{00,i} \approx -\frac{1}{2}g_{00,i} = \nabla\Phi$$
$$\Rightarrow \quad R_{00} = \nabla^2\Phi = \frac{1}{4\kappa}\rho$$

Remembering that Newtons law of gravitation is given by $\nabla^2\Phi = 4\pi G\rho$ we find $\kappa = 1/(16\pi G)$ yielding Einsteins field equations

$$R_{\mu\nu} - \frac{1}{2}Rg_{\mu\nu} = 8\pi G T_{\mu\nu} \tag{3.30}$$

These 16 equations are reduced to 10 by the symmetry in the indices $\mu\nu = \nu\mu$. Furthermore the fact that the equation is divergence free gives four more constraints giving 6 independent field equations. This reflects the fact that although the metric $g_{\mu\nu}$ contains ten degrees of freedom, four of these are related to our freedom of choice of coordinates. What we are left with is therefore a set of 6 coordinate independent, coupled second order differential equations which are also non-linear and they are therefore extremely difficult to solve. However, by assuming that spacetime has some additional symmetries it is possible to find explicit equations which can be solved numerically and sometimes also analytically (although the examples are sparse) and next we will look at two examples, namely the case of a static, spherically symmetric spacetime and the spatially homogeneous and isotropic spacetime.

3.5 Einstein's Equations in Symmetric Spacetimes

This section involves a lot of tedious tensor calculations and to make the section easier to read, the calculations are given in appendix A. We follow the same procedure in both the following cases: First we use the symmetries imposed to restrain the form of the metric, then we use the restrained metric to calculate the curvature tensors, and finally we plug them into Einsteins field equations together with a stress energy tensor, approximated as a perfect fluid, to obtain the equations governing the gravitational dynamics.

3.5.1 Static Spherically Symmetric Spacetime

The first case we are going to consider is that of a static spherically symmetric spacetime. Demanding that our spacetime is static and spherically symmetric reduces the six coupled second order Einstein equations to only two coupled first order equations, which are the relativistic equations of hydrostatic equilibrium known as the Tolman-Oppenheimer-Volkoff equation. This gives a good approximation to the spacetime inside and outside stars, where the rotation and spherical deviation of the star can be neglected and we will use these equations later in a slightly modified form when we discuss the effects of chameleon fields on neutron stars.

1. **Constraining the metric**

   For a static spherically symmetric spacetime it is possible to choose a set of coordinates where the metric takes the simple form

   $$ds^2 = -e^{2\alpha(r)}dt^2 + e^{2\beta(r)}dr^2 + r^2d\theta^2 + r^2\sin^2\theta d\phi^2 \tag{3.31}$$

   where $\alpha(r)$ and $\beta(r)$ are functions to be determined by the field equations, see [6, chap. 10]. The funny looking parametrization is chosen for convenience and we could just as well have written the metric in terms of $g_{tt}(r)$ and $g_{rr}(r)$. We are of course allowed to choose any coordinate system

we like for our calculations, but the point is that doing our calculations in this coordinate system dramatically simplifies the derivations of the equations and the actual physics will not depend on our choice.

2. **Einstein Tensor $E_{\mu\nu}$ and Stress Energy Tensor $T_{\mu\nu}$**

From the metric we can now calculate the Ricci tensor, and Ricci scalar R which can then be combined to form the Einstein tensor $E_{\mu\nu} = R_{\mu\nu} - \frac{1}{2}g_{\mu\nu}R$ corresponding to the left hand side of Einsteins field equations. The actual computations are found in appendix A. The non-vanishing components of the Einstein tensor $E_{\mu\nu}$ are

$$E_{tt} = \frac{1}{r^2}e^{2(\alpha-\beta)}\left[2r\partial_r\beta + e^{2\beta} - 1\right] \tag{3.32}$$

$$E_{rr} = \frac{1}{r^2}\left(2r\partial_r\beta - e^{2\beta} + 1\right) \tag{3.33}$$

$$E_{\theta\theta} = -r^2e^{-2\beta}\left[\partial_r^2\alpha + (\partial_r\alpha)^2 - \partial_r\alpha\partial_r\beta + \frac{1}{r}r\left(\partial_r\alpha - \partial_r\beta\right)\right] \tag{3.34}$$

$$E_{\phi\phi} = \sin^2\theta E_{\theta\theta} \tag{3.35}$$

where we notice that the angular components are related in the same way as the angular components of the metric. Next we turn to the right hand side of the field equations. Assuming matter to be in the form of a perfect fluid, the stress-energy tensor $T_{\mu\nu}$ takes the form given in equation 3.18, and since spacetime is static the same applies to the matter distribution, so in our choice of coordinates the four velocity of the fluid U^μ is given only in terms of the time component

$$\begin{aligned} & U^\mu U_\mu = g_{\mu\nu}U^\mu U^\nu = -e^{2\alpha}\left(U^0\right)^2 = -1 \\ \Rightarrow\ & U^\mu = \left(e^{-\alpha}, 0, 0, 0\right) \\ \Rightarrow\ & U_\mu = g_{\mu\nu}U^\nu = \left(-e^{\alpha}, 0, 0, 0\right) \end{aligned}$$

giving the stress energy tensor in terms of density and pressure

$$(T_{\mu\nu}) = \begin{pmatrix} e^{2\alpha}\rho & 0 & 0 & 0 \\ 0 & e^{2\beta}p & 0 & 0 \\ 0 & 0 & r^2p & 0 \\ 0 & 0 & 0 & r^2\sin^2\theta p \end{pmatrix} \tag{3.36}$$

Again we notice that the angular parts are related in the same way as in the metric, which means that the angular equations are the same.

3. **The TOV Equations**

Finally plugging into equation 3.30, we get the three equations

$$\boldsymbol{I} \quad \frac{1}{r^2}e^{-2\beta}\left[2r\partial_r\beta + e^{2\beta} - 1\right] = 8\pi G\rho \tag{3.37}$$

$$\boldsymbol{II} \quad \frac{1}{r^2}e^{-2\beta}\left[2r\partial_r\alpha - e^{2\beta} + 1\right] = 8\pi Gp \tag{3.38}$$

$$\boldsymbol{III} \quad e^{-2\beta}\left[\partial_r^2\alpha + (\partial_r\alpha)^2 - \partial_r\alpha\partial_r\beta + \frac{1}{r}\left(\partial_r\alpha - \partial_r\beta\right)\right] = 8\pi Gp \tag{3.39}$$

For convenience we express the equations in terms of a new function $m(r)$, instead of $\beta(r)$

$$
\begin{aligned}
e^{2\beta} &\equiv \left(1 - \frac{2Gm\left(r\right)}{r}\right)^{-1} \\
\Rightarrow \quad m\left(r\right) &= \frac{1}{2G}\left(r - re^{-2\beta}\right) \\
\partial_r m &= \frac{1}{2G}e^{-2\beta}\left(2r\partial_r\beta + e^{2\beta} - 1\right)
\end{aligned}
\tag{3.40}
$$

where $m(r)$ will be seen to be the mass contained inside a sphere of radius r. The first two equations written in terms of $m(r)$ become

$$
\begin{aligned}
\boldsymbol{I} \quad & \frac{1}{r^2}e^{-2\beta}\left(2r\partial_r\beta + e^{2\beta} - 1\right) = \frac{2G}{r^2}\partial_r m = 8\pi G\rho \\
\Rightarrow \quad & \partial_r m = 4\pi r^2\rho
\end{aligned}
\tag{3.41}
$$

$$
\begin{aligned}
\boldsymbol{II} \quad & \frac{1}{r^2}\left(1 - \frac{2Gm\left(r\right)}{r}\right)\left[2r\partial_r\alpha - \frac{1}{1 - \frac{2Gm(r)}{r}} + 1\right] = 8\pi Gp \\
\Rightarrow \quad & \partial_r\alpha = \frac{4\pi Gpr^3 + Gm\left(r\right)}{r\left[r - 2Gm\left(r\right)\right]}
\end{aligned}
\tag{3.42}
$$

Instead of using equation III it is more convenient to appeal to the conservation equation $\nabla_\mu T^{\mu\nu} = 0$ given by

$$
\left(T^{\mu\nu}\right) = \left(g^{\alpha\mu}g^{\beta\nu}T_{\alpha\beta}\right) = \begin{pmatrix} e^{-2\alpha}\rho & 0 & 0 & 0 \\ 0 & e^{-2\beta}p & 0 & 0 \\ 0 & 0 & r^{-2}p & 0 \\ 0 & 0 & 0 & r^{-2}\sin^{-2}\theta p \end{pmatrix}
$$

$$
\nabla_\mu T^{\mu\nu} = \partial_\mu T^{\mu\nu} + \Gamma^\mu{}_{\mu\lambda}T^{\lambda\nu} + \Gamma^\nu{}_{\mu\lambda}T^{\mu\lambda} = 0
$$

Using the fact that the stress energy tensor is diagonal we see that, without using Einstein's summation convention, the last equation can be written

$$
\sum_\mu \nabla_\mu T^{\mu\nu} = \partial_\nu T^{\nu\nu} + \sum_\mu \left(\Gamma^\mu{}_{\mu\nu}T^{\nu\nu} + \Gamma^\nu{}_{\mu\mu}T^{\mu\mu}\right) = 0
$$

where the only non-vanishing Christoffel symbols $\left(\Gamma^\mu{}_{\mu\nu},\ \Gamma^\nu{}_{\mu\mu}\right)$ and partial derivatives $\partial_\nu T^{\nu\nu}$ are

$$
\begin{aligned}
\Gamma^\mu{}_{\mu\nu} &\begin{cases} \neq 0 & , \quad \Gamma^\phi{}_{\phi\theta},\ \Gamma^t{}_{tr},\ \Gamma^r{}_{rr},\ \Gamma^\theta{}_{\theta r},\ \Gamma^\phi{}_{\phi r} \\ = 0 & , \quad \text{else} \end{cases} \\
\Gamma^\nu{}_{\mu\mu} &\begin{cases} \neq 0 & , \quad \Gamma^\theta{}_{\phi\phi},\ \Gamma^r{}_{tt},\ \Gamma^r{}_{rr},\ \Gamma^r{}_{\theta\theta},\ \Gamma^r{}_{\phi\phi} \\ = 0 & , \quad \text{else} \end{cases} \\
\partial_\nu T^{\nu\nu} &\begin{cases} \neq 0 & , \quad \partial_r T^{rr} \\ = 0 & , \quad \text{else} \end{cases}
\end{aligned}
$$

This means that both $\nabla_\mu T^{\mu t}$ and $\nabla_\mu T^{\mu\phi}$ vanish directly, while $\nabla_\mu T^{\mu\theta}$ vanishes by cancellation

$$\begin{aligned}\nabla_\mu T^{\mu\theta} &= \Gamma^\theta{}_{\phi\phi} T^{\phi\phi} + \Gamma^\phi{}_{\phi\theta} T^{\theta\theta} \\ &= -\frac{1}{r^2}\frac{\cos\theta}{\sin\theta} p + \frac{1}{r^2}\frac{\cos\theta}{\sin\theta} p = 0\end{aligned}$$

so that the only non-trivial conservation equation comes from $\nabla_\mu T^{\mu r}$

$$\begin{aligned}\nabla_\mu T^{\mu r} =& \partial_r T^{rr} + \sum_\mu \Gamma^\mu{}_{\mu r} T^{rr} + \Gamma^r{}_{\mu\mu} T^{\mu\mu} \\ &= \left(\partial_r p - 2p\partial_r\beta\right) e^{-2\beta} \\ &+ \left(\partial_r\alpha + \partial_r\beta + \frac{2}{r}\right) p e^{-2\beta} \\ &+ \left(p\partial_r\beta + \rho\partial_r\alpha - \frac{2}{r}p\right) e^{-2\beta} \\ &= \left(\partial_r p + p\partial_r\beta + \rho\partial_r\alpha\right) e^{-2\beta} = 0\end{aligned}$$

The conservation equation then gives us one extra constraint

$$\partial_r p = -\left(\rho + p\right)\partial_r\alpha$$

which we can now use to eliminate α from equation 3.42 to obtain

$$\partial_r p = -\frac{\left(\rho + p\right)\left[4\pi G p r^3 + G m\left(r\right)\right]}{r\left[r - 2G m\left(r\right)\right]}$$

This equation together with equation 3.41 are the equations describing the hydrostatic equilibrium of a star in general relativity, or simply the TOV(Tolman-Oppenheimer-Volkov) equations.

$$\frac{dp}{dr} = -\frac{\left(\rho + p\right)\left[4\pi G p r^3 + G m\left(r\right)\right]}{r\left[r - 2G m\left(r\right)\right]} \tag{3.43}$$

$$\frac{dm}{dr} = 4\pi r^2 \rho \tag{3.44}$$

From the second equation we see that integration over r yields

$$m(r) = \int_0^r 4\pi r^2 \rho dr$$

where the integrand is the the mass of an infinitesimal spherical shell of radius r and as such $m(r)$ can be viewed as the mass contained within a sphere of radius r. We also see that we have three variables $m(r), \rho(r)$ and $p(r)$ and to close the system of equations we need an additional equation telling us how the pressure is related to the density of the form of matter under consideration, known as an equation of state(EOS).

$$p = p(\rho) \tag{3.45}$$

To end this treatment of the static spherically symmetric spacetime, we find the metric in vacuum outside a spherically symmetric mass distribution of radius R, where we denote $m(R) \equiv M$. In vacuum, equation 3.37 and 3.38 both vanish, and by comparing the two we find

$$\frac{d\alpha}{dr} = -\frac{d\beta}{dr} \quad \Rightarrow \quad \alpha = -\beta + C$$

The constant C can be made to vanish by rescaling the time coordinate and using the definition 3.40 we can re-express α and β in terms of $m(r)$ which for $r > R$ is simply M. This gives us the metric components g_{tt} and g_{rr}

$$g_{rr} = e^{2\beta} \equiv \left(1 - \frac{2GM}{r}\right)^{-1} \quad \Rightarrow \quad g_{tt} = -e^{2\alpha} = -e^{-2\beta} = -\left(1 - \frac{2GM}{r}\right)$$

giving us the vacuum line element known as *the Schwarzschild line element*

$$ds^2 = -\left(1 - \frac{2GM}{r}\right)dt^2 + \left(1 - \frac{2GM}{r}\right)^{-1} dr^2 + r^2 d\theta^2 + r^2 \sin^2\theta d\phi^2 \tag{3.46}$$

It can actually be shown that this is the unique vacuum solution with spherical symmetry so this solution can be derived without assuming a static spacetime. The theorem was first discovered by the Norwegian physicist Jørg Tofte Jebsen and rediscovered two years later by the American mathematician George David Birkhoff so we will call it the *Jebsen-Birkhoff theorem*. The theorem implies that the spacetime outside collapsing or pulsating stars remains static as long as spherical symmetry still applies.

3.5.2 Homogeneous and Isotropic Spacetime

The second case we are going to consider is that of a spatially homogeneous and isotropic spacetime. By homogeneous we mean that the metric is the same everywhere in space and by isotropic we mean that the metric has no preferred spatial direction. When we look at the universe from earth, we see that on large scales it looks approximately the same in every direction and combining this with the Copernican principle, which states that there is nothing special about our place in the universe, we find that on large scales the universe is approximately homogeous and isotropic and as such should be described by a metric with these properties. Following the same recipe as above this will give us the equations governing the dynamics of the universe known as the Friedmann equations

1. **Constraining the metric**

   For a spatially homogeneous and isotropic spacetime it is possible to choose a set of coordinates, known as *comoving coordinates*, where the metric takes the simple form

   $$ds^2 = -dt^2 + a^2(t)\left[\frac{1}{1-kr^2}dr^2 + r^2 d\Omega^2\right] \quad , \quad d\Omega^2 = d\theta^2 + \sin^2\theta d\phi^2 \tag{3.47}$$

   known as the Robertson-Walker metric, see [6, chap. 12.2 for details]. $a(t)$ is known as the *scale factor* and gives us the relative size of space while the parameter k describes the curvature of the spatial part of the metric. When $k > 0$ space is said to be positively curved and the spatial geometry is spherical. If space is positively curved it is called *closed* because its spatial extension will be finite. If $k < 0$ space is said to have negative curvature and the spatial geometry is hyperbolic. As such the spatial extension can be infinite and space is said to be *open*. The limiting case where $k = 0$ has no curvature and space is flat, see figure 3.4.

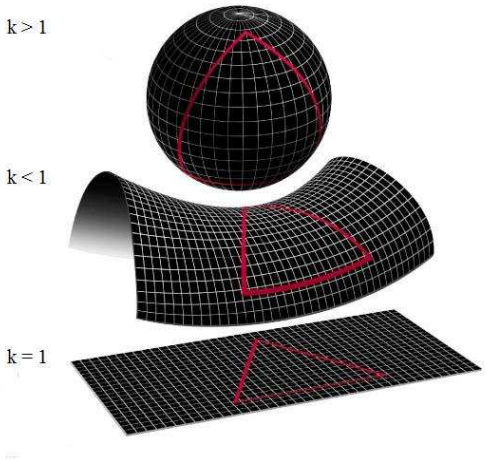

Figure 3.4: 2-D analogies to the curvature of av 3-D space given by k . The image is taken from Nasa's WMAP Universe cite `http://map.gsfc.nasa.gov/universe/uni_shape.html`

2. **Einstein Tensor $E_{\mu\nu}$ and Stress Energy Tensor $T_{\mu\nu}$**

   Again we calculate the Ricci tensor, and Ricci scalar R and form the Einstein tensor $E_{\mu\nu}$ yielding the non-vanishing components

$$E_{tt} = \frac{3}{a^2}\left[\dot{a}^2 + k\right] \tag{3.48}$$
$$E_{rr} = \left(1 - kr^2\right)^{-1}\left[-2a\ddot{a} - \dot{a}^2 - k\right] \tag{3.49}$$
$$E_{\theta\theta} = r^2\left[-2a\ddot{a} - \dot{a}^2 - k\right] \tag{3.50}$$
$$E_{\phi\phi} = \sin^2\theta E_{\theta\theta} \tag{3.51}$$

   The angular parts again are related as in the metric, an effect of our assumption of isotropy, but due to the homogeneity the same is true for the radial equation. The stress-energy tensor $T_{\mu\nu}$ can also in this case be approximated as a perfect fluid and in comoving coordinates the fluid is at rest so the four velocity U^μ is given only in terms of the time component

$$\begin{aligned} & U^\mu U_\mu = g_{\mu\nu}U^\mu U^\nu = -\left(U^0\right)^2 = -1 \\ \Rightarrow\ & U^\mu = (1,0,0,0) \\ \Rightarrow\ & U_\mu = g_{\mu\nu}U^\nu = (-1,0,0,0) \end{aligned}$$

   giving the stress energy tensor in terms of density and pressure

$$(T_{\mu\nu}) = \begin{pmatrix} \rho & 0 & 0 & 0 \\ 0 & \frac{a^2}{1-kr^2}p & 0 & 0 \\ 0 & 0 & a^2r^2p & 0 \\ 0 & 0 & 0 & a^2r^2\sin^2\theta p \end{pmatrix} \tag{3.52}$$

   In this case we see that the spatial equations reduce to only one.

3. **The Friedmann Equations**

   Plugging into equation 3.30, we get two equations

$$\begin{aligned} \boldsymbol{I} \quad & \frac{3}{a^2}\left[\dot{a}^2 + k\right] = 8\pi G\rho \\ \boldsymbol{II} \quad & -2a\ddot{a} - \dot{a}^2 - k = 8\pi G a^2 p \end{aligned}$$

which can be further simplified by using equation I to eliminate $\dot{a}$ and k in equation II. Doing this we get the conventional Friedmann equation forming the foundation of modern cosmology

$$\dot{a}^2 + k = \frac{8\pi G}{3}\rho a^2 \tag{3.53}$$

$$\frac{\ddot{a}}{a} = -\frac{4\pi G}{3}(\rho + 3p) \tag{3.54}$$

Again we see that we have two equations and three variables a, ρ and p, and to close the equations we need an equation of state. In cosmology we usually approximate matter by a simple equation of state

$$p(t) = \omega\rho(t) \tag{3.55}$$

where ω is a constant determined by the matter species under consideration. On cosmological scales baryonic matter is approximated as a pressureless fluid so $\omega_m = 0$, while standard thermodynamics tells us that the pressure of a photon gas is one third of its energy density, see [10], so radiation is described by $\omega_r = 1/3$. We can derive another useful relation from equations 3.53 and 3.54 by differentiating the first equation with respect to the time coordinate t and comparing it to the second one giving us the *adiabatic equation*

$$\dot{\rho} = -\frac{3\dot{a}}{a}(\rho + p) \tag{3.56}$$

Assuming that matter is given by the simple equation of state given above, the solution to this equation tells us that the density of a matter species i is related to the scale factor a by

$$\rho = \rho_0 \left(\frac{a_0}{a}\right)^{3(1+\omega)} \tag{3.57}$$

where ρ_0 and a_0 are initial values at some time t_0, which we usually take to be the density today and the scale factor today, often normalized $a_0 = 1$. It can be shown that if we have more than one matter component, then as long as the equation of state for any species i is independent of the other species, $p_i = p_i(\rho_i)$, then equation 3.56 holds for each species separately, see [11, chap. 1.10.4]. This means that we can write the total density of matter in the universe as a sum of the individual species.

$$\rho = \sum_i \rho_{i0} a^{-3(1+\omega_i)} \tag{3.58}$$

For later convenience we will end this section by rewriting equation 3.53 in terms of a new set of parameters. First we define the Hubble parameter $H(t)$

$$H(t) \equiv \frac{\dot{a}}{a} \tag{3.59}$$

and the critical density ρ_c, which is the density of a flat universe found by setting $k = 0$ in equation 3.53

$$H^2 \equiv \frac{8\pi G}{3}\rho_c(t) \quad \Rightarrow \quad \rho_c = \frac{3H^2}{8\pi G} \tag{3.60}$$

We can now re-express the densities in terms of a set of dimensionless density parameters Ω_i , where it is conventional to also express the curvature in terms of a parameter Ω_k .

$$\Omega_i \equiv \rho_i/\rho_c \quad , \quad \Omega_k \equiv -\frac{k}{(Ha)^2}$$

By again looking at equation 3.53 and 3.57 we see that the density parameters obey the relations

$$\sum_i \Omega_i = 1 \quad , \quad H^2\Omega_i = H_0^2\Omega_{i0}a^{-3(1+\omega_i)} \tag{3.61}$$

where we treat the curvature as a density with $\omega_k = -1/3$. Although we treat curvature as if it was an energy density here we can't do so in general, because it doesn't appear in the second Friedmann equation 3.54 as a proper density should. With these conventions the first Friedmann equation takes the form

$$H^2 = H_0^2 \sum_i \Omega_{i0}a^{-3(1+\omega_i)} \tag{3.62}$$

To see how our universe evolves according to the Friedmann equations, we have to know what kind of matter our universe is composed of and this is ultimately linked to observations. Almost all the phenomena of nature here on earth can be described by atoms (baryonic matter) and their electromagnetic interactions (radiation), so a natural assumption is to say that these forms of matter also dominate the evolution of our universe. Whether this is true or not is ultimately decided by observations, and it is possible that there exists forms of matter that are almost undetectable here on earth but plays important roles on cosmological scales. This will be the topic of the next part of this thesis.

3.6 A Numerical example: Neutron Star Equilibrium

We end this chapter with a numerical solution to the TOV equations derived in the last chapter. Since the goal of this thesis is to study neutron stars in the presence of a chameleon it is convenient to look at the ordinary case first. Realistic Neutron stars generally have large angular momenta and as such the matter distribution is neither static nor spherically symmetric so that the spherical symmetric approximation discussed in the last chapter isn't really valid. In this thesis we settle for a crude approximation where we look at the ideal case of a non-rotating spherically symmetric neutron star in which case the static spherically symmetric discussion applies. The first step in solving the equation set given by equations 3.43 and 3.44, is to close them by providing an appropriate equation of state

Equation of State for Matter

We assume the neutron star to be composed of a completely degenerate ideal neutron gas, for which analytic expressions for the pressure p and density ρ of the gas can be found by using quantum statistics [10, chap. 7]. Further one can show that in the relativistic and non-relativistic limit they can be related by a polytropic equation of state [12, chap. 3.9]

$$p = K\rho^\Gamma \tag{3.63}$$

where K is called the polytropic constant and Γ is called the polytropic index. We will restrict ourselves to looking at the non-relativistic case where the energy density $\rho \approx n_n m_n c^2$, where n_n is the neutron number density and m_n is the neutron rest mass. This is valid for densities $\rho << 5.4 \cdot 10^{35}\ J/m^3$ which covers all but the most extreme conditions. In this case the explicit expressions for Γ and K , see[13, chap. 2.3], are given by

$$\Gamma = \frac{5}{3}, \quad K = \frac{3^{2/3}\pi^{4/3}}{5}\frac{\hbar^2}{\left(m_n^8 c^{10}\right)^{1/3}} = 2,9837 \cdot 10^{-25}\ \left(J/m^3\right)^{-2/3} \tag{3.64}$$

Dimensionless TOV

To reduce the risk of numerical instability in the algorithm we will first write the equations on dimensionless form before solving the equations numerically. The dimensions will be put back in at the end of the computation. For convenience we restate the TOV equations given by equations 3.43 and 3.44

$$\textbf{I} \quad \frac{dp}{dr} = -\frac{(\rho + p)\left[4\pi G p r^3 + Gm\left(r\right)\right]}{r\left[r - 2Gm\left(r\right)\right]}$$

$$\textbf{II} \quad \frac{dm}{dr} = 4\pi r^2 \rho$$

To bring the equations on dimensionless form we follow [14] and start by re-expressing the dimensionfull quantities ρ, p, r and m in terms of the dimensionless quantities $\hat{\rho}, \hat{p}, \hat{r}$ and $\hat{m}$

$$\begin{array}{ll} \rho = P_d\hat{\rho} & p = P_d\hat{p} \\ m = M_d\hat{m} & r = R_d\hat{r} \end{array}$$

where the dimensions are put into the constants P_d, R_d and M_d . Inserting this into the TOV equations we find

$$\textbf{I} \quad \frac{d\hat{p}}{d\hat{r}} = -\frac{(\hat{\rho} + \hat{p})\left[4\pi G P_d R_d^3 \hat{p}\hat{r}^3 + GM_d\hat{m}\right]}{\hat{r}\left[R_d\hat{r} - 2GM_d\hat{m}\right]}$$

$$\textbf{II} \quad \frac{d\hat{m}}{d\hat{r}} = \frac{4\pi P_d R_d^3}{M_d}\hat{r}^2\hat{\rho}$$

We are free to choose the numerical values of the constants and we choose them in such a way that they disappear from the equations. This means that the numerical constants P_d, R_d and M_d fulfill the conditions

$$R_d = GM_d \quad , \quad \frac{4\pi P_d R_d^3}{M_d} = 1$$

giving

$$M_d = \frac{1}{\sqrt{4\pi G^3 P_d}} \quad , \quad R_d = \frac{1}{\sqrt{4\pi G P_d}} \tag{3.65}$$

where P_d can be chosen freely. A natural choice of magnitude for P_d is the central density ρ_c so that the dimensionless central density becomes $\hat{\rho}_c = 1$. With these dimensionfull quantities the equations become

$$\textbf{I} \quad \frac{d\hat{p}}{d\hat{r}} = -\frac{(\hat{\rho} + \hat{p})\left[\hat{p}\hat{r}^3 + \hat{m}\right]}{\hat{r}\left[\hat{r} - 2\hat{m}\right]} \tag{3.66}$$

$$\textbf{II} \quad \frac{d\hat{m}}{d\hat{r}} = \hat{r}^2\hat{\rho} \tag{3.67}$$

Finally we also need a dimensionless polytropic constant $\hat{K} = K/K_d$ where K_d is found to be

$$P_d\hat{p} = K\left(P_d\hat{\rho}\right)^{\Gamma}$$

$$\Rightarrow \qquad \hat{p} = \hat{K}\hat{\rho}^{\Gamma} \quad , \quad \hat{K} = \frac{K}{K_d} = P_d^{\Gamma-1}K \quad \Rightarrow \quad K_d = P_d^{1-\Gamma} \tag{3.68}$$

$$\Gamma = \frac{5}{3} \quad \Rightarrow \quad K_d = P_d^{-2/3} \tag{3.69}$$

Numerical Solutions

We now solve the dimensionless equations using Matlab's ODE suite. We do this for several different central densities ρ_c and calculate the the radius of the star R given by the radial coordinate where the pressure vanishes $p(R) = 0$, and the corresponding mass given by $M = m(R)$. We find that the star radius R decreases with increasing central density and that the total mass of the star M increases up to a maximum $M_{max} \approx 1\ M_\odot$ at central density $\rho_c \approx 5 \cdot 10^{35}\ J/m^3$ after which the total mass starts to decrease with increasing density. Figure 3.5 shows the total mass M and radius R as functions of central density ρ_c together with the mass radius relation $M(R)$.

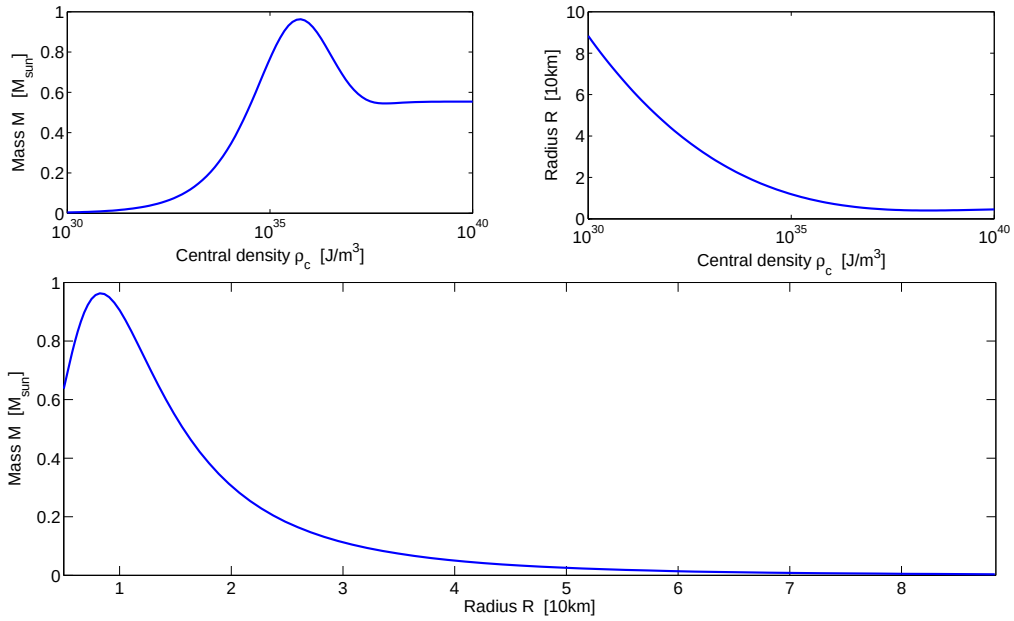

Figure 3.5: The two figures on the top shows the mass M and radius R of a neutron star as a function of central density ρ_c while the figure on the bottom shows the mass radius relationship $M(R)$, where the region to the left of the peak corresponds to unstable solutions. We see that the maximum mass neutron star corresponds to a star with central density $\rho_c \approx 5.5 \cdot 10^{35}\ J/m^3,\ R \approx 8\ km$ and $M \approx 1\ M_\odot$

When the mass of the star exceeds M_{max} , the star becomes unstable as there are no static solutions of larger mass then M_{max} . This maximum mass limit is known as the TOV-limit and more sophisticated models places the true limit somewhere between $1.5\ M_\odot$ and $3.0\ M_\odot$. For each central density we also get the radial profile of the density and pressure $\rho(r)$ and $p(r)$ together with the mass profile $m(r)$. These are plotted in figure 3.6

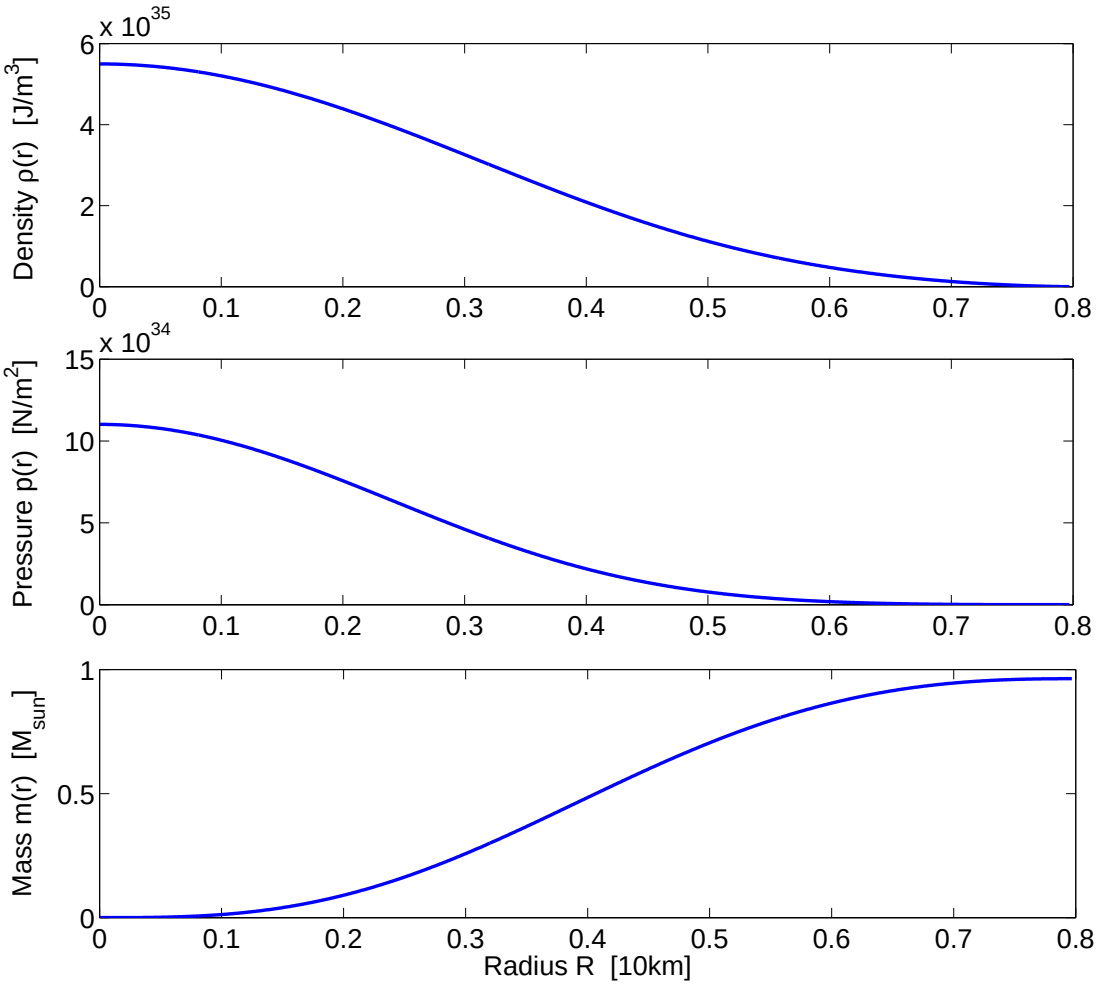

Figure 3.6: Plots of the density, pressure and mass profiles $\rho(r), p(r)$ and $m(r)$ for a star with central density $\rho_c = 5.5 \cdot 10^{35}\ J/m^3$

It should be noted that the central density of the maximum mass neutron star is actually too large for the non-relativistic approximation, which requires $\rho_c << 5.4 \cdot 10^{35}\ J/m^3$, to be valid, but at the level of accuracy we are dealing with here this is not important. Both the mass-radius relation and the profiles seems qualitatively correct and gives us a basis for considering the effects of the chameleon behavior in, and effects on, neutron stars. Our approach when solving the chameleon case will be to generalize the TOV equations and redo the analysis.

Part II

Dark Energy

Chapter 4

The Accelerating Universe

This chapter is based mainly on [11], [4], [15] and [16]. We ended the preliminary part of this thesis by stating that the matter content of the universe is ultimately determined by observations, and at the end of the last century observations revealed some surprising new insights on the subject. Independently, two teams of astronomers going by the names *High-Z Supernova Search Team* and *Supernova Cosmology Project*, looked at the light from distant supernovae and found that the light was too dim to be explained by a universe containing only baryonic matter and radiation. For the observations to be consistent with a universe described by the Friedmann equations 3.53 and 3.54, about 70 % of all the matter in the universe would have to be in the form of some unknown *dark energy* causing the universe to expand at an accelerating rate and ultimately explaining the supernova data. In this chapter we will give a brief review of the observational evidence for dark energy with emphasis on the supernova study.

4.1 Redshifts, Distances and Standard Candles

The universe looks approximately the same in all directions as seen from earth when we look out to distances larger than 300 million light years, so on large scales we can approximate the universe to be isotropic at least from our point of view. Assuming there is nothing special about our place implies that the universe should be isotropic everywhere and therefore homogeneous. This means that the Robertson-Walker metric given by equation 3.47 should be a good approximation to the geometry of the universe on large scales. The evolution of the size of our universe is then given by the scalefactor $a(t)$, which evolves according to equations 3.53 and 3.54. The solutions to these equations depend on the matter content and spatial curvature of the universe, so if we can measure the value of the curvature parameter k and how the scalefactor $a(t)$ evolves, we can determine the matter content of the universe. Since the main source of information about our universe is light, we need to know how light is affected by the shape and evolution of our universe as it travels towards us.

Cosmological redshift

The wavelength of light is proportional to the scale factor so we can infer the evolution of the scalefactor by looking at how light is *redshifted*. The redshift is usually given by the parameter z given by

$$z = \frac{\lambda_s}{\lambda_o} - 1 \tag{4.1}$$

where λ_s and λ_o are the emitted and the observed wavelength respectively. The relation between the scale factor $a(t)$ and the redshift z can be seen from equation 3.57 which tells us that the density of non-relativistic matter is proportional to inverse cube of the scale factor, $\rho \propto a^{-3}$, while for relativistic matter the relation is $\rho \propto a^{-4}$. The physical reason for these relations can be found from the relativistic expression for energy $\epsilon = \sqrt{m^2 + p^2}$. If we consider matter to consist of a set of N particles with average energy ϵ and momentum p, the energy density is given by $\rho = \epsilon \cdot N/V$. For non-relativistic

particles we have $\epsilon \approx m$ which is not affected by a change in a, so the change in energy density comes from the volume $V \propto a^3$ yielding $\rho \propto a^{-3}$. For relativistic particles the rest energy can be neglected so $\epsilon \approx p$, where the momentum of the particle is proportional to the wavelength of the particle, $p \propto 1/\lambda \propto 1/a$ yielding $\rho \propto 1/(V \cdot \lambda) \propto a^{-4}$. Since the wavelength of particles are proportional to the scale factor, a universe which evolves in time will give rise to a shift in the wavelength similar to the Doppler shift of light from moving sources. This is called the *cosmological redshift* and is given by

$$z \equiv \frac{\lambda_o}{\lambda_s} - 1 = \frac{a(t_o)}{a(t_s)} - 1$$

where λ_s and t_s denotes the emitted wavelength and time of emission. As mentioned earlier, the scale factor is usually normalized so that it is unity today, $a_{\text{today}} \equiv 1$, and since we are usually the observers, it is common to simply write

$$z = \frac{1}{a(t)} - 1 \quad \Rightarrow \quad a = (z+1)^{-1} \tag{4.2}$$

where it is now implicit that z is the redshift observed by us.

Luminosity Distance

The evolution and structure of the universe can be explored by measuring distances. Usually we think of the distance between two objects as the spatial separation at a given time, but measuring a distance will inevitably take time and if space itself is allowed to change, this notion of distance is not actually measurable. It is therefore convenient to use different definitions of distances directly relatable to both observable quantities and the metric, which is restated here for convenience

$$ds^2 = -dt^2 + a^2\left[\frac{1}{1-kr^2}dr^2 + r^2 d\Omega^2\right] \quad , \quad d\Omega^2 = d\theta^2 + \sin^2\theta d\phi^2$$

There are several ways of doing this, and the different definitions are not necessarily equivalent. This is not a big concern since what we really want is to determine the curvature parameter k and the scale factor a, which again gives us information about the matter content of the universe. We restrict ourselves to looking at the *luminosity distance* d_L, which is a convenient definition when we measure the flux of light received from a light source. This distance measure is based on how the intrinsic luminosity L of a spherically symmetric object is related to the flux F observed by an observer at a distance, d_L from the source. In flat space the flux F is related to the luminosity L by

$$F = \frac{L}{4\pi d_L^2} \quad \Rightarrow \quad d_L = \sqrt{\frac{L}{4\pi F}}$$

where we take this to be the definition of the luminosity distance d_L. In euclidean geometry the flux from a light source at a distance d is given by $F = L/A$ where A is the surface area of a sphere centered at the source with radius d. In a universe described by the RW-metric the wavelength λ of photons will be changed on the way from the source to the surface, and the frequency $\nu = 1/\lambda$ of photons passing through the surface per unit time, will also be altered, so the flux is scaled by a factor

$$F \;\rightarrow\; \left(\frac{\lambda_s}{\lambda_o}\right)\cdot\left(\frac{\nu_o}{\nu_s}\right)F = \frac{a^2(t_s)}{a^2(t_o)}F = a^2(t_s)\frac{L}{A}$$

where we consider ourselves to be the observers so that $a_o = 1$. The area A of the sphere is found by keeping t and r fixed and integrating over the solid angle $d\Omega$ given the surface area $A = 4\pi a^2(t_o)r^2 = 4\pi r^2$. Putting all this together yields

$$F = \frac{a^2(t_s)L}{A} = \frac{a^2(t_s)L}{4\pi r^2} \quad \Rightarrow \quad d_L = \frac{r}{a(t_s)}$$

and by replacing the scale factor a with the redshift z given by equation 4.2 we get the luminosity distance

$$d_L = (1+z)r$$

Finally we can replace the coordinate distance r by looking at the path taken by the light we receive today. As we mentioned in chapter 3.1, light rays follow lightlike paths given by $ds^2 = 0$ which means that a light ray received by us today at $t = t_0$, follows a path given by

$$-dt^2 + a^2\frac{dr^2}{1-kr^2} = 0 \quad \Rightarrow \quad -\int_r^0 \frac{dr}{\sqrt{1-kr^2}} = \int_t^{t_0}\frac{dt}{a(t)}$$

$$-\int_r^0 \frac{dr}{\sqrt{1-kr^2}} = S_k^{-1}(r) \quad , \quad S_k^{-1}(x) = \begin{cases} \sin^{-1}(\sqrt{|k|}x)/\sqrt{|k|} & , \quad k>0 \\ x & , \quad k=0 \\ \sinh^{-1}(\sqrt{|k|}x)/\sqrt{|k|} & , \quad k<0 \end{cases}$$

which yields the comoving radial coordinate r

$$r = S_k\left(\int_t^{t_0}\frac{dt}{a(t)}\right) \tag{4.3}$$

The integral over the scale factor can be re-expressed in terms of the redshift z given by equation 4.2 and the Hubble parameter H given by equation 3.59

$$\int_t^{t_0}\frac{dt}{a(t)} = \int_0^z \frac{dz}{H(z)}$$

Finally we can write out the explicit z-dependence of $H(z)$ by expressing equation 3.62 in terms of the redshift. We thus find the explicit expression for the luminosity distance in terms of z

$$d_L(z) = (1+z)S_k\left(\int_0^z \frac{dz}{H_0\sqrt{\sum_i \Omega_{i0}(z+1)^{3(1+\omega_i)}}}\right) \tag{4.4}$$

To actually measure the luminosity distance d_L , we have to know the intrinsic luminosity L , and objects for which the intrinsic luminosity is believed to be known, are called *standard candles*.

Standard Candles

Standard candles are as mentioned, objects for which the absolute luminosity is known. Comparing the intrinsic luminosity L with the observed flux we observed, the distance to the object can be inferred. In astronomy this is usually stated in terms of the *absolute magnitude* M and the *apparent magnitude* m which are related to the Luminosity and flux as described by [16]

$$M = -\frac{5}{2}\log_{10}\left[\frac{L}{L_0}\right] \quad , \quad L_0 = 3.02\cdot 10^{42} J/s \tag{4.5}$$

$$m = -\frac{5}{2}\log_{10}\left[\frac{F}{F_0}\right] \quad , \quad F_0 = 2.52\cdot 10^{2} J/s \tag{4.6}$$

Using this notation we can write $m - M$ called the *distance modulus* in terms of the luminosity distance d_L

$$m - M = 5\log_{10}\left[\frac{d_L}{pc}\right] - 5 \quad , \quad pc = 30.857\cdot 10^{15} m \tag{4.7}$$

By numerically integrating equation 4.4 we can find the theoretical predictions for the distance modulus as a function of z using equation 4.7.

Figure 4.1 shows the results for three different models, where $\Omega_{\Lambda 0}$ is the density parameter for a component with equation of state $\rho = -p$ (the choice of models and density parameters will become clear later)

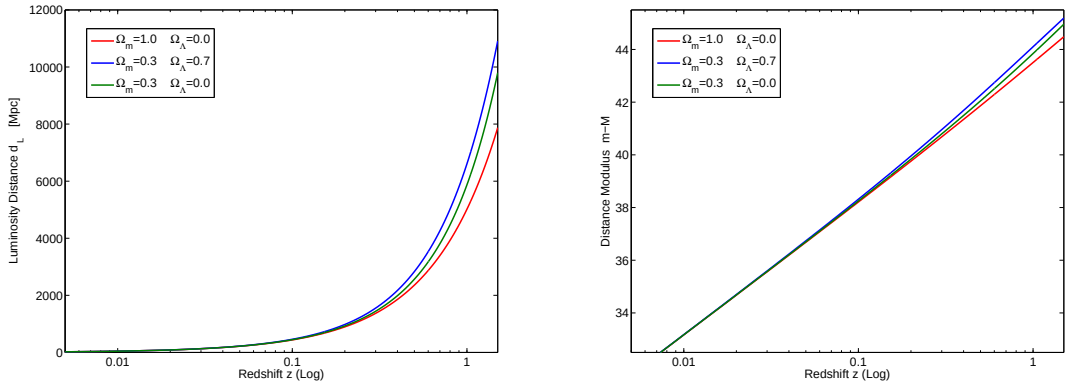

Figure 4.1: Theoretical Predictions for the distance modulus $m - M$ and luminosity distance d_L for three different values of the curvature and density parameters. The blue line corresponds to a flat model with ordinary matter Ω_m and a component with negative pressure Ω_Λ , the red line to a negatively curved universe with matter and the green line to a flat universe containing only matter.

The results can be explained by looking at equation 4.4. The matter component Ω_m is assumed to have no pressure so the equation of state parameter $\omega_m = 0$, giving a matter term that goes as $(z+1)^3$. Similarly curvature has $\omega_k = -1/3$ giving $(z+1)^2$ and the negative pressure component has $\omega_\Lambda = -1$ yielding a constant term. This means that since the integrand depends inversely on the size of these parameters, both the curvature and the negative pressure component grow slower than the matter component as z increases and helps making the integrand larger compared to what it would have been with only matter. This means that the radial comoving coordinate r given by the integral, and consequently the luminosity distance d_L is larger when curvature or energy with negative pressure exists. In addition, for negative curvature (positive Ω_k) the function $S_k(x) = \sinh(\sqrt{|k|}x)/\sqrt{|k|}$ comes into play making d_L larger. A perhaps more physical explanation goes like this: The effect of negative pressure can be explained by looking at Friedmann equation 3.54 that tells us that if $\rho = -p$ then $\ddot{a} > 0$, meaning the universe today is accelerating. If the universe is accelerating today it means it must have been expanding at a slower rate at earlier times, and in effect light rays must have used a longer time to obtain a given redshift z . If light has traveled longer in time it has also traveled longer in space and from regular euclidean geometry the flux F becomes smaller yielding a larger luminosity distance d_L . In the case of curvature there is no extra contribution causing the expansion to accelerate, but the matter density is still smaller then in a universe with $\Omega_m = 1$ and as such the cosmic deceleration caused by matter is smaller. By a similar argument as for cosmic acceleration this leads to the conclusion that d_L would be larger. In addition negative curvature makes spatial areas larger than in a flat euclidean universe and as such the flux F would be smaller in a negatively curved universe, leading to an even larger inferred luminosity distance (the $\sinh$ effect). Another thing we see is that even though the choice of density parameters are very different, the effects on the luminosity distance becomes visible only at large redshifts $z > 0.1$. As a consequence we need very bright standard candles in order to detect the highly redshifted and dispersed photons and as of today the best sources are a type of stellar explosion known as *type Ia supernovae*

Type Ia Supernovae

Type Ia supernovae are believed to occur when white dwarf stars in binary systems accrete to much mass from its partner for the pressure to sustain the gravitational pull. When this happens, the star becomes unstable causing a thermonuclear explosion so luminous that it can be seen thousands of megaparsecs

away. In terms of absolute magnitudes the supernova typically has $M \sim -19.5$, which is comparable to the brightness of an entire galaxy. The mass limit where this occurs, $M \approx 1.4\ M_\odot$, is known as the *Chandrasekhar limit* and is nearly universal, so the luminosity of the explosion depends little on when in the history of the universe it happens, or what the original mass of the white dwarf is. There is still a significant amount of variation in peak luminosity and these variations are believed to be due to differences in the composition of the white dwarf atmospheres. Fortunately these differences are very closely correlated with the differences in the shape of their light curves: Dimmer supernovas decline more rapidly after peak luminosity then brighter ones. When this correlation is taken into account, the luminosity uncertainty inferred from data has an uncertainty of about 15%, compared to an uncertainty of about 40% whithout it, and this is sufficient to distinguish between cosmological models. A problem with using Supernovae as standard candles is that they are extremely rare occurences. In a Milky way sized galaxy there are typically a few supernovae per century, and as such it is hard to find enough supernova occurences to get a statistically representative set of data.

4.2 Our Universe

We are now ready to see what observations tell us about what our universe looks like. At the time when Einstein published his theory of general relativity in 1916 he believed the universe to be static, which at the time was consistent with the observational data available. However Einsteins own field equations in its original form given by equation 3.30 seemed to indicate something else, as can be seen by looking at the first Friedmann equation

$$\frac{\ddot{a}}{a} = -\frac{4\pi G}{3}(\rho + 3p)$$

We see that since the scale factor a is always positive and "ordinary" matter like atoms and radiation has positive density and pressure, a FRW universe consisting only of ordinary matter cannot be static but must either expand at a decelerating rate or contract at an accelerating rate. To solve this problem Einstein introduced a cosmological constant Λ in his field equations

$$R_{\mu\nu} - \frac{1}{2}Rg_{\mu\nu} = 8\pi G\left(T_{\mu\nu} - \frac{\Lambda}{8\pi G}g_{\mu\nu}\right) \tag{4.8}$$

which is the same as introducing a new energy component with negative pressure, $p = -\rho$. By fine tuning Λ Einstein was able to counter balance the attractive gravitational pull of ordinary matter to create a static, but unstable universe model. In 1929 the American astronomer Edwin Hubble, building on earlier results by Slipher, discovered that on average the light from galaxies seemed to be redshifted by a factor z proportional to their distance from us. More precisely Hubble, and Slipher before him, looked at standard candles known as Cepheid variables, see [16, chap. 1.3] to determine the distances to galaxies out to about $2\ Mpc$, and Hubble found there was a rough relation between the observed redshift z and the measured distance d. This relation is known as Hubble's law

$$z = \frac{\lambda_s}{\lambda_o} - 1 = H_0 d \tag{4.9}$$

where λ_s and λ_o are the emitted and the observed wavelength respectively and the proportionality factor H_0 is the Hubble parameter today as can be seen from the luminosity distance: The redshifts Hubble observed where small, $z \lesssim 0.02$ so $(1+z) \approx 1$, which means we can approximate the luminosity distance given by equation 4.4 as

$$d_L \approx S_k\left(\int_0^z \frac{dz}{H_0\sqrt{\sum_i \Omega_{i0}}}\right) = S_k\left(\int_0^z \frac{dz}{H_0}\right) = S_k\left(\frac{z}{H_0}\right)$$

If the spatial curvature of the universe is also negligible for small redshifts, we get Hubble's law

$$d_L \approx \frac{z}{H_0} \quad \Rightarrow \quad z \approx H_0 d_L$$

Hubble found H_0 to be positive indicating that the universe is not static but expanding. When Einstein heard of these results he was forced to give up the idea of a static universe and removed the cosmological constant from his equations, calling it his biggest blunder. Current observational data suggests that the value of the Hubble parameter today is approximately equal to $H_0 \approx 70 \pm 10\ km/s/Mpc$.

The expansion of the universe tells us that the universe must have been smaller at earlier times and as we go further and further back it becomes denser and denser until we finally end up at a singularity, where the scale factor a goes to zero and the density ρ becomes infinite, and this singularity is called the *Big Bang*. By using thermodynamics the physical consequences of the Big Bang hypothesis was explored, and among the great achievements was the prediction of the *cosmic microwave radiation* (CMB) around 1950, a background radiation from when protons, neutrons and electrons came together to form neutral atoms. The CMB was then detected in 1965 and the new found CMB made the Big Bang model the standard model of cosmology and gave a wealth of new data about the universe. In particular the temperature of the CMB $T_{CMB} \approx 2.7\ K$ suggested that the radiation density was small, $\Omega_r \approx 10^{-4}$. Today it is one of the most important sources of information about our universe, see [17] for more details.

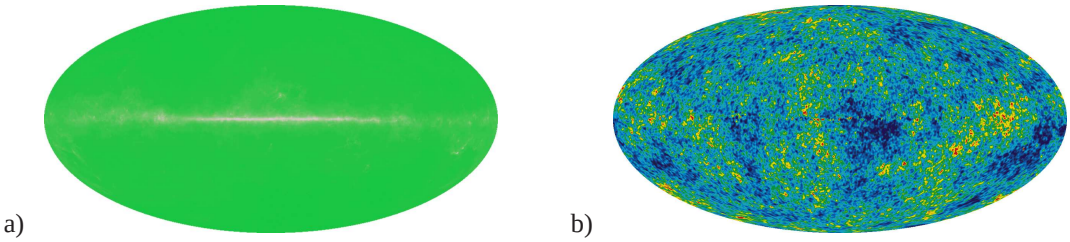

a) b)

Figure 4.2: a) A map of the cosmic microwave background as seen by Penzias and Wilson, showing no structure. b) Current more detailed CMB map of 5 year data from WMAP which clearly shows structure, and this structure contains large amounts of information about our universe. Taken from http://map.gsfc.nasa.gov/

During the 70's it became clear that ordinary baryonic matter was not enough to describe the gravitational effects on galaxies, and the idea that most of the matter in our universe is in the form of a non-relativistic *cold dark matter* which only interacts gravitationally, grew hold. In the 80's the theory of *inflation*, which introduces a short period of exponential expansion early in the evolution, was proposed and offered explanations to many cosmological problems, see [11]. The original inflationary scenario given by Guth in 1981 predicted a flat universe, and observations indicated that the density of non-relativistic matter (both dark and baryonic) was small, $\Omega_m \sim 0.1$, although the uncertainties were large enough for a flat universe scenario with $\Omega_m \approx 1$ to be viable. Even though the low matter content estimates were very uncertain, it was enough to make some physicists suggest that the contradiction between the predicted flatness from inflation and the low matter content was due to a component similar to Einsteins cosmological constant Λ , with $\rho = -p$.

As the 90's emerged, the observational evidence for a universe with a small matter component Ω_{m0} grew. In particular the discovery of anisotropies in the CMB was consistent with inflation, suggesting that the universe is close to spatially flat, and observations of the large scale structure of the universe [18] seemed to prefer a model containing a nonzero Λ as well as matter, called the ΛCDM *model* , rather then a model containing only non-relativistic matter. Although these data were consistent with the ΛCDM model, it was not sufficient to rule out other models, and the most serious contenders were an inflationary scheme known as *Open inflation* [19] and the *CHDM model* with a low Hubble constant $H_0 \sim 50\ km/s/Mpc$ and relativistic *hot dark matter* [20], non of which causes accelerated expansion. The evidence for cosmic acceleration, and as such a non zero $\Omega_{\Lambda 0}$, where made by looking at supernovae redshifts. To probe the matter content of the universe using redshift surveys we need to look out to sufficiently large redshifts, $z \gtrsim 0.3$, to detect the effects of curvature and the time evolution of H , see [21]. At such large distances type Ia supernovae are the best means to measure distance, but due to their rareness they are hard to

detect and it was not until the 1990's that the technique of using type Ia supernovae as standard candles was good enough to give any reliable results. With the new techniques the *High-Z Supernova Team* and the *Supernova Cosmology Project* began surveying the sky at large redshifts and in 1998, the Supernova Cosmology Project published a study consisting of 42 type Ia supernovae with z ranging from 0.18 to 0.83 together with a set of closer supernovae with z smaller than 0.1 from another supernova survey. The data ruled out $\Omega_{\Lambda 0} = 0$ with a confidence level of $99\,\%$, and for a flat universe the estimated values of the density parameters Ω_{m0} and $\Omega_{\Lambda 0}$ were

$$\Omega_{m0} \approx 0.28 \quad , \quad \Omega_{\Lambda 0} \approx 0.72$$

Soon after, the High-z Supernova Search Team published their study which included 16 type Ia supernovae of redshifts between $z = 0.16$ and $z = 0.97$ including 2 from the Supernova Cosmology Project. They concluded that $\Omega_\Lambda > 0$ with a confidence level of $99.7\,\%$ and the same estimates for Ω_{m0} and $\Omega_{\Lambda 0}$. The original data in figure 4.2a and the combined constraints on Ω_{m0} and $\Omega_{\Lambda 0}$ including later results from the CMB surveys BOOMERANG and MAXIMA1 [22] are given in figure 4.2b.

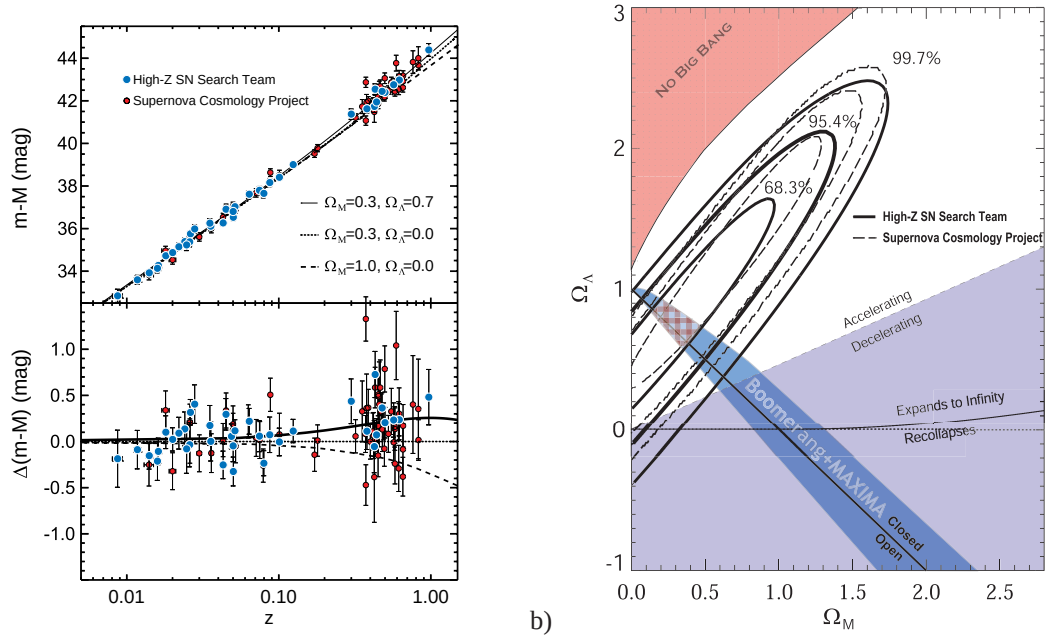

a) b)

Figure 4.3: a) The combined data of the Supernova Cosmology Project and the High-Z Supernova Team together with the theoretical predictions from three different models. The observations seem to prefer a universe with 30% matter and 70% dark energy. b) Constraints from the supernova search and from the CMB surveys BOOMERANG and MAXIMA1. Taken from the High-z Supernova Search Team homepage `http://www.cfa.harvard.edu/supernova//HighZ.html`

From the end of the 90's and up to the present these results have been reinforced and refined by additional supernova observations and other observational probes, and the most recent constraints on Ω_{m0} and $\Omega_{\Lambda 0}$ are shown in figure 4.4a. The data does not require the extra component $\Omega_{\Lambda 0}$ to be due to a cosmological constant Λ, but rather suggests the presence of a component with an equation of state $\rho \approx -p$ or in terms of the equation of state parameter given by equation 3.55, $\omega_{\Lambda 0} \approx -1$. The more general term used to describe such an energy component is *dark energy*, reflecting the fact that we don't really know what it is. Assuming a flat universe, the current data prefer a value of $\omega_{\Lambda 0} = -0.94 \pm 0.1$, see figure 4.4b.

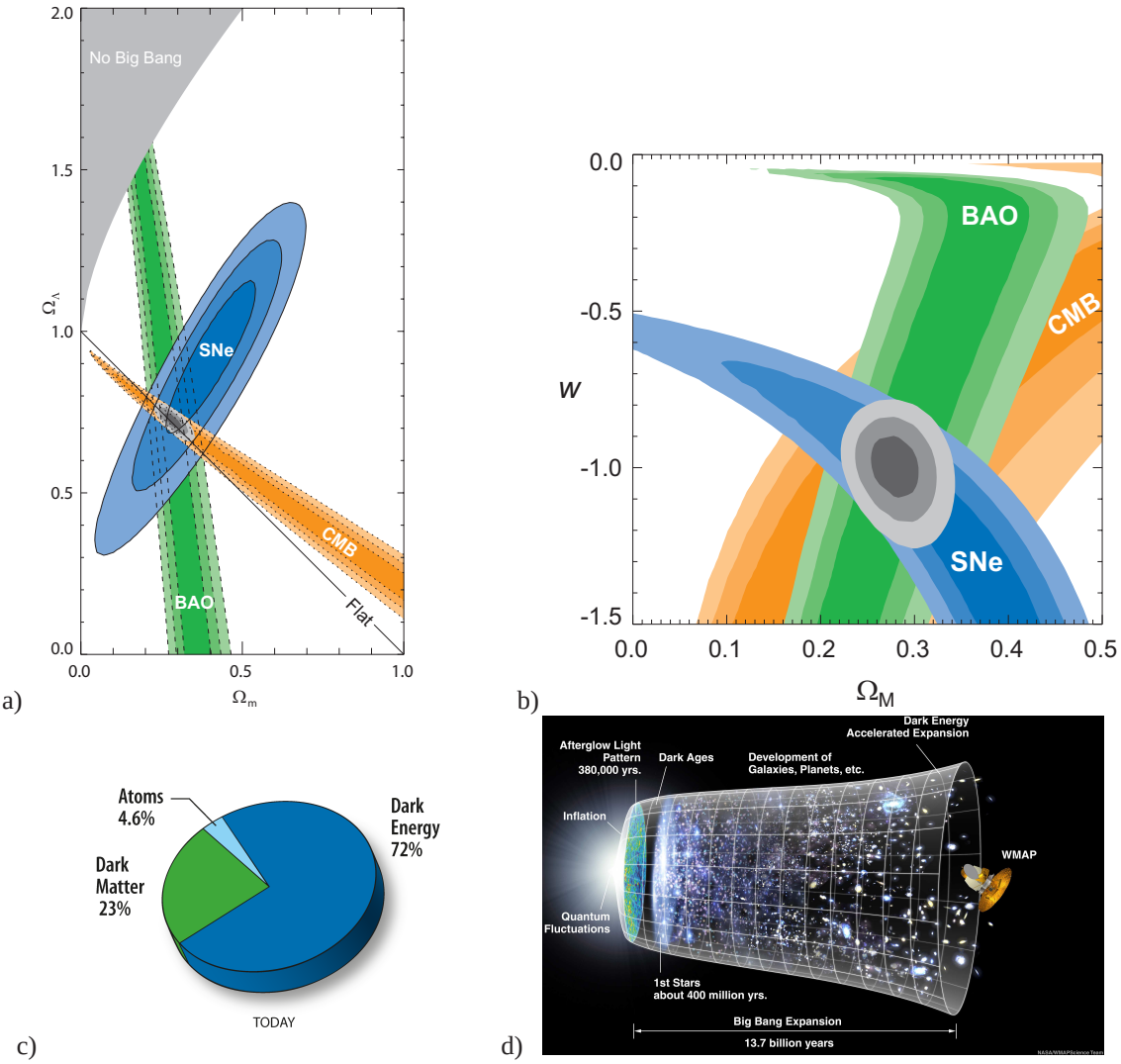

Figure 4.4: a) Most recent constraints on the parameters Ω_{m0} and $\Omega_{\Lambda 0}$ from supernovae, CMB and large scale structure (BAO). b) Constraints on Ω_{m0} and the equation of state parameter $\omega_{\Lambda 0}$ assuming $\Omega_{k0} = 0$. From Kowalski et al. [23]. c) Approximate composition of the universe, where the small radiation component has been neglected. d) An intuitive way of representing the evolution of the size of the universe suggested by theory and experiments. Taken from http://map.gsfc.nasa.gov/

This dark energy, that makes the expansion of the universe accelerate and tries to tear it apart, will be the topic of the next chapter.

Chapter 5

Dark Energy Models

This chapter is mainly based on [24], [16], [15] and [25]. Although most physicists agree that the cosmic acceleration is real, what causes it is still unclear. The simplest explanation is that it is caused by a cosmological constant Λ, usually interpreted as the energy density of vacuum, but there is a plethora of other models, all having both pros and cons. These dark energy models can be roughly classified as shown in figure 5.1

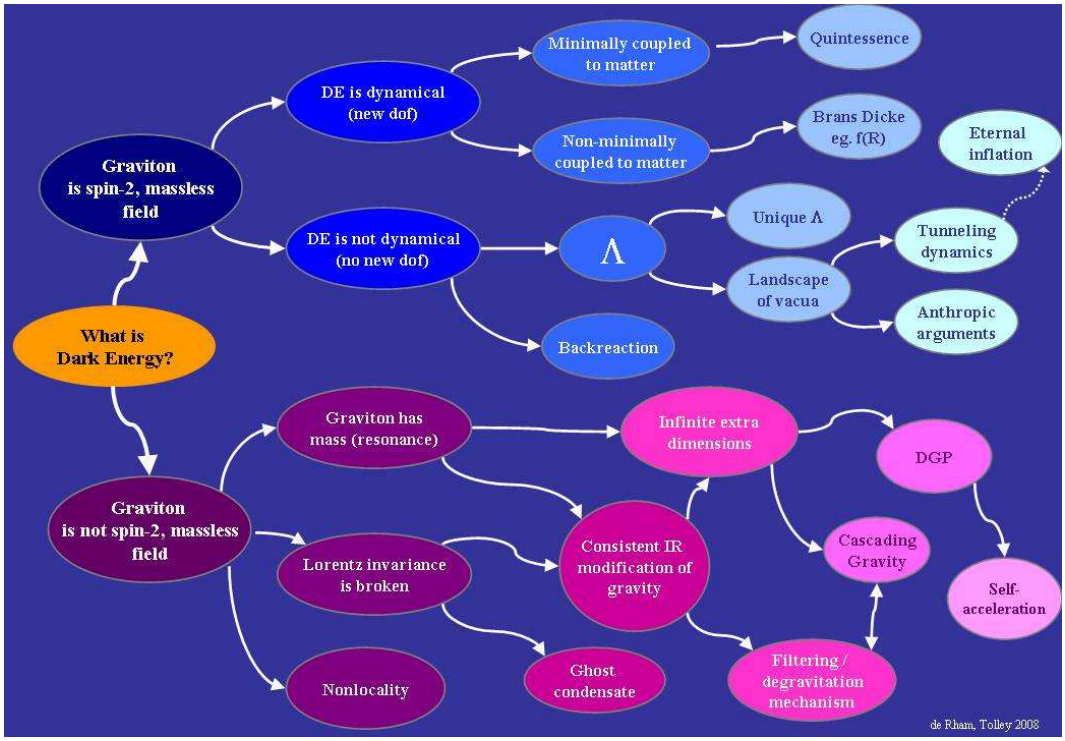

Figure 5.1: A bubble diagram classifying dark energy models in a nice way. In this thesis we will pursue some of the ideas built on the assumption that gravity can be viewed as a massless spin 2 field (upper half). Taken from Claudia de Rham and Andrew J. Tolley, "The Cosmological Constant Challenge" Nordita summer school on de Sitter Cosmology, 9-17 August 2008, to appear.

The classification scheme used here might seem strange, but as we briefly mentioned in the preliminaries it is possible to look at the metric $g_{\mu\nu}$ as a massless spin 2 field and as such the first classification indicates whether the cosmic acceleration is caused by dark energy or by modifications to Einsteins theory at a

fundamental level. We will assume that the cosmic acceleration is due to dark energy. In this case the next classification is whether dark energy is dynamical or not. The cosmological constant Λ is the simplest non dynamical explanation, but it has also been suggested that the apparent accelerated expansion is an effect of the universe not being homogeneous as is assumed in Friedmann cosmology [26]. We restrict ourselves to looking at the cosmological constant scenario. Dark energy can also be dynamical, meaning that rather than having a constant density, it is allowed to vary with space and time. In these models dark energy can be described by scalar fields $\Phi(x,t)$ and can be classified by whether they couple *minimally* or *non-minimally* to matter. The distinction between non-minimal and minimal coupling refers to how the scalar field couples to matter through gravity, and not any explicit matter coupling. If the scalar field is coupled through the metric by for example a kinetic term $g_{\mu\nu}\partial_\mu\Phi\partial_\nu\Phi$ it is said to be minimally coupled but if it couples directly through the curvature, for example by a term ΦR, the coupling is non-minimal, see [25]. Although these models give approximately the same predictions for the present day universe, the different models can yield different predictions for the history and ultimate fate of the universe. In this chapter we give a brief overview of the cosmological constant scenario and dynamical dark energy described by scalar fields, before we take a closer look at the scalar field model known as *Chameleon dark energy* in the following chapters.

5.1 The Cosmological Constant Λ

The simplest explanation is that the cosmic acceleration is due to a cosmological constant Λ. If we look at Einstein field equations with Λ included, 4.8,we see that the stress-energy tensor for such a component would be proportional to the metric

$$T^{\Lambda}_{\mu\nu} = \frac{\Lambda}{8\pi G} g_{\mu\nu} \tag{5.1}$$

and by using the perfect fluid approximation 3.18 in comoving coordinates, this yields the pressure p and density ρ

$$\rho_\Lambda = \frac{\Lambda}{8\pi G} \quad , \quad p_\Lambda = -\frac{\Lambda}{8\pi G} \tag{5.2}$$

and as such an equation of state parameter $\omega_\Lambda = -1$ and from equation 3.57 a constant density ρ_Λ. Further solving the first Friedmann equation 3.53 for a universe dominated by a Λ component yields an exponentially expanding universe

$$\ln a \propto t$$

Using SI units observations seems to indicate that $\Omega_{\Lambda 0} \approx 0.73$, $H_0 \approx 2.27 \cdot 10^{-18}\ s$ and $G \approx 6.7 \cdot 10^{-11}\ m^3/(kgs^2)$ giving an energy density ρ_Λ (using units $c = 3 \cdot 10^8\ m/s$)

$$\rho_\Lambda = \Omega_\Lambda \rho_{c0} \approx 0.73 \frac{3H_0^2 c^2}{8\pi G} \approx 2 \cdot 10^{-10}\ J/m^3 \tag{5.3}$$

This energy with the peculiar property of having negative pressure $p < 0$ is believed to be the energy density of empty space itself. As we briefly mentioned at the end of chapter 2, matter is described by quantum fields on small scales, where the free quantum field can be thought of as an infinite collection of harmonic oscillators with particles identified as the excitations of these oscillators. From quantum mechanics we know that the ground state energy of a harmonic oscillator is given by its frequency ν, $E_0 = \frac{1}{2}\hbar\nu$, which means that even in the absence of particles each quantum field has a vacuum energy given as an infinite sum of zero point energies. The total contribution from such zero point energies will formally yield an infinite vacuum energy since we are summing over an infinite collection of oscillators, but if we discard the highest frequency modes on the grounds that the predictions of quantum field theory can only be trusted up to some maximal energy, we can get a finite estimate. It is believed that both quantum field theory and Einsteins gravitational theory breaks down at what is known as the *Planck scale*, where quantum gravitational effects become important, and this is usually taken as the cut off. A rough approximation can then be found by constructing a mass known as the *reduced Planck mass* M_{Pl} from the fundamental constants of gravity and quantum mechanics. For simplicity we use $8\pi G$ as the fundamental

constant of gravity rather than G, and the *Planck constant* $\hbar$ as the fundamental constant of quantum theory. In SI units we have $8\pi G = 1.68 \cdot 10^{-9}\ [m^3/(kgs^2)]$ and $\hbar = 1.05 \cdot 10^{-34}\ kgm^2/s$ and combining these together with the light speed c we get a constant with units of mass called the reduced Planck mass M_{Pl}

$$M_{Pl} = \sqrt{\frac{\hbar c}{8\pi G}} \approx 4.33 \cdot 10^{-9} kg \tag{5.4}$$

or with units $c = \hbar = 1$ simply $M_{Pl} = (8\pi G)^{-1/2}$. The Planck mass M_{Pl} can now be related to the corresponding Planck energy E_Pl through Einsteins relation $E = mc^2$ and if we take this to be the largest contribution to the zero point energy, the corresponding vacuum energy density ρ^{Λ}_{Pl} becomes

$$\rho^{\Lambda}_{Pl} = \frac{E^4_{Pl}}{(\hbar c)^3} \sim 10^{110}\ J/m^3 \tag{5.5}$$

Now if our cut off at the Planck scale is correct, each quantum field is believed to give a contribution of this magnitude, with bosons giving positive contributions and fermions negative ones. Additional contributions are smaller contributions to the vacuum energy from scalar fields as well as the possibility of a non-zero bare cosmological constant Λ_0, see [24] for more details. It is conceivable that the sum of all these contributions approximately cancels, yielding a small effective cosmological constant consistent with observations, but without any arguments for how or why the contributions should cancel to such a degree accuracy (so as to only leave $\rho_\Lambda \sim 10^{-10} J/m^3$), it seems very unlikely. This problem is known as the *Cosmological constant problem* and is one of the most important unsolved problems in fundamental physics. A related problem is called *the coincidence problem* and relates to the fact that we observe the energy density of vacuum $\rho_{\Lambda 0}$ to be of the same order of magnitude as the density of matter ρ_{m0} today. If we look at equation 3.57 which relates the densities to the scale factor, we see that while the vacuum energy density is constant $\rho_\Lambda = \text{constant}$, the matter density goes as $\rho_m \propto a^{-3}$. This means that if ρ_m and ρ_Λ are comparable today, then in the past the vacuum energy would have been undetectably small compared to the matter density, and in the future the density of matter will be negligible. Now if they are so different both in the past and in the future, why do we live in an era where they are comparable? One suggested solution to both these problems (and many others) involves what is called the *Anthropic principle*, which uses our rareness to explain why we live in a rare environment. From this point of view we could imagine that there is much more to the world than we observe, but that we must live in a part that supports life, and it can be shown that if Λ is very different from what we observe, then galaxies would never form and human life would not exist. Another possible explanation to this apparent coincidence might be found if the detected cosmic acceleration is not due to a non-zero vacuum energy but rather to a dynamical field closely mimicking the properties of vacuum energy.

5.2 Quintessence

It is perhaps more plausible that the sum of vacuum energy contributions cancels exactly through some symmetry of nature rather than a cancellation leaving a fraction of order 10^{-120} of the original contributions. If this is the case then the observed cosmic acceleration might be due to a new dynamical degree of freedom and the simplest possibility is a real scalar field Φ. Such models are sometimes called *Quintessence*, a name dating back to the ancient Greeks who thought nature was built up from five fundamental elements: Fire, earth, wind and water, and an additional fifth element (in Latin “quinta essentia”), the aether, permeating all of space. In terms of the components Ω this new scalar degree of freedom would be the fifth in line, the others being radiation, baryonic matter, dark matter and curvature, and as such quintessence was seen as a suitable name for this new form of energy. To illustrate the idea of Quintessence we choose as a starting point the minimally coupled action

$$S_Q = \int \mathcal{L}_Q d^4x$$
$$\mathcal{L}_Q = \mathcal{L}_G + \mathcal{L}_m + \mathcal{L}_\Phi$$

where the first two terms are the same as in the ordinary gravitational Lagrangian given in chapter 3.4 and $\mathcal{L}_\Phi$ is the curved spacetime version of the free scalar field Lagrangian given in equation 2.6 with $\sqrt{-g}$ included as usual (no other changes needs to be made since $\nabla_\mu \Phi = \partial_\mu \Phi$ for scalar fields)

$$\mathcal{L}_\Phi = -\sqrt{-g}\left(\frac{1}{2}g^{\mu\nu}\partial_\mu\Phi\partial_\nu\Phi + V(\Phi)\right) \tag{5.6}$$

We will state the results obtained from the Lagrangian without proof, saving a more detailed discussion for chapter 6. Dark Energy seems to be relatively smoothly distributed, or it would have been detected by its local gravitational field[4, chap. 8]. This means that on cosmological scales we can approximate the field Φ to be spatially homogeneous in which case the Lagrangian simplifies to

$$\mathcal{L}_\Phi = \frac{1}{2}\dot{\Phi}^2 - V(\Phi) \tag{5.7}$$

which through equation 3.29, assuming dark energy to be a perfect fluid, yields the pressure and density

$$\rho_\Phi = \frac{1}{2}\dot{\Phi}^2 + V(\Phi) \quad , \quad p_\Phi = \frac{1}{2}\dot{\Phi}^2 - V(\Phi) \quad \Rightarrow \quad \omega_\Phi = \frac{p_\Phi}{\rho_\Phi} = \frac{\frac{1}{2}\dot{\Phi}^2 - V(\Phi)}{\frac{1}{2}\dot{\Phi}^2 + V(\Phi)} \tag{5.8}$$

The observed cosmic acceleration today indicates that $\omega_\Phi \approx -1$ today, which can be obtained if the field evolves slowly in time compared to the potential, so that $\dot{\Phi}^2 \ll V(\Phi)$

$$\omega_\Phi = \frac{\frac{1}{2}\dot{\Phi}^2 - V(\Phi)}{\frac{1}{2}\dot{\Phi}^2 + V(\Phi)} \approx \frac{-V(\Phi)}{+V(\Phi)} = -1$$

If this is the case the scalar field behaves as a slowly varying dark energy with $\rho_\Phi \approx V(\Phi(t))$. We can find further constraints on the potential $V(\Phi)$ by looking at the cosmic evolution given by the equation of motion derived from 5.7 using an RW-metric 3.47

$$\ddot{\Phi} + 3H\dot{\Phi} = -\frac{dV}{d\Phi} \tag{5.9}$$

This equation is analogous to the classical problem of a ball with position $\Phi(t)$ rolling in a potential $V(\Phi)$. Using this analogy we see that the field will try to "roll" down to the potential where the Hubble term $3H\dot{\Phi}$ serves as a friction force, slowing down any time evolution in the field. Generally Quintessence potentials are required to be very flat compared to the friction in order to work, meaning that the effective mass of the field m_Φ given by the curvature of the potential must be smaller than the Hubble parameter, $m_\Phi = \sqrt{V_{,\Phi\Phi}} << H$ [27]. However the Hubble parameter is extremely small by particle physics standards and in units of eV , $H_0 = 10^{-33}eV$. This means that for quintessence to work the mass of the associated scalar particle m_Φ would have to be fine tuned to an extraordinary small value compared to all other known particles. For quintessence to work it also has to be dark, meaning that it couples very weakly to other particles. The reason for this is that the mass of the scalar particle is inversely proportional to the range of the force mediated by it, and because m_Φ is required to be extremely small, a direct coupling to matter would yield a new long range force inconsistent with observations unless the coupling is very weak as well. As we will see in the following chapters the chameleon model provides a way out of this problem. Most quintessence models also require a fine tuning of initial conditions in order to acquire the desired dynamics, but there exist potentials that give rise to so called attractor solutions, so that the same late time cosmic acceleration occurs for a broad range of different initial conditions.
The original potential proposed, known as the *Ratra-Peebles potential*

$$V(\Phi) = M^{4+n}\Phi^{-n} \tag{5.10}$$

exhibits such behavior. Here M is a constant with units of mass (for $\hbar = c = 1$) and n is positive but otherwise arbitrary. For such a potential the cosmic equation of motion 5.9 has a dark energy attractor solution towards which a large class of initially different solutions converge with time. To obtain this solution it is necessary to require that the universe was radiation dominated at sufficiently early times, which is also required for Big Bang nucleosynthesis to work [16] and what is then found is that the energy

density of Φ falls off with time, but slower than the densities of both matter and radiation. This continues to hold for the matter dominated era and eventually dark energy will come to dominate both matter and radiation. When this happens the kinetic term $\dot{\Phi}$ decays faster than the potential term $V(\Phi)$ yielding a negative pressure solution, and as such cosmic acceleration at late times. The cosmic acceleration caused by such a Quintessence model will be somewhat smaller then that caused by a cosmological constant

$$\ln a = t^{2/(4+n)}$$

In this scenario the coincidence problem is not as severe because the energy density of vacuum decays in a similar fashion as the densities of matter and radiation and its smallness today is a consequence of the universe being old. It also helps that the solution is an attractor leaving the model less sensitive to the initial values of Φ and $\dot{\Phi}$, but we still have to fine tune the values of M and n to obtain matter dark energy equality close to the present. For the cosmic acceleration to have started only recently we need

$$M^{4+n} \approx G^{-(1+n/2)} H_0^2 \tag{5.11}$$

To end this chapter we will look at non-minimally coupled dark energy models, and show that such models can be transformed into a theory with no non-minimal coupling but with an interesting direct matter coupling through what is known as a *conformal transformation*.

5.3 Scalar Tensor Theories

Before we delve into the main topic of this thesis, namely Chameleon Fields, we will briefly discuss how this model arises from a non minimally coupled scalar tensor theory, where the scalar field couples directly to the curvature scalar R. In the dark energy models we have looked at so far, we have basically only added a new term to the stress-energy tensor $T_{\mu\nu}$ in Einstein's field equations, and assumed that that the new term is due to either some new form of matter or the energy of vacuum. In scalar-tensor models on the other hand, it is the gravitational part of the Lagrangian $\mathcal{L}_G$ that is modified by coupling a scalar field ϕ directly to the curvature scalar R through some function $f(\phi)$. In this sense scalar tensor theories are not strictly dark energy models but rather a modified theory of gravity where the metric degree of freedom $g_{\mu\nu}$ is given a scalar companion ϕ which is non-minimally coupled to the metric through the $f(\phi)R$ term. The theory was initially invented by Pascual Jordan who in the late 50's found a way to project five dimensional spacetime into a four dimensional one, where the projection gave rise to an effective four dimensional Lagrangian with a non-minimally coupled scalar field. In the early 60's Robert Dicke and Carl Brans employed such a non-minimally coupled Lagrangian to construct an alternative theory to Einstein's general relativity where the scalar field served as a time varying gravitational constant in accordance with arguments made by Dirac, [25]. In this theory the coupling is given by a parameter ω where ordinary GR is believed to be recovered in the limit $\omega \to \infty$. Although Brans-Dicke theory is consistent with observations, the value of ω has been constrained to such a high value, $\omega > 4 \cdot 10^4$, that many see it as unlikely. Rather than using the original Lagrangian proposed by Brans and Dicke we will follow [25] and take as our starting point the more general Lagrangian $\mathcal{L}^J_{ST}$ (the J will become clear shortly) where we for later convenience write the metric and metric related quantities with a tilde on top ($\tilde{g}_{\mu\nu}, \tilde{R},$ etc), and denote the self interaction potential of the scalar field by $U(\phi)$. With these conventions the starting point is given by

$$\mathcal{L}^J_{ST} = \mathcal{L}_{\phi\tilde{R}} + \mathcal{L}_\phi + \mathcal{L}_m \tag{5.12}$$

where $\mathcal{L}_{\phi R}$ is the Einstein Hilbert term but with a non minimal coupling $f(\phi)$. For convenience we use units with $M_{Pl} = 1$ for the moment giving $\mathcal{L}_{\phi R}$

$$\frac{1}{2}\sqrt{-\tilde{g}} f(\phi) \tilde{R} \tag{5.13}$$

Further $\mathcal{L}_\phi$ is a slightly generalized form of the scalar field Lagrangian

$$\mathcal{L}_\phi = -\sqrt{-\tilde{g}} \left(\frac{\epsilon}{2} \tilde{g}^{\mu\nu} \partial_\mu \phi \partial_\nu \phi + U(\phi) \right) \tag{5.14}$$

and $\mathcal{L}_m(g_{\mu\nu}, \Psi)$ is the Lagrangian for the matter fields Ψ and the metric $g_{\mu\nu}$. The equations of motion for this Lagrangian can now be obtained in the usual way by varying the Lagrangian with respect to the degrees of freedom. In particular the analogue to Einsteins field equations found by varying $\mathcal{L}^J_{ST}$ with respect to the metric becomes

$$\tilde{E}_{\mu\nu} = f^{-1}(\phi)\left(\tilde{T}^m_{\mu\nu} + \tilde{T}^\phi_{\mu\nu} + \tilde{\nabla}_\mu\tilde{\nabla}_\nu f(\phi) - \tilde{g}_{\mu\nu}\Box f(\phi)\right) \tag{5.15}$$

where $\tilde{E}_{\mu\nu}$ is the Einstein tensor defined by the left hand side of equation 3.30, the stress energy tensors $\tilde{T}^i_{\mu\nu}$ are defined in the usual way $T^i_{\mu\nu} \equiv -2/\sqrt{-\tilde{g}}\,(\partial\mathcal{L}_i/\partial\tilde{g}_{\mu\nu})$ and $\Box$ is the d'Alemertian defined by $\Box \equiv \eta^{\mu\nu}\partial_\mu\partial_\nu$. Although the presence of a scalar field suggests that cosmic acceleration might be explained by this model, the field equations are considerably more complicated than Einstein's field equation which are already hard to solve. It is however possible to cast the Lagrangian $\mathcal{L}^J_{ST}$ into a simpler form by using conformal transformations[1]. This is done by rewriting the Lagrangian in terms of a new metric $g_{\mu\nu}$ given by

$$\tilde{g}_{\mu\nu} = \Omega^2(x)g_{\mu\nu} \quad , \quad \tilde{g}^{\mu\nu} = \Omega^{-2}(x)g^{\mu\nu} \tag{5.16}$$

where $\Omega(x)$ is some spacetime dependent function. The change of metric is said to be a conformal transformation and by re-expressing the Lagrangian in terms of g, R and ∇_μ derived from $g_{\mu\nu}$ using the methods of chapter 3, we can move from one conformal frame to another. The original conformal frame with the non-minimal coupling term is known as the Jordan frame and we will now use conformal transformations to obtain the Lagrangian in the Einstein frame, where the curvature part of the Lagrangian becomes that of Einstein's theory but now with a scalar field Φ coupled to matter. Actually applying the conformal transformations is easy in principle but rather tedious, so we refer to references [25, 4] for the actual transformations and just state the results. Rewriting the curvature part $\mathcal{L}_{\phi R}$ in terms of the geometric quantities in the new frame we get

$$\mathcal{L}_{\phi R} = \frac{1}{2}\sqrt{-g}f\Omega^2\left(R - 6g^{\mu\nu}\frac{\partial_\mu\Omega\partial_\nu\Omega}{\Omega^2}\right) + S(g,\Omega)$$

where $S(\tilde{g},\Omega)$ is a surface term that vanishes when integrated (see section 3.4) and as such can be neglected. Since both $f(\phi)$ and $\Omega(x)$ are arbitrary functions so far we are free to choose them so that

$$f\Omega^2 \equiv 1 \quad \Rightarrow \quad \Omega = f^{-\frac{1}{2}} \tag{5.17}$$

so that the non-minimal coupling vanishes from the curvature part and $\mathcal{L}_{\phi R}$ becomes

$$\mathcal{L}_{\phi R} = \sqrt{-g}\left(\frac{1}{2}R - \frac{3}{4}\left(\frac{\partial_\phi f}{f}\right)^2 g^{\mu\nu}\partial_\mu\phi\partial_\nu\phi\right)$$

The choice 5.17 of relation between $f(\phi)$ and $\Omega(x)$ defines the Einstein frame. In a Similar manner we can also re-express $\mathcal{L}_\phi$ which gives

$$\mathcal{L}_\phi = -\sqrt{g}\left(\frac{\epsilon}{2}f^{-1}g^{\mu\nu}\partial_\mu\phi\partial_\nu\phi + f^{-2}U(\phi)\right)$$

and by combining the two terms we get a pure curvature term $\mathcal{L}_R$ and a scalar term $\mathcal{L}_\phi$

$$\mathcal{L}_R = \frac{1}{2}\sqrt{-g}R \quad , \quad \mathcal{L}_\phi = -\sqrt{g}\left(\frac{1}{2}\Delta(\phi)g^{\mu\nu}\partial_\mu\phi\partial_\nu\phi + f^{-2}U(\phi)\right) \quad , \quad \Delta(\phi) = \frac{3}{2}\left(\frac{\partial_\phi f}{f}\right)^2 + \frac{\epsilon}{f}$$

Finally we can make $\mathcal{L}_\phi$ look exactly like the ordinary scalar field Lagrangian given by equation 2.6 by rewriting it in terms of a new scalar field Φ defined by

$$\frac{d\Phi}{d\phi} = \sqrt{\Delta} \quad \Rightarrow \quad \frac{\partial\Phi}{\partial x^\mu} = \frac{d\Phi}{d\phi}\frac{\partial\phi}{\partial x^\mu} = \sqrt{\Delta}\frac{\partial\phi}{\partial x^\mu} \tag{5.18}$$

[1] The following treatment is a slightly modified version of the treatment given in [25, chap. 3]

and defining the self interaction of Φ as $V(\Phi) \equiv f^{-2}U(\phi)$. Finally reinserting M_{Pl} we have the Einstein frame Lagrangian

$$\mathcal{L}^{E}_{ST} = \sqrt{-g}\left(\frac{M^2_{Pl}}{2}R - \frac{1}{2}g^{\mu\nu}\partial_\mu\Phi\partial_\nu\Phi - V(\Phi)\right) + \mathcal{L}_m(\Omega^2 g_{\mu\nu}, \Psi) \tag{5.19}$$

In the Einstein frame the non-minimal coupling term has vanished, but we now have a new scalar field Φ which couples to matter through the metric $\tilde{g}_{\mu\nu}$, and this Lagrangian is the starting point for the chameleon dark energy models which will be the focus for the remainder of this thesis. For completeness we also re-express the original Jordan frame Lagrangian in terms of the new field Φ and the conformal coupling Ω using 5.18 and 5.17 together with the definition of Δ .

$$\mathcal{L}^{J}_{ST} = \frac{\sqrt{-\tilde{g}}}{\Omega^2}\left(\frac{M^2_{Pl}}{2}\tilde{R} - \frac{1}{2}\left[1 + 6\left(\frac{\partial_\Phi\Omega}{\Omega}\right)^2\right]\tilde{g}^{\mu\nu}\partial_\mu\Phi\partial_\nu\Phi - \frac{V(\Phi)}{\Omega^2}\right) + \mathcal{L}_m(\tilde{g}_{\mu\nu}, \Psi) \tag{5.20}$$

This is the same as in [28] and [29]. The Jordan and Einstein frame Lagrangians given by 5.20 and 5.19 are mathematically equivalent, but that does not necessarily mean that they are physically equivalent. In the Jordan frame the non-minimal coupling can be interpreted as a spacetime dependent gravitational constant $G(x,t)$ while in the Einstein frame the scalar field is coupled to particles through the metric so the coupling can be interpreted as a spacetime dependent particle physics scale. The question is whether both descriptions give the same predictions for anything we in principle can measure and there is still heated debate over what the answer is. We will not speculate on the subject and refer the interested reader to the more detailed discussions in [30, 25, 31]. In this thesis we will use the Einstein frame most of the time, but in some situations we will follow the literature and use Jordan frame arguments to justify our assumptions.

Part III

Chameleon Fields

Chapter 6

Foundation

This chapter is based mainly on [25, 32] and [33]. Following up on the short general discussion of scalar tensor theories, we now move on to discuss the class of scalar tensor theories known as chameleon dark energy models. In these models the non minimal coupling given by $\Omega(\Phi)$ and the self interaction $V(\Phi)$ is chosen so as to allow a strong coupling between the matter fields Ψ and the scalar field Φ, without breaking experimental constraints. As we briefly mentioned in our discussion of Quintessence in section 5.2, the scalar field has to have a very small mass, $m_\Phi \lesssim H_0$ in order to give cosmic acceleration, and if coupled to matter such a low mass field would give rise to a long ranged force. Such forces have been tightly constrained by experiments done on earth and in the solar system, which means that if dark energy is due to Quintessence, the scalar field would have to have an unnaturally weak matter coupling, see [34]. In the Chameleon models invented by Justin Khoury and Amanda Weltman these tight constraints can be circumvented by choosing the self interaction and matter coupling in such a way that the effective potential and therefore the mass $m_\Phi = \sqrt{V_{,\Phi\Phi}}$ becomes larger in regions with higher densities, giving a shorter force range. Since our most stringent constraints on additional forces comes from earth and solar system experiments where the matter density is high compared to the matter density on cosmological scales, this allows for a larger coupling. Since the field adapts to its environment in this way it's called a Chameleon field. Although there are many choices for self interactions and coupling that gives rise to such a chameleon, we will choose to work with a prototype model where the self interaction is given by the Ratra-Peebles potential 5.10 and an exponential matter coupling term $\Omega(\Phi)$

$$V(\Phi) = M^{4+n}\Phi^{-n} \quad , \quad \Omega(\Phi) = e^{\beta\Phi/M_{Pl}} \tag{6.1}$$

where β is a dimensionless coupling constant . This explicit choice of potential and coupling then gives the Jordan frame Lagrangian $\mathcal{L}_C^J$

$$\mathcal{L}_C^J = \frac{\sqrt{-\tilde{g}}}{e^{-2\beta\Phi/M_{Pl}}}\left(\frac{M_{Pl}^2}{2}\tilde{R} - \frac{1}{2}\left[1 + 6\left(\frac{\beta}{M_{Pl}}\right)^2\right]\tilde{g}^{\mu\nu}\partial_\mu\Phi\partial_\nu\Phi - \frac{M^{4+n}}{e^{2\beta\Phi/M_{Pl}}}\Phi^{-n}\right) + \mathcal{L}_m(\tilde{g}_{\mu\nu}, \Psi) \tag{6.2}$$

and the Einstein frame Lagrangian $\mathcal{L}_C^E$

$$\mathcal{L}_C^E = \sqrt{-g}\left(\frac{M_{Pl}^2}{2}R - \frac{1}{2}\partial^\mu\Phi\partial_\mu\Phi - M^{4+n}\Phi^{-n}\right) + \mathcal{L}_m\left(e^{2\beta\Phi/M_{Pl}}g_{\mu\nu}, \Psi\right) \tag{6.3}$$

In this thesis we will focus on the Einstein frame formulation. In order to see where the chameleon effect comes from we must first find the equations of motion for the chameleon.

6.1 Chameleon Equations of Motion

The derivation of the equations of motion does not depend on the specific choice of coupling or potential so we will work with the general Lagrangian 5.19 for now. The Chameleon equations of motion is most easily

found by applying the curved spacetime version of the Euler-Lagrange equations given by equation 3.16 to the Φ dependent part of the Lagrangian $\mathcal{L}_\Phi$

$$\mathcal{L}_\Phi = -\sqrt{-g}\left(\frac{1}{2}\partial^\alpha\Phi\partial_\alpha\Phi - V(\Phi)\right) + \mathcal{L}_m\left(\Omega(\Phi)g_{\mu\nu}, \Psi\right)$$
$$\frac{d\mathcal{L}_\Phi}{d\Phi} = -\sqrt{-g}\frac{dV}{d\Phi} + \frac{d\mathcal{L}_m}{d\Phi}$$
$$\frac{\partial\mathcal{L}_\Phi}{\partial\left(\partial_\mu\Phi\right)} = -\sqrt{-g}\partial^\mu\Phi = -\sqrt{-g}\nabla^\mu\Phi$$

Putting the two terms together and using $\nabla_\alpha g_{\mu\nu} = 0$, we find

$$\nabla_\mu\nabla^\mu\Phi = \frac{dV}{d\Phi} - \frac{1}{\sqrt{-g}}\frac{d\mathcal{L}_m}{d\Phi}$$

The matter term can be rewritten in a more familiar form by using the relationship between the Einstein and Jordan frame metrics

$$\frac{d\mathcal{L}_m}{d\Phi} = \frac{\partial\mathcal{L}_m}{\partial\tilde{g}^{\mu\nu}}\frac{d\tilde{g}^{\mu\nu}}{d\Phi}$$

$$\frac{\partial\tilde{g}^{\mu\nu}}{\partial\Phi} = -2\frac{\partial_\Phi\Omega}{\Omega^3}g^{\mu\nu} \quad , \quad \frac{\partial\mathcal{L}_m}{\partial\tilde{g}^{\mu\nu}} = \frac{\partial\mathcal{L}_m}{\partial g^{\alpha\beta}}\frac{\partial g^{\alpha\beta}}{\partial\tilde{g}^{\mu\nu}} = \Omega^2\frac{\partial\mathcal{L}_m}{\partial g^{\mu\nu}}$$

$$\Rightarrow \quad \frac{d\mathcal{L}_m}{d\Phi} = -2\frac{\partial_\Phi\Omega}{\Omega}\frac{\partial\mathcal{L}_m}{\partial g^{\mu\nu}}g^{\mu\nu}$$

and by using the definition of the stress-energy tensor $T^m_{\mu\nu} \equiv -2/\sqrt{-g}\left(\partial\mathcal{L}_m/\partial g^{\mu\nu}\right)$ and the trace $T^m = T^m_{\mu\nu}g^{\mu\nu}$ we get

$$\frac{1}{\sqrt{-g}}\frac{d\mathcal{L}_m}{d\Phi} = \frac{\partial_\Phi\Omega}{\Omega}T^m$$

yielding the equation of motion

$$\nabla_\mu\nabla^\mu\Phi = \frac{dV}{d\Phi} - \frac{\partial_\Phi\Omega}{\Omega}T^m \tag{6.4}$$

Before we continue we will briefly discuss some of the properties of the stress energy tensor $T^m_{\mu\nu}$ and the conformally related Jordan frame tensor $\tilde{T}^m_{\mu\nu}$. The stress-energy tensor for matter does not obey the usual energy conservation equation in the Einstein frame since the matter fields are coupled to the chameleon so the trace T^m and the corresponding density and pressure $\rho_{m\Phi}$ and $p_{m\Phi}$ must be considered functions of Φ . On the other hand the full stress-energy tensor $T^M_{\mu\nu} = T^m_{\mu\nu} + T^\Phi_{\mu\nu}$ is conserved, so in the Einstein frame we have

$$\nabla^\mu T^m_{\mu\nu} \neq 0 \quad , \quad \nabla^\mu T^\Phi_{\mu\nu} \neq 0 \tag{6.5}$$

$$\nabla^\mu T^M_{\mu\nu} = \nabla^\mu\left(T^m_{\mu\nu} + T^\Phi_{\mu\nu}\right) = 0 \tag{6.6}$$

In the Jordan frame however there is no direct matter-chameleon coupling and as such the stress-energy tensor $\tilde{T}^m_{\mu\nu} \equiv -2/\sqrt{-\tilde{g}}\left(\partial\mathcal{L}_m/\partial\tilde{g}^{\mu\nu}\right)$ is conserved in the Jordan frame, i.e $\tilde{\nabla}^\mu\tilde{T}^m_{\mu\nu} = 0$. The relation between these two tensors $T^m_{\mu\nu}$ and $\tilde{T}^m_{\mu\nu}$ and the corresponding traces T^m and $\tilde{T}^m$ are found to be

$$T^m_{\mu\nu} = -\frac{2}{\sqrt{-g}}\frac{\partial \mathcal{L}_m}{\partial g^{\mu\nu}} = \Omega^4 \frac{\partial \tilde{g}^{\alpha\beta}}{\partial g^{\mu\nu}}\left(-\frac{2}{\sqrt{-\tilde{g}}}\frac{\partial \mathcal{L}_m}{\partial \tilde{g}^{\alpha\beta}}\right) = \Omega^2 \tilde{T}^m_{\mu\nu} \tag{6.7}$$

$$T^{\mu\nu}_m = g^{\mu\alpha}g^{\nu\beta}T^m_{\alpha\beta} = \Omega^6 \tilde{g}^{\mu\alpha}\tilde{g}^{\nu\beta}\tilde{T}^m_{\alpha\beta} = \Omega^6 \tilde{T}^{\mu\nu}_m$$

$$T^m = T^m_{\mu\nu}g^{\mu\nu} = \Omega^4 \tilde{T}^m_{\mu\nu}\tilde{g}^{\mu\nu} = \Omega^4 \tilde{T}^m \tag{6.8}$$

With these matters out of the way we return to the equations of motion. If we consider T^m to describe a perfect fluid, we can use equation 3.18 to write the trace in terms of the density and pressure, which we denote by $\rho_{m\Phi}$ and $p_{m\Phi}$ to keep in mind that $T^m_{\mu\nu}$ also depends on Φ

$$T^m = T^{\mu\nu}_m g_{\mu\nu} = U^\mu U_\mu \left(\rho_{m\Phi} + p_{m\Phi}\right) + \delta^\mu_\mu p_{m\Phi} = -\rho_{m\Phi} + 3p_{m\Phi}$$

and by plugging this into equation 6.4 we find the equations of motion

$$\nabla_\mu \nabla^\mu \Phi = \frac{dV}{d\Phi} + \frac{\partial_\Phi \Omega}{\Omega}\left(\rho_{m\Phi} - 3p_{m\Phi}\right) \tag{6.9}$$

or in terms of our prototype model

$$\nabla_\mu \nabla^\mu \Phi = -nM^{4+n}\Phi^{-n+1} - \frac{\beta}{M_P l}\left(\rho_{m\Phi} - 3p_{m\Phi}\right) \tag{6.10}$$

We end this section by giving the explicit left hand sides of the equations of motion for the two spacetimes considered in section 3.5

Static Spherically Symmetric Spacetime

First we calculate the covariant derivative $\nabla_\mu\left(\partial^\mu \Phi\right)$ using the Christoffel symbols given in appendix A.2.

$$\begin{aligned}
\nabla_\mu\left(\partial^\mu\Phi\right) =& \partial_{\ \mu}\partial^\mu\Phi + \Gamma^\mu_{\ \lambda\mu}\partial^\lambda\Phi \\
=& \partial_{\ \mu}\partial^\mu\Phi + \left(\Gamma^t_{\ rt} + \Gamma^r_{\ rr} + \Gamma^\theta_{\ r\theta} + \Gamma^\phi_{\ r\phi}\right)\partial^r\Phi \\
&+ \Gamma^\phi_{\ \theta\phi}\partial^\theta\Phi \\
=& \partial_{\ \mu}\partial^\mu\Phi + \left[\partial_r\left(\alpha+\beta\right) + \frac{2}{r}\right]e^{-2\beta}\partial_r\Phi \\
&+ \frac{1}{r^2}\frac{\cos\theta}{\sin\theta}\partial_\theta\Phi
\end{aligned}$$

and continue by re-expressing the $\partial_r\Phi$ -term in terms of m, p and ρ using the relations obtained in section 3.5.1, where $\rho = \rho_m + \rho_\Phi$ and $p = p_m + p_\Phi$ comes from the full stress energy tensor $T^M_{\mu\nu}$

$$e^{-2\beta} = 1 - \frac{2Gm}{r} \quad , \quad \partial_r\alpha = \frac{4\pi G p r^3 + Gm}{r\left[r - 2Gm\right]} \quad , \quad \partial_r m = 4\pi r^2\rho \quad , \quad \partial_r\beta = \frac{4\pi G\rho r^3 - Gm}{r\left[r-2Gm\right]}$$

$$\left[\partial_r\left(\alpha+\beta\right) + \frac{2}{r}\right]e^{-2\beta} = \left(1 - \frac{2Gm}{r}\right)\left[\frac{2}{r} + \frac{4\pi G r^3\left(\rho + p\right)}{r\left[r-2Gm\right]}\right]$$

Now since spacetime is static and spherically symmetric we also require this of Φ so that $\partial_t\Phi = \partial_\theta\Phi = \partial_\phi\Phi = 0$, giving the double partial derivative

$$\partial_\mu\partial^\mu\Phi = \partial_r g^{rr}\partial_r\Phi = e^{-2\beta}\left(\partial_r^2\Phi - 2\partial_r\beta\partial_r\Phi\right) = \left(1 - \frac{2Gm}{r}\right)\left[\frac{d^2\Phi}{dr^2} - \frac{8\pi G\rho r^3 - 2Gm}{r\left[r-2Gm\right]}\frac{d\Phi}{dr}\right]$$

and the covariant double derivative $\nabla_\mu \nabla^\mu \Phi$

$$\nabla_\mu \nabla^\mu \Phi = \left(1 - \frac{2Gm}{r}\right)\left[\frac{d^2\Phi}{dr^2} + \left(\frac{2}{r} - \frac{4\pi G r^3(\rho - p) - 2Gm}{r\,[r - 2Gm]}\right)\frac{d\Phi}{dr}\right] \tag{6.11}$$

We thus have the equation of motion 6.9 for Φ in a static spherically symmetric spacetime

$$\left(1 - \frac{2Gm}{r}\right)\left[\frac{d^2\Phi}{dr^2} + \left(\frac{2}{r} - \frac{4\pi G r^3(\rho - p) + 2Gm}{r\,[r - 2Gm]}\right)\frac{d\Phi}{dr}\right] = \partial_\Phi V + \frac{\partial_\Phi \Omega}{\Omega}(\rho_{m\Phi} - 3p_{m\Phi}) \tag{6.12}$$

Spatially Homogeneous and Isotropic Spacetime

Again we follow the same procedure but this time we calculate the covariant derivative $\nabla_\mu(\partial^\mu\Phi)$ using the Christoffel symbols given in appendix A.1

$$\begin{aligned}
\nabla_\mu(\partial^\mu\Phi) =& \partial_\mu \partial^\mu \Phi + \Gamma^\mu{}_{\lambda\mu}\partial^\lambda\Phi \\
=& \partial_\mu \partial^\mu \Phi + \left(\Gamma^r{}_{tr} + \Gamma^\theta{}_{t\theta} + \Gamma^\phi{}_{t\phi}\right)\partial^t\Phi \\
&+ \left(\Gamma^\theta{}_{r\theta} + \Gamma^\phi{}_{r\phi}\right)\partial^\phi\Phi + \\
=& \partial_\mu \partial^\mu \Phi - 3\frac{\dot{a}}{a}\dot{\Phi} \\
&+ \frac{2}{a^2 r}\partial_r\Phi + \frac{1}{r^2}\frac{\cos\theta}{\sin\theta}\partial_\theta\Phi
\end{aligned}$$

where all but the time derivative terms disappear due to the spatial isotropy and homogeneity, $\partial_r\Phi = \partial_\theta\Phi = \partial_\phi\Phi = 0$. In this case the the ordinary partial derivative simply reduces to $-\ddot{\Phi}$ since $g^{tt} = -1$ and the simplified covariant double derivative $\nabla_\mu \partial^\mu \Phi$ becomes

$$\nabla_\mu \nabla^\mu \Phi = -\ddot{\Phi} - 3\frac{\ddot{a}}{a}\dot{\Phi}$$

yielding the equation of motion 6.9 for Φ in a spatially homogeneous and isotropic spacetime

$$\ddot{\Phi} + 3\frac{\dot{a}}{a}\dot{\Phi} = -\frac{dV}{d\Phi} + \frac{\partial_\Phi\Omega}{\Omega}(\rho_{m\Phi} - 3p_{m\Phi}) \tag{6.13}$$

This is very similar to the Quintessence equation 5.9 except for an additional term due to the matter-chameleon coupling. Now the equations we have obtained works perfectly well, except we haven't really looked at how one should interpret the density and pressure $\rho_{m\Phi}$ and $p_{m\Phi}$. It is convenient, at least from a cosmological point of view , to define the matter density ρ_m and pressure p_m in such a way that the corresponding stress energy tensor obeys the conservation equation 3.17. Then we can follow the usual procedure in cosmology and use the continuity equation 3.56 to write the density and pressure of the different forms of matter in terms of the scale factor a. Soon we will show how we can rewrite $\rho_{m\Phi} = f(\Phi)\rho_m$ so that ρ_m obeys the continuity equation,. but before we do this we need to discuss the other part of the full stress energy tensor $T^M_{\mu\nu}$, namely the stress energy tensor for the free scalar field.

6.2 Chameleon Stress-Energy Tensor

In the following chapters we are also going to need the stress energy tensor for the Chameleon $T^\Phi_{\mu\nu}$. Using the definition of $T^{\mu\nu}$ from Einsteins field equations given in equation 3.29, together with the free chameleon Lagrangian $\mathcal{L}^{\text{free}}_\Phi$

$$T_{\mu\nu} \equiv -\frac{2}{\sqrt{-g}}\frac{\partial \mathcal{L}^{\text{free}}_\Phi}{\partial g^{\mu\nu}} \quad , \quad \mathcal{L}^{\text{free}}_\Phi = -\sqrt{-g}\left(\frac{1}{2}\partial^\mu\Phi\partial_\mu\Phi + V(\Phi)\right)$$

we first find $\partial\mathcal{L}_\Phi^{\text{free}}/\partial g^{\mu\nu}$

$$\frac{\partial\mathcal{L}_\Phi}{\partial g^{\mu\nu}} = -\frac{\partial\sqrt{-g}}{\partial g^{\mu\nu}}\left(\frac{1}{2}\partial_\alpha\Phi\partial^\alpha\Phi + V(\Phi)\right) - \frac{\sqrt{-g}}{2}\frac{\partial g^{\alpha\beta}}{\partial g^{\mu\nu}}\partial_\alpha\Phi\partial_\beta\Phi$$

$$\frac{\partial\sqrt{-g}}{\partial g^{\mu\nu}} = -\frac{1}{2}\sqrt{-g}g_{\mu\nu} \quad , \quad \frac{\partial g^{\alpha\beta}}{\partial g^{\mu\nu}} = \delta^\alpha_\mu\delta^\beta_\nu$$

$$\Rightarrow \quad \frac{\partial\mathcal{L}_\Phi}{\partial g^{\mu\nu}} = \frac{\sqrt{-g}}{2}\left[g_{\mu\nu}\left(\frac{1}{2}\partial_\alpha\Phi\partial^\alpha\Phi + V(\Phi)\right) - \partial_\mu\Phi\partial_\nu\Phi\right]$$

and plug it in to the stress energy tensor $T^\Phi_{\mu\nu}$, giving full expression

$$T^\Phi_{\mu\nu} = -g_{\mu\nu}\left(\frac{1}{2}\partial_\alpha\Phi\partial^\alpha\Phi + V(\Phi)\right) + \partial_\mu\Phi\partial_\nu\Phi \tag{6.14}$$

Using this expression and assuming the chameleon to behave as a perfect fluid we can find the density ρ_Φ and pressure p_Φ of the chameleon fluid. As usual we also find the explicit expressions in the two spacetimes given by the metrics 3.31 and 3.47 .

Spatially Homogeneous and Isotropic Spacetime

On cosmological scales we approximate the cosmic fluid to be homogeneous and isotropic implying that on these scales $\Phi \approx \Phi(t)$. Using comoving coordinates given by the RW-metric 3.47, where we assume flat spacetime, $k = 0$, together with the perfect fluid equation 3.18 and 6.14 we find

$$T^\Phi_{00} = -\left(\frac{1}{2}\dot\Phi^2 + V(\Phi)\right) + \dot\Phi^2 = \rho_\Phi$$
$$T^\Phi_{rr} = -a^2\left(-\frac{1}{2}\dot\Phi^2 + V(\Phi)\right) = a^2 p_\Phi$$

which yields the chameleon pressure and density on cosmological scales

$$\rho_\Phi = \frac{1}{2}\dot\Phi^2 + V(\Phi) \tag{6.15}$$
$$p_\Phi = \frac{1}{2}\dot\Phi^2 - V(\Phi) \tag{6.16}$$

Static Spherically Symmetric Spacetime

In this case spacetime and as such the energy distribution, is assumed to be static and spherically symmetric so $\Phi \approx \Phi(t)$. Following the same procedure as above, but this time with the metric 3.31, re-expressed in terms of the mass m using definition 3.40, and with radial derivatives written as Φ' . This gives

$$T^\Phi_{00} = e^{2\alpha}\left[\frac{1}{2}\left(1 - \frac{2Gm}{r}\right)\Phi'^2 + V(\Phi)\right] = e^{2\alpha}\rho_\Phi$$
$$T^\Phi_{rr} = -\left(1 - \frac{2Gm}{r}\right)^{-1}\left[\frac{1}{2}\left(1 - \frac{2Gm}{r}\right)\Phi'^2 + V(\Phi)\right] + \Phi'^2 = \left(1 - \frac{2Gm}{r}\right)^{-1} p_\Phi$$

which in turn yields the energy density ρ_Φ and pressure p_Φ for the Chameleon in a static spherically symmetric spacetime

$$\rho_\Phi = \frac{1}{2}\left(1 - \frac{2Gm}{r}\right)\Phi'^2 + V(\Phi) \tag{6.17}$$

$$p_\Phi = \frac{1}{2}\left(1 - \frac{2Gm}{r}\right)\Phi'^2 - V(\Phi) \tag{6.18}$$

6.3 Matter Density in The Einstein Frame

In order to find a conserved matter density we will use the fact that the full stress energy tensor $T^M_{\mu\nu}$ is conserved, which means that if we look at the full density $\rho = \rho_\Phi + \rho_{m\Phi}$ and pressure $p = p_\Phi + p_{m\Phi}$, then all the equations derived from Einsteins field equations in section 3.5 applies to the total densities ρ and p. In particular we have the continuity equation 3.56 which becomes

$$\begin{aligned} \dot{\rho} &= -3\frac{\dot{a}}{a}(\rho + p) \\ \Rightarrow \quad \dot{\rho}_{m\Phi} + \dot{\rho}_\Phi &= -3\frac{\dot{a}}{a}(\rho_{m\Phi} + p_{m\Phi} + \rho_\Phi + p_\Phi) \\ \Rightarrow \quad \dot{\rho}_\Phi + 3\frac{\dot{a}}{a}(\rho_\Phi + p_\Phi) &= -\dot{\rho}_{m\Phi} - 3\frac{\dot{a}}{a}(\rho_{m\Phi} + p_{m\Phi}) \end{aligned}$$

We already found the pressure and density of the chameleon given by 6.15 and 6.16 so plugging in on the left hand side we find in terms of Φ

$$\ddot{\Phi} + 3\frac{\dot{a}}{a}\dot{\Phi} = -\frac{dV}{d\Phi} - \frac{\dot{\rho}_{m\Phi} + 3\frac{\dot{a}}{a}(\rho_{m\Phi} + p_{m\Phi})}{\dot{\Phi}}$$

which is the equation of motion for Φ. By comparing this matter term to the original one, and assuming that the density can be written as $\rho_{m\Phi} = F(\Phi)\rho_m$ and that matter obeys the simple equation of state $p_m = \omega\rho_m$ we find

$$\dot{\rho}_m + 3\frac{\dot{a}}{a}(\rho_m + p_m) = \left((1 - 3\omega)\frac{\partial_\Phi \Omega}{\Omega}\dot{\Phi} - \frac{\dot{F}}{F}\right)\rho_m \tag{6.19}$$

We see that a vanishing right-hand side gives the continuity equation 3.56, so the requirement that matter obeys this equation means that

$$\frac{\dot{F}}{F} = (1 - 3\omega)\frac{\partial_\Phi \Omega}{\Omega}\dot{\Phi}$$

which we can rewrite

$$(1 - 3\omega)\frac{\partial_\Phi \Omega}{\Omega}\dot{\Phi} = \frac{d\ln\Omega^{(1-3\omega)}}{dt} \quad , \quad \frac{\dot{F}}{F} = \frac{d\ln F}{dt}$$

$$\Rightarrow \quad \frac{d\ln\Omega(1 - 3\omega)}{dt} = \frac{d\ln F}{dt} \tag{6.20}$$

which means that up to a constant factor, $F(\Phi)$ is given by

$$F(\Phi) = \Omega^{1-3\omega} \tag{6.21}$$

$$\Rightarrow \quad \rho_{m\Phi} = \Omega^{1-3\omega}\rho_m \tag{6.22}$$

In particular we see that for radiation with $\omega_m = +1/3$, $\rho_{m\Phi}$ is conserved, reflecting the fact that radiation does not couple to the chameleon at a classical level, and for pressureless matter $\omega_m = 0$, $F(\Phi)$ is simply equal to Ω. Finally plugging into the general and prototype equation of motion 6.9 and 6.10

$$\nabla_\mu \nabla^\mu \Phi = \frac{dV}{d\Phi} + \frac{\partial_\Phi \Omega}{\Omega} \Omega^{1-3\omega} (1 - 3\omega) \rho_m \tag{6.23}$$

$$\nabla_\mu \nabla^\mu \Phi = -nM^{4+n} \Phi^{-n+1} + (1 - 3\omega) \frac{\beta}{M_{Pl}} e^{(1-3\omega)\beta\Phi/M_{Pl}} \rho_m \tag{6.24}$$

This is the equations of motion usually used in the literature and which we will use in chapter 7.

6.4 Chameleon Forces

Following the procedure used in [32] we now derive the chameleon force. As we mentioned in section 3.3, freely falling objects follows trajectories through spacetime known as geodesics, given by the geodesic equation 3.19. In the Einstein frame matter couples to the chameleon so in this frame particles are subjected to forces, but in the Jordan frame there is no matter coupling and as such they follow the geodesics of $\tilde{g}_{\mu\nu}$.

$$\frac{d^2 x^\alpha}{d\tau^2} + \tilde{\Gamma}^\alpha_{\ \mu\nu} U^\mu U^\nu = 0$$

where the four velocity notation $U^\mu = \frac{dx^\mu}{d\tau}$ is used for simplicity and the Christoffel symbols $\tilde{\Gamma}^\alpha_{\ \mu\nu}$ are given by equation 3.14

$$\tilde{\Gamma}^\alpha_{\ \mu\nu} = \frac{1}{2} \tilde{g}^{\alpha\lambda} \left(\tilde{g}_{\mu\lambda,\nu} + \tilde{g}_{\lambda\nu,\mu} - \tilde{g}_{\mu\nu,\lambda} \right)$$

By rewriting the Christoffel symbols $\tilde{\Gamma}^\alpha_{\ \mu\nu}$ in terms of the Einstein frame metric $g_{\mu\nu}$ we can find the deviation from geodesic motion in the Einstein frame and find the associated force by taking the Newtonian limit. In this section we denote the Chameleon by Φ and the Newtonian potential by ϕ. First we rewrite $\tilde{\Gamma}^\alpha_{\ \mu\nu}$ using $\tilde{g}^{\mu\nu} = \Omega^{-2} g^{\mu\nu}$ and $\tilde{g}_{\mu\nu} = \Omega^2 g_{\mu\nu}$

$$\begin{aligned}
\tilde{\Gamma}^\alpha_{\ \mu\nu} &= \frac{1}{2} \Omega^{-2} g^{\sigma\alpha} \left[\partial_\nu \left(\Omega^2 g_{\mu\lambda} \right) + \partial_\mu \left(\Omega^2 g_{\lambda\nu} \right) - \partial_\lambda \left(\Omega^2 g_{\mu\nu} \right) \right] \\
\partial_\lambda \left(\Omega^2 g_{\mu\nu} \right) &= \Omega^2 g_{\mu\nu,\lambda} + 2\Omega\Omega_{,\Phi} \Phi_{,\lambda} g_{\mu\nu} \\
\Rightarrow \quad \tilde{\Gamma}^\alpha_{\ \mu\nu} &= \Gamma^\alpha_{\ \mu\nu} + \frac{\partial_\Phi \Omega}{\Omega} \left(\delta^\alpha_\mu \partial_\nu \Phi + \delta^\alpha_\nu \partial_\mu \Phi - g_{\mu\nu} \partial^\alpha \Phi \right)
\end{aligned} \tag{6.25}$$

We can now plug this into the Jordan frame geodesic equation. Using that the inner product of the four velocity is simply $U_\mu U^\mu = -1$ we find

$$\frac{d^2 x^\alpha}{d\tau^2} + \Gamma^\alpha_{\ \mu\nu} U^\mu U^\nu + \frac{\partial_\Phi \Omega}{\Omega} \left(2U^\alpha \frac{d\Phi}{d\tau} - g^{\alpha\lambda} \partial_\lambda \Phi \right) = 0 \tag{6.26}$$

An alternative approach to obtain the same result is to use the covariant Euler-Lagrange equations for discrete system on the Lagrangian for a free particle as is done in [5, sec. 5.6] but with the metric $\tilde{g}_{\mu\nu}$ instead of $g_{\mu\nu}$. Now taking the non-relativistic weak field limit as we did at the beginning of section 3.3, the Christoffel term yields the regular Newtonian gravitational force which we denote by ϕ_N while the additional term corresponds to the contribution from the chameleon. To lowest order we find

$$\frac{d^2 x}{dt^2} = -\nabla \phi_N - \frac{\partial_\Phi \Omega}{\Omega} \nabla \Phi \tag{6.27}$$

or in terms of the explicit coupling of our prototype model

$$\frac{d^2x}{dt^2} = -\nabla\left(\phi_N + \frac{\beta}{M_P l}\Phi\right) \tag{6.28}$$

We see that at a classical level, our prototype model will not violate the universality of free fall (i.e the weak equivalence principle) since β is universal. However when we solve the equations of motion in chapter 7 we will see that the chameleon does not yield an inverse square law as Newtonian gravity does, and as such the parameters of the theory can be constrained by experiments looking for deviations from this law. Further more it is possible for the coupling to be different for different matter species i so that rather than having one coupling, β , we have several, β_i . In this case we see that the correction term would differ from species to species and the weak equivalence principle (WEP) would be violated. Generally quantum corrections will lead to such variations and as such even chameleon models with a universal coupling at the classical level will eventually lead to WEP violations due to quantum effects [33].

6.5 Experimental Constraints

We end this chapter by briefly giving the experimental constraints on chameleon models. The best bounds on chameleon theories comes from laboratory experiments such as the Eöt-Wash experiment which searches for deviations from the Newtonian inverse square law, and Lunar Laser Ranging tests for violations of the weak equivalence principle (WEP). At very small distances the tightest constraints come from measurements of the Casimir force. The experimental constraints have already been discussed extensively in [33], so rather then giving a discussion here, we only show the results and refer to [33] for details. The combined constraints on β and M are shown in figure 6.1 for $n = 1, 4, 6, -4, -6, -8$.

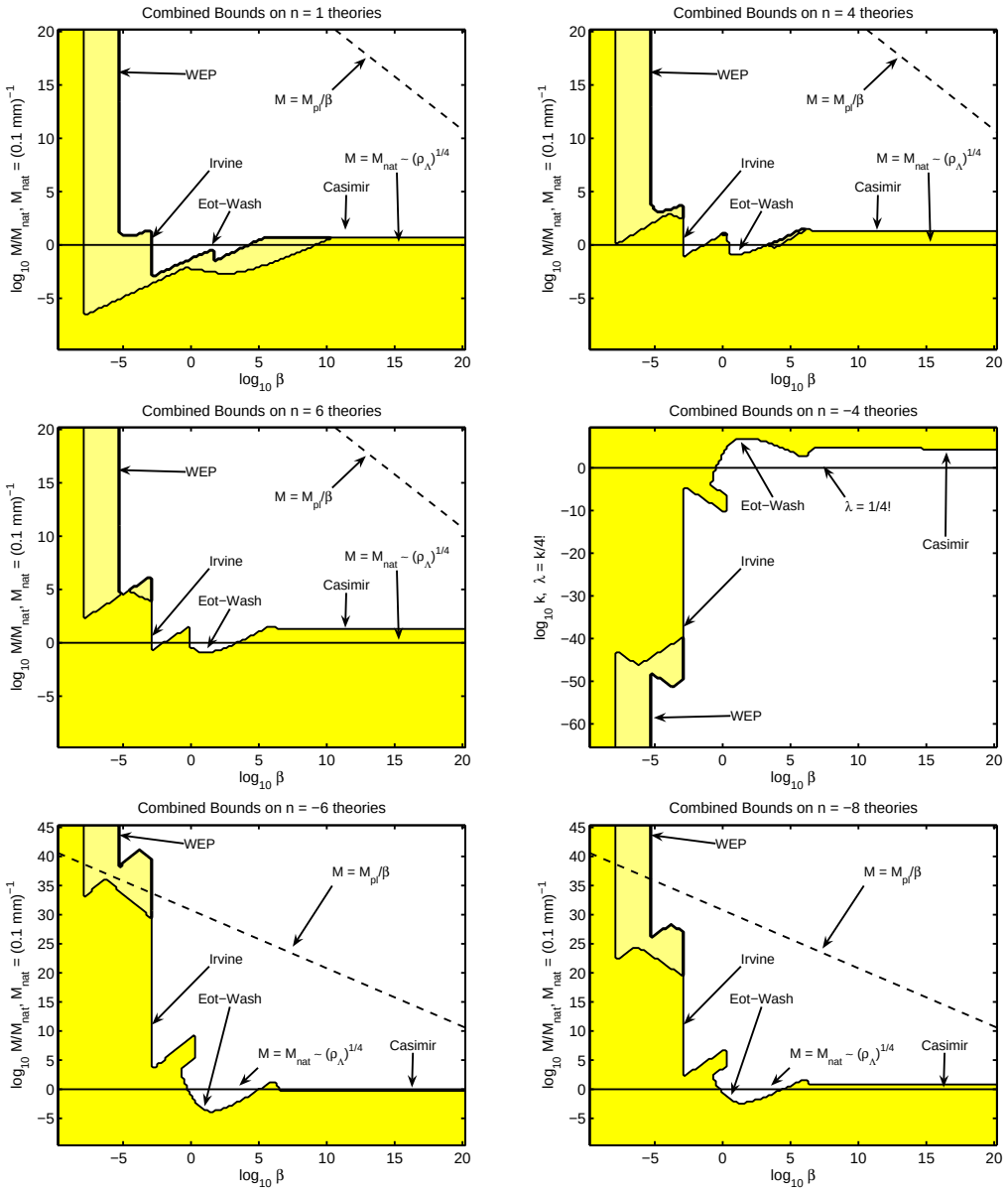

Figure 6.1: Combined constraints on β and M for $n = 1, 4, 6, -4, -6, -8$. The shaded yellow regions shows the parameter values that are allowed by current experiments. The dotted line indicates $M = M_{Pl}/\beta$ Taken from [33].

Part IV

Chameleons and Compact Objects

Chapter 7

A First Approximation

We have now arrived at the main part of this thesis where we consider how inhomogeneities in the matter distribution affects the chameleon field. In the first chapter of this part we find an analytic approximation, using the original treatment by Khoury and Weltman, [34, 35], as a basis and continue by numerically solving the equations and compare the results to the analytic predictions. In the following chapter we will use numerical methods to explore more generalized situations where we allow the matter density to vary and also take into account general relativistic effects.

Following Khoury and Weltman, we start by looking at the idealized situation where we have a static and homogeneous spherically symmetric matter distribution and where general relativistic effects can be neglected. In this case we can find analytic solutions applicable under conditions known as *thin shell* and *thick shell* conditions.

7.1 Analytic Approximation

To find an analytic approximation we start by considering a static spherical symmetric sphere of radius R_s and constant density ρ_s embedded in a homogeneous background of density ρ_b. If we neglect spacetime curvature, and use our prototype chameleon model given by the matter and self-coupling given in equation 6.1, together with the equation of motion 6.24 for non relativistic matter $\omega = 0$, we have as our starting point

$$\frac{d^2\Phi}{dr^2} + \frac{2}{r}\frac{d\Phi}{dr} = -nM^{4+n}\Phi^{-(n+1)} + \frac{\beta}{M_{Pl}}e^{\beta\Phi/M_{Pl}}\rho_m(r) \tag{7.1}$$

where the right hand side can be considered as the derivative of the effective potential $dV_{eff}/d\Phi$ where V_{eff} is given by

$$V_{eff} = M^{4+n}\Phi^{-n} + e^{\beta\Phi/M_{Pl}}\rho_m(r)$$

For later convenience we define Φ_s and Φ_b as the value of Φ at the minimum of this effective potential inside and outside the body where $\rho_m(r)$ is given by

$$\rho_m(r) = \begin{cases} \rho_s & , \quad r < R_s \\ \rho_b & , \quad r > R_s \end{cases}$$

Now since the equation of motion is a second order differential equation we need two conditions to determine the integration constants of the solutions and in this treatment they are fixed by supplying boundary conditions at $r = 0$ and $r = \infty$. For the solution to be non-singular we require that the gradient of Φ vanishes at $r = 0$, and as $r \to \infty$, we require that Φ converges towards Φ_b. The last requirement is argued to be physically sensible because this implies that the gradient of Φ, and thus also the fifth forces, vanish at infinity. This gives the following boundary conditions

$$\frac{d\Phi}{dr} = 0 \text{ at } r = 0$$
$$\Phi \to \Phi_b \text{ as } r = 0$$

To obtain an approximate analytic solution we need to get an idea of how the solutions evolve and this can be done by comparing equation 7.1 to the equation of motion governing the cosmological evolution of the quintessence field given by equation 5.9. In that case we used the analogy between the field evolution and the classical problem of a ball rolling in a one dimensional potential, treating Φ as the spatial coordinate, to get an intuitive picture of the time evoultion. We can apply the same analogy here except that the radial derivatives have the opposite sign compared to the time derivative. This means that to apply the intuitive picture of a ball rolling in a potential we have to treat the negative of the true potential as the potential in which the ball is rolling, which we will denote by V_{roll} , see figure 7.1. In this picture the gradient

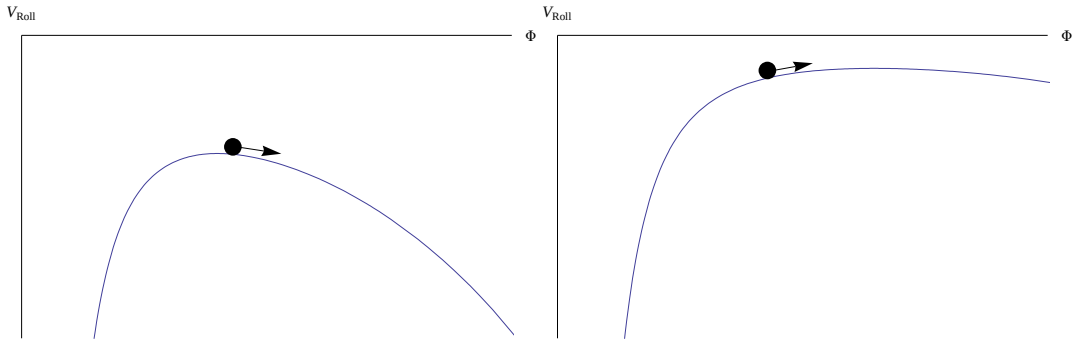

Figure 7.1: Schematic picture of Φ rolling inside the star (left) and in the background (right)

term serves as a friction term which is infinitely large at the core $r = 0$, and tends to zero as $r \to \infty$, which means that if Φ starts close to Φ_s , then due to the large friction term it should stay approximately constant until the friction term is sufficiently small to allow Φ to start rolling. We denote the radial coordinate at which the field starts to roll by R_{roll} and consider the two regimes: The thin shell regime where $R_s - R_{\text{roll}} << R_s$, which requires $\Phi(0) - \Phi_s << \Phi_s$ and the thick shell regime where we take the limit $R_{\text{roll}} \to 0$, which requires Φ to start out sufficiently far away from the maxima of V_{roll} so as to practically start rolling at once but at the same time sufficiently close so that it ends up to the left of the maxima of V_{roll} in the background, $\Phi(0) \gtrsim \Phi_s$. We start by looking at the thin shell regime

- **Thin Shell** $\Phi(0) - \Phi_s << \Phi_s$

  In the thin shell regime the solution can be split into three different parts, first we have the region $r < R_{\text{roll}}$ in which Φ is approximately constant, secondly the region in the interior $R_{\text{roll}} < r < R_s$, where Φ is rolling and finally the exterior solution $r > R_s$.

  - **Region 1** $r < R_{\text{roll}}$

    The first region is trivial because by definition $\Phi \approx \Phi_s$.

    $$\Phi_1(r) \approx \Phi_s \quad , \quad r < R_{\text{roll}}$$

– **Region 2** $R_{\text{roll}} < r < R_s$

In the second region the matter term of the potential comes to dominate almost immediately and if we also assume that $\beta\Phi/M_{Pl} << 1$ we get the approximate equation of motion for this region

$$\frac{d^2\Phi_2}{dr^2} + \frac{2}{r}\frac{d\Phi_2}{dr} \approx \frac{\beta}{M_{Pl}}\rho_s \tag{7.2}$$

This equation is linear which means we can superpose solutions. The general solution can be found by guessing that the solution takes the form $\Phi_2 = C_n r^n$ and allowing values of n such that the left hand side either vanishes or becomes a constant. Plugging into equation 7.2

$$\big[n(n-1) + 2n\big] C r^{n-2} = \frac{\beta}{M_{Pl}}\rho_s$$

we see that for $n = -1, 0$ the left hand side vanishes so these are the complimentary solutions while $n = 2$ gives a constant which must be equal to the constant on the right hand side and we thus have the general solution

$$\Phi_2(r) = \frac{\beta\rho_s}{6M_{Pl}} r^2 + C_1 r^{-1} + C_2$$

The two integration constants are found by demanding consistency between Φ_1 and Φ_2 at $r = R_{\text{roll}}$

$$\begin{aligned}
\Phi(R_{\text{roll}}) &= \frac{\beta\rho_s}{6M_{Pl}} R_{\text{roll}}^2 + \frac{C_1}{R_{\text{roll}}} + C_2 = \Phi_s \\
\frac{d\Phi(R_{\text{roll}})}{dr} &= \frac{\beta\rho_s}{3M_{Pl}} R_{\text{roll}} - \frac{C_1}{R_{\text{roll}}^2} = 0 \\
\Rightarrow \quad C_1 = \frac{\beta\rho_s R_{\text{roll}}^3}{3M_{Pl}} \quad &, \quad C_2 = \Phi_s - \frac{\beta\rho_s R_{\text{roll}}^2}{2M_{Pl}}
\end{aligned}$$

which yields the final solution

$$\Phi_2(r) = \frac{\beta\rho_c}{3M_{Pl}}\left(\frac{r^2}{2} + \frac{R_{\text{roll}}^3}{r}\right) - \frac{\beta\rho_s R_{\text{roll}}^2}{2M_{Pl}} + \Phi_s \quad , \quad R_{\text{roll}} < r < R_s$$

Khoury & Weltman argues that the validity of the solutions in region 1 and 2 requires $R_s - R_{\text{roll}} << R_s$ and the argument is that otherwise we would need one solution valid over the whole interval.

– **Region 3** $r > R_s$

On the outside of the object, the density drops to ρ_b so that Φ is now climbing up the potential. We ultimately want a solution that never goes over the top of the potential or rolls back down, i.e $\Phi \overset{r\to\infty}{\longrightarrow} \Phi_b$, which means that depending on the density contrast and the curvature of the potential the field has to either be rolling fast compared to the curvature of the potential, or be close to the minima Φ_b , as the density changes. Either way we can approximate the potential by a Taylor expansion about Φ_b so that $\Phi = (\Phi_b - \delta\Phi)$, yielding the approximate equation of motion

$$\frac{d^2\Phi_3}{dr^2} + \frac{2}{r}\frac{d\Phi_3}{dr} \approx m_b^2\left(\Phi_3 - \Phi_b\right)$$

where $m_b^2 = \frac{d^2V_{eff}}{d^2\Phi}$ is the squared mass of the chameleon in the background. For simplicity we first substitute $u = \Phi_3 - \Phi_b$ before assuming a series solution of the form

$$u = \sum_{n=0}^{\infty} a_n r^{n+\sigma} \;\Rightarrow\; \frac{du}{dr} = \sum_{n=0}^{\infty}(n+\sigma)a_n r^{n+\sigma-1} \;\Rightarrow\; \frac{d^2u}{dr^2} = \sum_{n=0}^{\infty}(n+\sigma)(n+\sigma-1)a_n r^{n+\sigma-2}$$

where the free parameter σ is inserted since the equation is singular. Plugging this into the equation we find

$$\sum_{n=0}^{\infty}\left[(n+\sigma)(n+\sigma-1)+2(n+\sigma)\right]a_n r^{n+\sigma-2} = \sum_{n=0}^{\infty} m_b^2 a_n r^{n+\sigma}$$

We see that we need the $r^{n+\sigma-2}$ and $r^{n+\sigma-1}$ terms on the left hand side to vanish to get the same form as on the right-hand side and this is where σ comes in. By choosing $\sigma = -1$ both the $n = 1$ and the $n = 2$ terms vanish on the left hand side and by shifting $n \to n+2$ we obtain

$$\frac{1}{r}\sum_{n=0}^{\infty}\left[(n+1)n+2(n+1)\right]a_{n+2}r^n = \frac{1}{r}\sum_{n=0}^{\infty} m_b^2 a_n r^n$$

We are thus left with the recurrence relation

$$a_{n+2} = \frac{m_b^2}{(n+3)(n+2)}$$

where we have two free parameters a_0 and a_1 . Plugging into the first few coefficients a_n we see that if $a_1 = m_b a_0$ the series would correspond to the Taylor expansion of the exponential function and by rewriting the free parameters a_0 and a_1 in terms of two new ones C_1 and C_2 so that

$$a_0 = C_1 + C_2 \quad , \quad a_1 = m_b(C_1 - C_2)$$

We can write the solution in two exponential terms

$$\begin{aligned} u &= \frac{C_1}{r}\sum_{n=0}^{\infty}\frac{m_b^n}{n!}r^n + \frac{C_1}{r}\sum_{n=0}^{\infty}(-1)^n\frac{m_b^n}{n!}r^n \\ &= \frac{C_1}{r}e^{m_b r} + \frac{C_2}{r}e^{-m_b r} \end{aligned}$$

Finally we substitute back $\Phi_3 = u + \Phi_b$ and require that $\Phi_3 \to \Phi_b$ as $r \to \infty$ and $\Phi_3(R_s) = \Phi_2(R_s)$ to determine C_1 and C_2

$$\begin{aligned} &\Phi(\infty) = m_b C_1 e^{m_b\infty} - m_b C_2 e^{-m_b\infty} + \Phi_b = \Phi_b \\ &\Phi(R_s) = \frac{C_1}{R_s}e^{m_b R_s} + \frac{C_2}{R_s}e^{-m_b R_s} + \Phi_b = \Phi_2(R_s) = \Phi_{R_s} \\ \Rightarrow\;& C_1 = 0 \quad , \quad C_2 = (\Phi_{R_s} - \Phi_b)R_s e^{m_b R_s} \end{aligned}$$

giving the full exterior solution

$$\Phi_3(r) = (\Phi_{R_s} - \Phi_b)\frac{R_s}{r}e^{-m_b(r-R_s)} + \Phi_b \quad , \quad r > R_s$$

We determine R_{roll} by requiring that the profile is smooth at $r = R_s$. If we where to determine R_{roll} exactly we would have to solve a nasty cubic equation, which would yield only one extremely long and ugly real solution, however remembering that the validity of Φ_1 and Φ_2 required $R_s - R_{\text{roll}} << R_s$ we can replace $R_{\text{roll}} = (1 - \Delta R) R_s$ where $\Delta R = (R_s - R_{\text{roll}}) / R_s << 1$ and keep only first order terms in ΔR.

$$\begin{aligned}
\frac{d\Phi_2(R_s)}{dr} &= \frac{\beta\rho_s}{3M_{\text{Pl}}}\left(R_s - \frac{R_{\text{roll}}^3}{R_s^2}\right) \\
&= \frac{R_s\beta\rho_s}{3M_{\text{Pl}}}\left(3\Delta R - 3\Delta R^2 + \Delta R^3\right) \\
&\approx \frac{R_s\beta\rho_s}{M_{\text{Pl}}}\Delta R \\
\frac{d\Phi_3(R_s)}{dr} &= \frac{(1+m_bR_s)(\Phi_b - \Phi_s)}{R_s} - \frac{\beta\rho_s(1+m_bR_s)(R_{\text{roll}} - R_s)^2(2R_{\text{roll}} + R_s)}{6M_{\text{Pl}}R_s^2} \\
&= \frac{(1+m_bR_s)(\Phi_b - \Phi_s)}{R_s} + \frac{R_s\beta\rho_s(1+m_bR_s)}{6M_{\text{Pl}}}(3\Delta R^2 - 2\Delta R^3) \\
&\approx \frac{(1+m_bR_s)(\Phi_b - \Phi_s)}{R_s}
\end{aligned}$$

Finally we demand that the gradients at R_s are equal to first order in ΔR which gives us the thin shell condition, which when rewritten in terms of the mass of the sphere $M_s = 4\pi R_s^3\rho_s/3$ becomes

$$\Delta R \approx C_{\text{Thin}} \equiv \frac{4\pi M_{\text{Pl}}R_s(1+m_bR_s)}{3\beta M_s}(\Phi_b - \Phi_s) << 1 \tag{7.3}$$

This expression differs from the condition given in the original paper by a factor $1 - m_bR_s$ where they probably assume $m_bR_s << 1$,which would be the case in most scenarios. With this thin shell condition the approximate radius where the field starts to roll R_{roll} becomes

$$R_{\text{roll}} = (1 - \Delta R)R_s \approx \left(1 - \frac{4\pi M_{\text{Pl}}R_s(1+m_bR_s)}{3\beta M_s}(\Phi_b - \Phi_s)\right)R_s \tag{7.4}$$

In summary, the thin shell approximation yields a solution

$$\Phi(r) \approx \Phi_s \quad , \quad r < R_{\text{roll}} \tag{7.5}$$

$$\Phi(r) = \frac{\beta\rho_s}{3M_{Pl}}\left(\frac{r^2}{2} + \frac{R_{\text{roll}}^3}{r}\right) - \frac{\beta\rho_sR_{\text{roll}}^2}{2M_{Pl}} + \Phi_s \quad , \quad R_{\text{roll}} < r < R_s \tag{7.6}$$

$$\Phi(r) \approx -(\Phi_b - \Phi_{R_s})R_s\frac{e^{-m_b(r-R_s)}}{r} + \Phi_b \quad , \quad r > R_s \tag{7.7}$$

$$\Phi_{R_s} = \Phi_s + \frac{\beta\rho_sR_s^2(3\Delta R^2 - 2\Delta R^3)}{6M_{Pl}} \tag{7.8}$$

where Φ_{R_s} is given by equation 7.6 at $r = R_s$.

- **Thick Shell** $\Phi(0) \gtrsim \Phi_s$

  If Φ is sufficiently displaced from Φ_s at the center of the star the friction dominated region will be negligible and the profile of the chameleon is given by the rolling equation throughout the whole star. The solution to the rolling equation in this case is easily obtained by letting $R_{roll} \to 0$ and replacing Φ_s by a, yet to be determined, initial value Φ_i, which can be determined in terms of mass and radius of the star by demanding consistency with the outer solution at $r = R_s$. The solutions are

– **Region 1** $r < R_s$

Taking the $R_{roll} \to 0$ limit and replacing Φ_s by Φ_i we get

$$\Phi_1(r) = \frac{\beta\rho_s}{6M_{Pl}} r^2 + \Phi_i \quad , \quad r < R_s$$

– **Region 2** $r > R_s$

Again we assume that the potential outside the sphere can be approximated by a harmonic potential. Requiring the field to reach the minimum Φ_b as $r \to \infty$ and that the profile is continuous at $r = R_s$ we find

$$\Phi_2(r) = \left(\frac{\beta\rho_s}{6M_{Pl}} R_s^2 + \Phi_i - \Phi_b\right) \frac{R_s}{r} e^{-m_b(r-R_s)} + \Phi_b$$

Φ_i is determined by requiring a smooth profile at $r = R_s$, i.e $\Phi_1'(R_s) = \Phi_2'(R_s)$

$$\frac{d\Phi_1(R_s)}{dr} = \frac{d\Phi_1(R_s)}{dr}$$
$$\frac{\beta\rho_s}{3M_{Pl}} R_s = -\left(\frac{\beta\rho_s}{6M_{Pl}} R_s^2 + \Phi_i - \Phi_b\right)\left(\frac{1}{R_s} + m_b\right)$$

$$\Rightarrow \quad \Phi_i = \Phi_b - \frac{\beta\rho_s R_s^2}{6M_{Pl}}\left(1 + \frac{2}{(1+m_b R_s)}\right) \tag{7.9}$$

It should be noted that this answer is different from what was obtained in the original paper which also means the solutions Φ_1 and Φ_2 are slightly different, but the numerics seem to favor these results over the ones originally obtained, where we get a discontinuity at $r = R_s$.

Anyways plugging Φ_i into the solutions we find that in the thick shell limit the profile of the chameleon is approximately given by

$$\Phi(r) = \frac{\beta\rho_s}{6M_{Pl}} r^2 - \frac{\beta\rho_s R_s^2}{6M_{Pl}}\left(1 + \frac{2}{(1+m_b R_s)}\right) + \Phi_b \quad , \quad r < R_s \tag{7.10}$$

$$\Phi(r) = -\frac{\beta\rho_s R_s^3}{3M_{Pl}\,(1+m_b R_s)} \frac{e^{-m_b(r-R_s)}}{r} + \Phi_b \quad , \quad r > R_s \tag{7.11}$$

Finally we can derive a thick shell condition by using the fact that $\Phi_i > \Phi_s$, and writing it in terms of M_s

$$\Phi_i = \Phi_b - \frac{\beta\rho_s R_s^2}{6M_{Pl}}\left(1 + \frac{2}{(1+m_b R_s)}\right) > \Phi_s$$

$$C_{\text{thick}} \equiv \frac{8\pi M_{Pl} R_s\,(1+m_b R_s)}{3\beta M_s}\,(\Phi_b - \Phi_s) - \frac{m_b R_s}{3} > 1 \tag{7.12}$$

We see that we now have different conditions for the thick shell and the thin shell regimes because our expression differs from the original one by more then the factor of $(1 + m_b R_s)$ due to the difference in Φ_i . We will see that although the expressions look different, the numerical result will be the same (which is not the case if we use the original expressions!).

7.2 Parameter Dependence of Thin Shell ΔR from Rolling Ball Analogy

We will now use the analogy of the ball rolling with friction to roughly explain the parameter dependence of the thin shell ΔR. When the shell is thin, $\Delta R = (R_s - R_{roll})/R_s << 1$, its size is given approximately by equation 7.3, where we express M_s in terms of R_s and ρ_s

$$\Delta R \approx \frac{M_{\rm Pl}\,(1 + m_b R_s)}{\beta R_s^2 \rho_s}\,(\Phi_b - \Phi_s) << 1$$

From this expression we see that the shell becomes thinner with increasing radius R_s, coupling β and interior density ρ_s, and it becomes thicker with increasing exterior potential curvature given by m_b and the separation between the interior and exterior maximum of V_{roll}, given by $\Phi_b - \Phi_s$. We can explain this dependence in terms of the rolling ball analogy. The thin shell decreases with R_s, β and ρ_s because a larger radius gives a smaller friction term in the rolling regime, and β and rho_b increases the curvature of the potential inside the sphere, and this allows for a greater change in Φ and its derivative in a shorter radial region. The thin shell gets thicker as the separation between the interior and exterior maxima grows, because the ball ha to travel a larger distance in order to reach the top of the exterior potential. Finally the shell must gets thicker for a larger exterior chameleon mass term m_b because the increase in the curvature of the exterior potential makes it harder for the ball to reach the exterior potential maximum.

If we also have $\beta\Phi/M_{Pl} << 1$ we can write Φ_s and Φ_b in terms of β, M, n, ρ_s and ρ_b

$$\Phi_i = \left(\frac{nM^{4+n}M_{Pl}}{\beta\rho_i}\right)^{1/(n+1)} \quad , \quad i = \{s, b\}$$

giving ΔR

$$\Delta R \approx \frac{n^{1/(n+1)}\,(1 + m_b R_s)}{R_s^2}\left(\frac{M^{2/(n+1)}M_{\rm Pl}}{\beta\rho_s}\right)^{(n+2)/(n+1)}\left[\left(\frac{\rho_s}{\rho_b}\right)^{1/(n+1)} - 1\right]$$

This can be simplified further by noting that both $n^{1/(n+1)}$ and $(n+2)/(n+1)$ is close to unity for all $n > 1$ which means we can approximate

$$\Delta R \approx \frac{(1 + m_b R_s)}{R_s^2}\left(\frac{M^{2/(n+1)}M_{\rm Pl}}{\beta\rho_s}\right)\left[\left(\frac{\rho_s}{\rho_b}\right)^{1/(n+1)} - 1\right]$$

from this we see that an increase in M leads to a thicker shell both through the explicit dependence and because the mass m_b also increases with M, but as n grows the shell becomes less and less dependent on the actual value of M, but also brings the density contrast term ρ_s/ρ_b closer to 1 thus leading to a thinner shell.

7.3 Fifth Forces Revisited

With an analytic approximation for the Φ-profile at hand we can show how fifth forces outside objects are suppressed. We start out by noticing that the exterior solution in both the thin and thick shell limit takes the form

$$\Phi_{\rm ext} = -\kappa\frac{e^{-m_b(r-R_s)}}{r} + \Phi_b \tag{7.13}$$

$$\kappa_{\rm thin} = (\Phi_b - \Phi_{R_s})\,R_s \quad , \quad \kappa_{\rm thick} = \frac{\beta\rho_s R_s^3}{3M_{Pl}\,(1 + m_b R_s)} \tag{7.14}$$

where the difference lies in the constant κ. In section 6.4 we found that in the Newtonian limit the correction to the gravitational acceleration was given by equation 6.28 and written in terms of the exterior solutions Φ_{ext}, and the explicit Newtonian potential $\phi_N = -GM_s/r$ we find that the acceleration a of a test particle is given by

$$\begin{aligned} a &= \nabla\left(\frac{GM}{r} + \frac{\beta\kappa}{M_{Pl}}\frac{e^{-m_b(r-R_s)}}{r} + \Phi_b\right) \\ &= -\frac{GM_s}{r^2}\left(1 + \frac{\beta\kappa}{M_{Pl}GM_s}(1+m_b r)e^{-m_b(r-R_s)}\right) \end{aligned}$$

where κ is given by 7.14. From this general expression we can see that the chameleon force range depends on the mass of the chameleon through the exponential term which is unity at $r = R_s$ and vanishes as $r \to \infty$ and how fast it tends to zero depends on the background chameleon mass m_b. Since the $(1 + m_b r)$ term increases at a slower rate than the exponential term decays, we find that the maximal deviation from the Newtonian free fall occurs at the surface $r = R_s$ so that

$$\frac{\beta\kappa}{M_{Pl}}(1+m_b r)e^{-m_b(r-R_s)} < \frac{\beta\kappa}{M_{Pl}}(1+m_b R_s) \quad , \quad r > R_s$$

In the thick shell regime can express the constant in front of the exponential in terms of the mass of the object $M_s = 4\pi R_s^3\rho_s/3$ and G rather than M_{Pl}.

$$\frac{\beta\kappa_{\text{thick}}}{M_P l} = \frac{\beta^2\rho_s R_s^3}{3M_{Pl}^2\,(1+m_b R_s)} = \frac{2\beta^2}{1+m_b R_s}GM_s$$

yielding the free fall correction

$$a = -\frac{GM_s}{r^2}\left(1 + 2\beta^2\left(\frac{1+m_b r}{1+m_b R_s}\right)e^{-m_b(r-R_s)}\right) \tag{7.15}$$

From this equation we see that if $\beta = 1$ the correction term would be of the same order of magnitude as the Newtonian one. However in dense backgrounds the term drops off rapidly as the radius increases so the responsible force must be very local and as such helps to relieve the experimental constraints from experiments done in dense backgrounds. In the thin shell regime, we can write κ_{thin} in terms of κ_{thick} and a suppression factor S so that $\kappa_{\text{thin}} = S\kappa_{\text{thick}}$ with $S = \kappa_{\text{thin}}/\kappa_{\text{thick}}$. Plugging in from the expressions for κ_{thin} and κ_{thick} from equation 7.14 and using the definition of Φ_{Rs} from equation 7.8, we find that the suppression factor S becomes

$$\begin{aligned} S = \frac{\kappa_{\text{thin}}}{\kappa_{\text{thick}}} &= \frac{3M_{Pl}\,(1+m_b R_s)\,(\Phi_b - \Phi_{R_s})}{\beta\rho_s R_s^2} \\ &= \frac{3M_{Pl}\,(1+m_b R_s)\,(\Phi_b - \Phi_s)}{R_s^2\beta\rho_s} - \frac{\Delta R^2(-3+2\Delta R)\,(1+m_b R_s)}{2R_s} \\ &\approx \frac{3M_{Pl}\,(1+m_b R_s)\,(\Phi_b - \Phi_s)}{R_s^2\beta\rho_s} = \frac{4\pi M_{\text{Pl}} R_s\,(1+m_b R_s)}{\beta \text{M}_s}\,(\Phi_b - \Phi_s) = 3\Delta R \end{aligned} \tag{7.16}$$

where we in the last line neglected higher order ΔR-terms and used the thin shell condition 7.3 to write the remainder in terms of ΔR. Thus we see that when the object acquires a thin shell, the free fall correction term is additionally suppressed by a factor $3\Delta R << 1$ giving

$$a = -\frac{GM_s}{r^2}\left(1 + 6\Delta R\beta^2\left(\frac{1+m_b r}{1+m_b R_s}\right)e^{-m_b(r-R_s)}\right) \tag{7.17}$$

The thin shell compression factor can be compared to what was found in [35, 34].

7.4 Numerical Example: Ball of Beryllium in Air

Thin Shell

In [34] the validity of the analytic approximation is confirmed by comparing it to numerical calculations for a ball of beryllium with energy density $\rho_{\text{Be}} = 9 \cdot 10^{19}\ J/m^3$ and radius $R_{\text{Be}} = 40/M$ (giving a total mass $M_{\text{Be}} = 1.24 \cdot 10^{-3}\ kg$) in air with density $\rho_{\text{air}} = 9 \cdot 10^{15}\ J/m^3$. As theory parameters they use a self interaction potential with $n = 1$ and $M = 6 \cdot 10^3\ m^{-1}$ and matter coupling $\beta = 1$. With these numerical values we find the minima of the effective potential in the ball, Φ_{Be} , and in air, Φ_{air} by solving

$$\begin{aligned} & \frac{dV_{\text{eff}}(\Phi_{\text{Be}}, \rho_{\text{Be}})}{d\Phi} = -M^5\Phi_{\text{Be}}^{-2} - \frac{1}{M_{Pl}} e^{\Phi_{\text{Be}}/M_{Pl}}\rho_{\text{Be}} = 0 \\ \Rightarrow\ & \Phi_{\text{Be}} \approx 5.81 \cdot 10^3 \approx M \\ & \frac{dV_{\text{eff}}(\Phi_{\text{air}}, \rho_{\text{air}})}{d\Phi} = -M^5\Phi_{\text{air}}^{-2} - \frac{1}{M_{Pl}} e^{\Phi_{\text{air}}/M_{Pl}}\rho_{\text{air}} = 0 \\ \Rightarrow\ & \Phi_{\text{Be}} \approx 5.81 \cdot 10^5 \approx 100M \end{aligned} \tag{7.18}$$

which are in accordance with the minima obtained by Khoury & Weltman. We also need the mass of the field given by the curvature of the effective potential

$$m_{\text{Be}} = \sqrt{2M^5\Phi_{\text{Be}}^{-3} + \frac{1}{M_{Pl}^2} e^{\Phi_b/M_{Pl}}\rho_{\text{Be}}} \approx 8.9 \cdot 10^3\ m^{-1} \tag{7.19}$$

$$m_{\text{air}} = \sqrt{2M^5\Phi_{\text{air}}^{-3} + \frac{1}{M_{Pl}^2} e^{\Phi_{\text{air}}/M_{Pl}}\rho_{\text{air}}} \approx 8.9\ m^{-1} \tag{7.20}$$

Plugging into the thin shell condition, equation 7.3, we find

$$C_{\textbf{thin}} = \frac{4\pi M_{\text{Pl}} R_{\text{Be}}\,(1 + m_{\text{air}}R_{\text{Be}})}{3\beta M_{\text{Be}}}\,(\Phi_{\text{air}} - \Phi_{\text{Be}}) \approx 0.06$$

The analytic approximation using these numerical values is plotted in figure 7.2 and coincides with the result produced by Khoury & Weltman. Because reproducing the results numerically was harder then expected, and because no outline of the methods used to produce the original numerics were given, we will give a brief description of the algorithm used here. We start by putting the equations of motion on dimensionless form by writing

$$\Phi = \Phi_d\hat{\Phi} \quad , \quad \rho = P_d\hat{\rho} \quad , \quad r = R_d\hat{r}$$

where $\hat{\Phi}, \hat{\rho}$ and $\hat{r}$ are dimensionless quantities. Plugging into equation 7.1, we get the equations of motion expressed in terms of dimensionless variables

$$\frac{d^2\hat{\Phi}}{d\hat{r}^2} + \frac{2}{\hat{r}}\frac{d\hat{\Phi}}{d\hat{r}} = -A\hat{\Phi}^{-(n+1)} + Be^{C\hat{\Phi}}\hat{\rho}_m(r) \tag{7.21}$$

where A, B and C contains the dimensionfull, natural and theory dependent constants

$$A = \frac{nM^{4+n}R_d^2}{\Phi_d^{n+2}} \quad , \quad B = \frac{\beta R_d^2 P_d}{M_{Pl}\Phi_d} \quad , \quad C = \frac{\beta\Phi_d}{M_{Pl}} \tag{7.22}$$

Because of the discontinuity in ρ at R_{Be} we will choose two different values for the dimensionfull constants in the regions $r \in [0, R_{\text{Be}}]$ and $r > R_{\text{Be}}$. We choose to fix the dimensionless quantities R_d and Φ_d by requiring $A = B = 1$ and choosing P_d so that $\hat{\rho} = 1$. Provided the constant $C \lesssim 1$ this also yields $\hat{\Phi} \sim \mathcal{O}(1)$ close to the minimum of the potential which should be suitable since the solution we want is one in which the field spends most of its time around the minimum of the potential. Plugging in for $P_{d1} = 9 \cdot 10^{19} J/m^3$ and $P_{d2} = 9 \cdot 10^{15} J/m^3$ we find

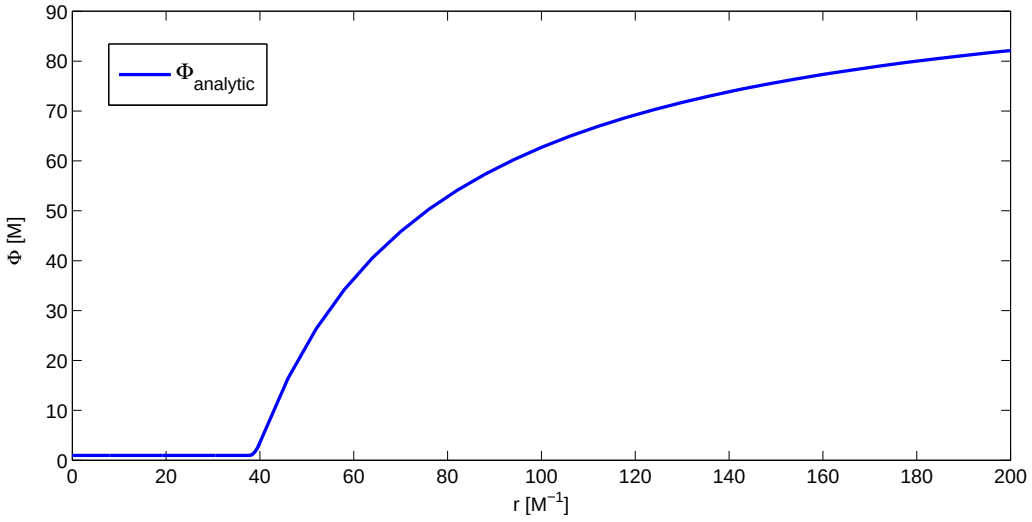

Figure 7.2: Approximate analytic solution of Φ for a ball of Beryllium in air for $n = \beta = 1, M = 6 \cdot 10^3 m^{-1}$

$P_{d1} \equiv 9 \cdot 10^{19}$	J/m^3	$P_{d2} \equiv 9 \cdot 10^{15}$	J/m^3
$\Phi_{d1} = 5.8 \cdot 10^3$	m^{-1}	$\Phi_{d2} = 5.8 \cdot 10^5$	m^{-1}
$R_{d1} = 1.6 \cdot 10^{-4}$	m	$R_{d2} = 1.6 \cdot 10^{-1}$	m
$C_1 = 4.7 \cdot 10^{-31}$		$C_2 = 4.7 \cdot 10^{-29}$	

Finally we rewrite the second order differential equation as two coupled first order equations, treating $\hat{\Phi}$ and $\hat{\lambda} = \frac{d\Phi}{dr}$ as independent variables

$$\begin{aligned} \frac{d\hat{\Phi}}{d\hat{r}} &= \hat{\lambda} \\ \frac{d\hat{\lambda}}{d\hat{r}} + \frac{2}{\hat{r}}\hat{\lambda} &= -\hat{\Phi}^{-(n+1)} + e^{C\hat{\Phi}}\hat{\rho}_m(r) \end{aligned} \tag{7.23}$$

and solve for the two regions using Matlab's built in ODE suite on the two regions, using the final values of the first solver as initial conditions for the second. What we want to show is that there exists an initial value $\Phi(0)$ that gives a solution similar to the analytic approximation but numerics show that if we start the first solver at $r = 0$ this seems to require fine tuning of the initial value of Φ beyond the number of significant digits allowed by Matlab (uses roughly 16 significant decimal digits). We therefore choose to start the solver at a value r_i where we are able to tune Φ_i and the validity of our approach thus rests on the assumption that there actually exists a value for $\Phi(0)$ that yields $\Phi(r_i) = \Phi_i$, together with a negligible gradient $\lambda(r_i) \approx 0$. By trial and error we find that starting at $r_i \approx 0.2R_{\text{Be}}$ we are able to find a solution that agrees well with the analytic approximation within the limitations of Matlab. The numerical solution is plotted together with the analytic one in figure 7.3 where it should be noted that the last digit in $\hat{\Phi}_i$ corresponds to the 15th decimal digit.It is also instructive to look at the solution space around the analytic approximation. In figure 7.4 and 7.5 we have plotted the solutions for ten additional initial $\hat{\Phi}_i^n = \hat{\Phi}_i \pm n \cdot 10^{-14}$ with $n = 1, 2, 3, 4, 5$ close to and far away from the beryllium ball The solution space close to the approximate analytic solution can be explained if we again use the analogy of the ball rolling in the potential V_{roll} , see figure 7.1. If $\Phi_i^n > \Phi_i$ the ball acquires a velocity while rolling down the potential inside the sphere that is large enough for it to roll over the top of the potential outside of the sphere and continue at an accelerating rate on the other side of the top. On the other hand if $\Phi_i^n < \Phi_i$ the velocity of the ball is too small for it to roll over and it rolls back instead. A slight complication is

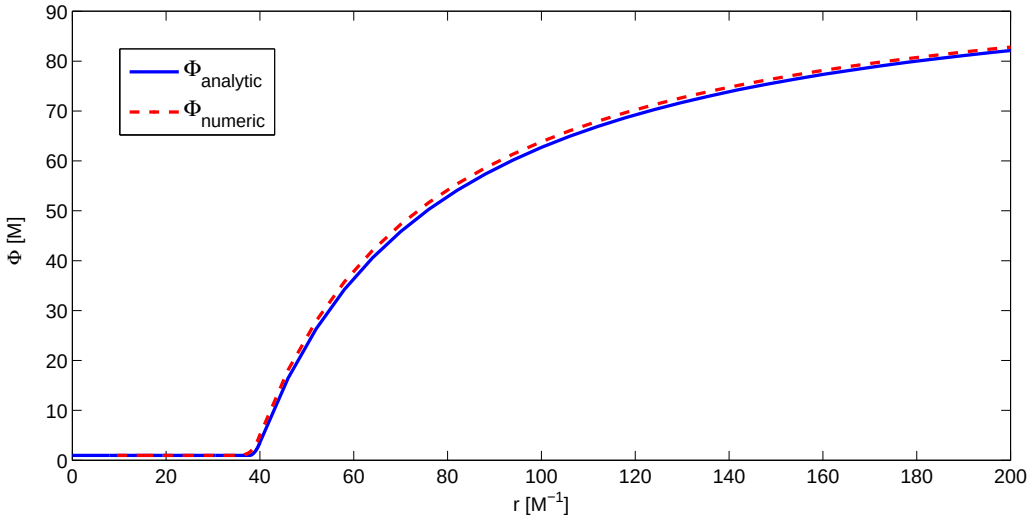

Figure 7.3: Analytic vs Numerical solution with initial conditions $\hat{\Phi}_i = 1 + 3.6994 \cdot 10^{-11}$ and $\hat{\lambda}_i = 0$ at $\hat{r}_i = 10$.

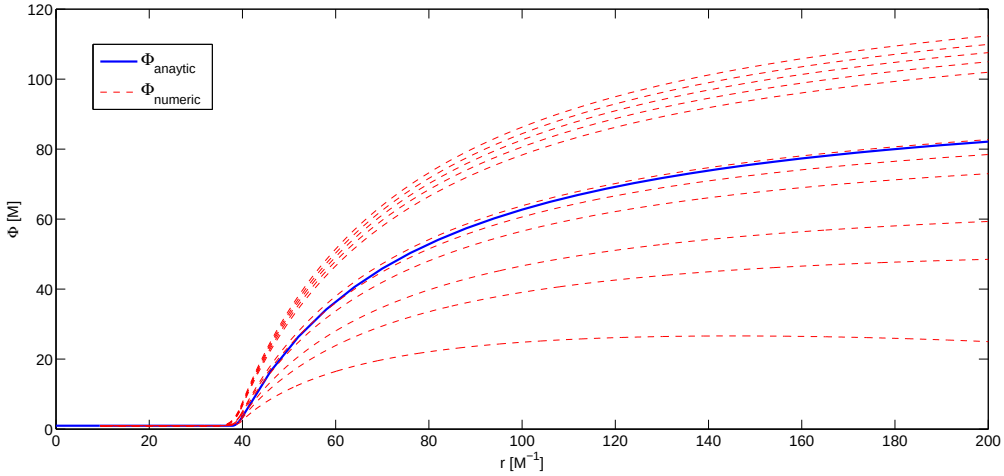

Figure 7.4: Solutions with initial values $\hat{\Phi}_i^n = \hat{\Phi}_i \pm n \cdot 10^{-14}$ with $n = 1, 2, 3, 4, 5$ together with the analytic approximation close to the sphere

the friction term which contributes to the deceleration of the ball independent of the potential and if the potential curvature drops at a significantly small radius it will cause a deceleration even for the solutions with $\Phi_i^n(R_s) > \Phi_b$. To conclude we see that all solutions except the one where the field actually reaches Φ_b as $r \to \infty$, diverges away from the analytic solution at an accelerating rate as the radius increases, in fact even the solution in figure 7.3 diverges as r becomes large enough. We must however remember that the field evolves with time on cosmological scales so the static approximation breaks down at large values of r .

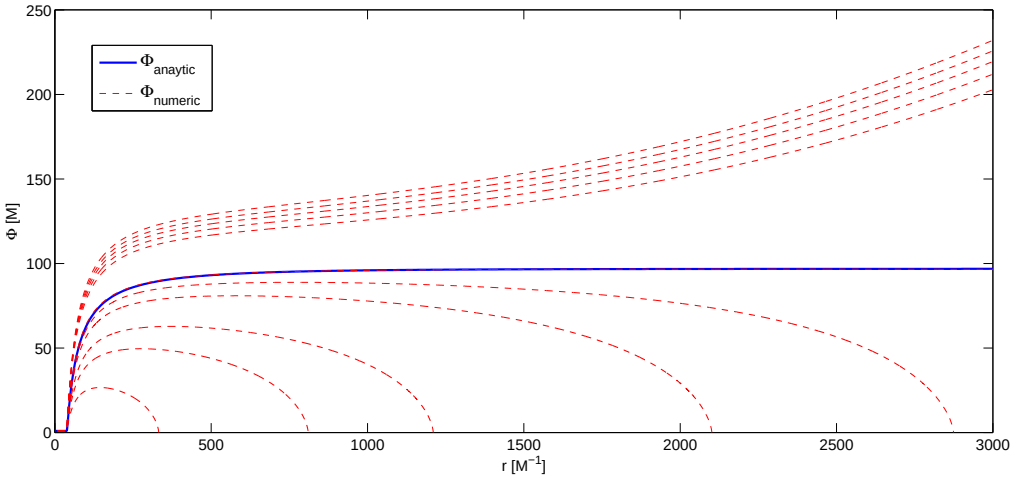

Figure 7.5: Solutions with initial values $\hat{\Phi}_i^n = \hat{\Phi}_i \pm n \cdot 10^{-14}$ with $n = 1, 2, 3, 4, 5$ together with the analytic approximation far away from the sphere

Thick Shell

Finally we proceed as in [34] and reduce the size of the ball by a factor of 40, $R_{\text{Be}} = M^{-1}$, giving a total mass $M_{\text{Be}} = 1.94 \cdot 10^{-8}\ kg$. Plugging this new values of R_{Be} and M_{Be} into the thick shell condition, equation 7.12, we find

$$C_{\text{thick}} = \frac{8\pi M_{Pl} R_{\text{Be}} \left(1 + m_{\text{air}} R_{\text{Be}}\right)}{3\beta M_{\text{Be}}} \left(\Phi_{\text{air}} - \Phi_{\text{Be}}\right) - \frac{m_{\text{air}} R_{\text{Be}}}{3} \approx 180$$

Which is much larger the 1 (90 with the original condition), implying that the thick shell approximation should be valid. Plugging in the new value of $R_{\text{Be}} = M^{-1}$ into the algorithm and using the initial value of Φ_i given for the thick shell approximation we find that staring at $r = 0$ is no longer a problem and the numerical solution fits very well with the analytic approximation, see figure 7.6

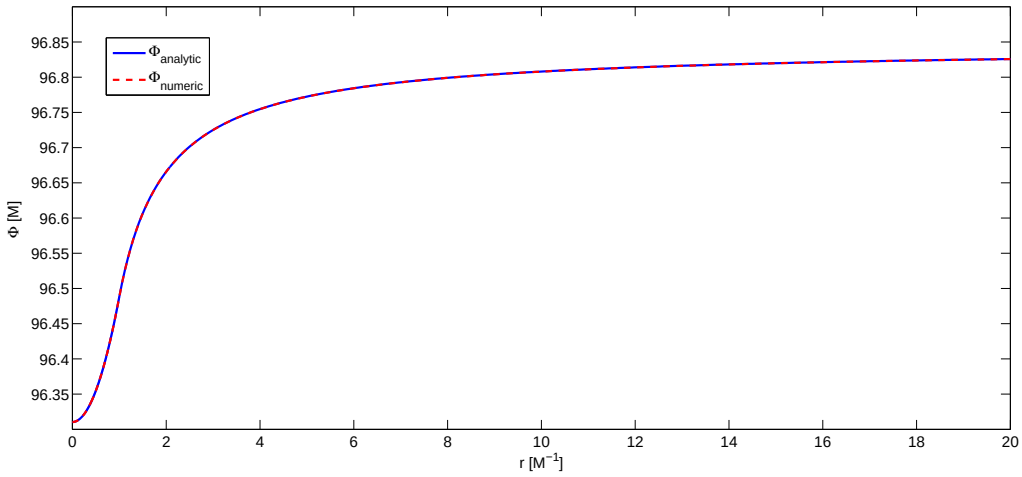

Figure 7.6: Analytic thick shell approximation vs. numerical solution for a ball of Beryllium of size $R_{\text{Be}} = M^{-1}$

As expected we see that the perturbation in the Φ field caused by the smaller beryllium ball is very small compared to the perturbations caused by the bigger one. The reason for this is that the friction term is large inside the entire sphere and to get the velocity required for the ball to reach the top of the potential outside the sphere, Φ has to start at a much larger value of Φ_i , corresponding to a much steeper potential, see figure 7.1. Looking at the solutions close to the analytic approximation, which are plotted for $\hat{\Phi}_i^n = \hat{\Phi}_i \pm n \cdot 10^{-1}$ with $n = 1, 2, 3, 4, 5$ in figure 7.7 and 7.8, we find that they are much less sensitive to variations in Φ_i then the thin shell solutions at small values of r, but as r increases and the friction term gets smaller, we see that the solutions start to diverge away from the analytic solution in a similar fashion as in the thin shell case.

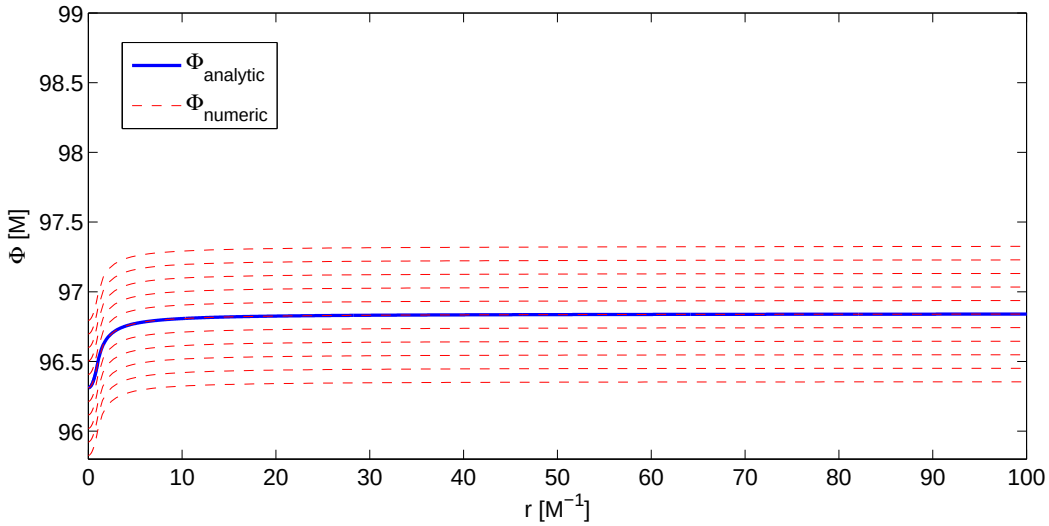

Figure 7.7: Solutions with initial values $\hat{\Phi}_i^n = \hat{\Phi}_i \pm n \cdot 10^{-1}$ with $n = 1, 2, 3, 4, 5$ together with the analytic approximation close to the sphere

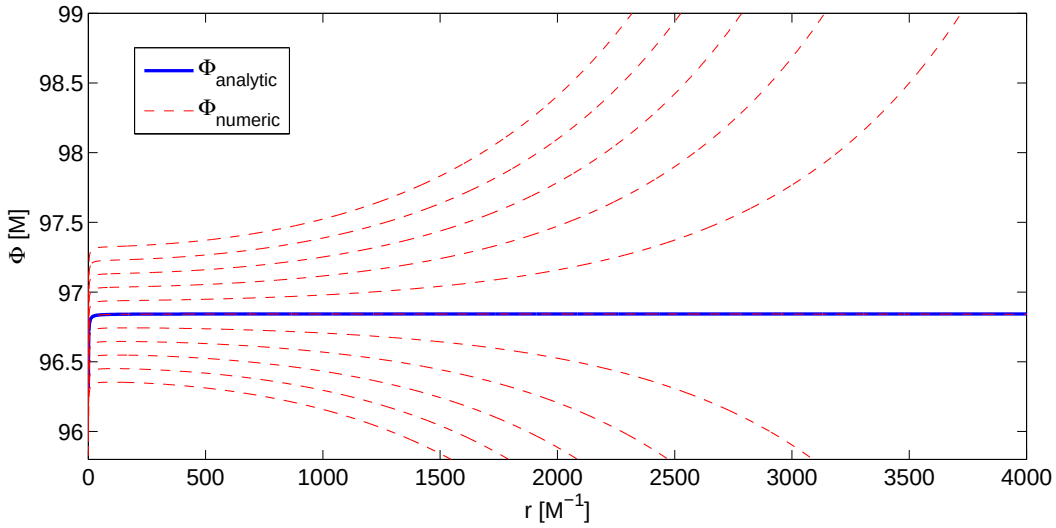

Figure 7.8: Solutions with initial values $\hat{\Phi}_i^n = \hat{\Phi}_i \pm n \cdot 10^{-1}$ with $n = 1, 2, 3, 4, 5$ together with the analytic approximation far away from the sphere

Chapter 8

A General Relativistic Approach

The first part of this chapter where we solve the ordinary TOV equations is mainly based on [14], while the following generalization to chameleon fields is the work of the author. The Problem of incorporating general relativistic effects has actually been studied already in a treatment by Tsujikawa, Tamaki and Tavakol [28], but because the treatment is very recent (dated April 3. 2009, and discovered by the author May 9. 2009) we unfortunately haven't had time to study their approach in any detail, let alone confirm their results. There are several differences between their treatment and ours, but the most crucial ones are that they actually manage to obtain physically viable solutions numerically and that they have found an analytic approximation as well. By using the approach chosen in this thesis we get solutions that fit with the intuition from the rolling ball analogy discussed in chapter 7 but we can't find the physically viable solutions where the field converges towards the minimum of V_{eff} in the background. Since the results obtained in [28] seems to be far more relevant than what is found here, we will give a very brief review of their approach and results before we give our treatment.

8.1 Treatment and Results of Tsujikawa, Tamaki and Tavakol

We now give a very brief review of the treatment in [28], where we use our notation in order to make it easier to compare results. Here they use the same chameleon coupling as we use in our prototype model so that $\Omega = e^{\beta\Phi/M_{Pl}}$, and find the coupled equations of motion for matter and chameleon in a spherical symmetric spacetime together with an analytic approximation to the Φ-profile which they confirm by numerical simulations. They start with the static spherically symmetric metric given by equation 3.31 and assume matter in the Einstein frame to be given simply by $T^m_{\mu\nu}$, neglecting the Φ-coupling in the stress-energy tensor. With this approach they get the chameleon equation of motion

$$\frac{d^2\Phi}{dr^2} + \left(\frac{2}{r} + \partial_r(\alpha - \beta)\right)\frac{d\Phi}{dr} = e^{2\beta}\left(\frac{dV}{d\Phi} + \frac{\beta}{M_{Pl}}(\rho_m - 3p_m)\right)$$

and by rewriting the equations in terms of ρ_m, p_m and m as in section 6.1 we get the equation of motion

$$(1 - 2\frac{Gm}{r})\left[\frac{d^2\Phi}{dr^2} + \left(\frac{2}{r} - \frac{4\pi G r^3(\rho_m - p_m) - 2Gm}{r(r - 2Gm)}\right)\frac{d\Phi}{dr}\right] = \frac{dV}{d\Phi} + \frac{\beta}{M_{Pl}}(\rho_m - 3p_m) \tag{8.1}$$

which is the same as our equation 6.12. They also find the TOV equations

$$\frac{dp_m}{dr} = -(\rho_m + p_m)\frac{d\alpha}{dr} + \frac{\beta}{M_{Pl}}\frac{d\Phi}{dr}(\rho_m - 3p_m) \tag{8.2}$$

$$\frac{dm}{dr} = 4\pi r^2 \rho_m \tag{8.3}$$

and by plugging in for $\partial_r\alpha$ using equation 3.42 we find

$$\frac{dp_m}{dr} = -\frac{(\rho_m + p_m)\left[4\pi G p_m r^3 + Gm\left(r\right)\right]}{r\left[r - 2Gm\left(r\right)\right]} + \frac{\beta}{M_{Pl}}\frac{d\Phi}{dr}\left(\rho_m - 3p_m\right) \tag{8.4}$$

$$\frac{dm}{dr} = 4\pi r^2 \rho_m \tag{8.5}$$

The second expression is the same as ours, with $\rho \approx \rho_m$, but the first expression is not easily comparable to our version found in section 8.2, because we write the equations in terms of the total density and pressure ρ and p . We'll continue this discussion when we get to section 8.2.

They now continue as we did in chapter 7, by looking at a sphere with radius R_s and a homogeneous matter density $\rho_m = \rho_s$ embedded in a homogeneous background of density $\rho_m = \rho_b$. By neglecting the Φ -dependence of equation 8.4 an analytic solution for p_m is obtained by integrating equations 8.4 and 8.5, and in terms of the Newtonian potential at the surface $\phi_{Ns} = \phi_N(R_s)$ they find

$$p_m(r) = \frac{\sqrt{1 - 2(r/R_s)\phi_{Ns}} - \sqrt{1 - 2\phi_{Ns}}}{3\sqrt{1 - 2\phi_{Ns}} - \sqrt{1 - 2(r/R_s)\phi_{Ns}}}\rho_s$$

which to first order in ϕ_{Ns} yields the equation of motion 8.1 inside the sphere

$$\Phi'' + \frac{2}{r}\left(1 - \frac{r^2}{2R_s^2}\phi_{Ns}\right)\Phi' = \left(V_{,\Phi} + \frac{\beta}{M_{Pl}}\rho_s\right)\left(1 + 2\phi_{Ns}\frac{r^2}{R_s^2}\right) - \frac{3\beta}{2M_{Pl}}\rho_s\phi_{Ns}\left(1 - \frac{r^2}{R_s^2}\right)$$

Using this expression, they are able to find an analytic approximation for the Φ -profile by treating Φ as a small perturbation to the flat spacetime solution Φ_0 , $\Phi = \Phi_0 + \delta\Phi$ discussed in the last chapter, where they use a slightly different approximation then we did. The solution they find is long and complicated and since we have not had time to go into the analytic work in any detail we refer to the original literature [28] for the explicit expressions.

What they find is that compared to the profile in Minkowski spacetime discussed in chapter 7, Φ is shifted near the center of the body due to the relativistic pressure correction and for large values of ϕ_{Ns} and $m_s R_s$, the chameleon gradient Φ' becomes negative in the innermost region, but becomes positive in the rolling regime and when $\Delta R << 1/(m_s R_s)$ the field acquires sufficient kinetic energy in this regime to reach the top of the potential V_{roll} outside of the body. These analytic results are confirmed numerically in gravitational backgrounds with $\phi_{Ns}(R_s) \lesssim 0.3$ by using the analytic solutions to obtain appropriate boundary conditions. Their results are given in figure 8.1

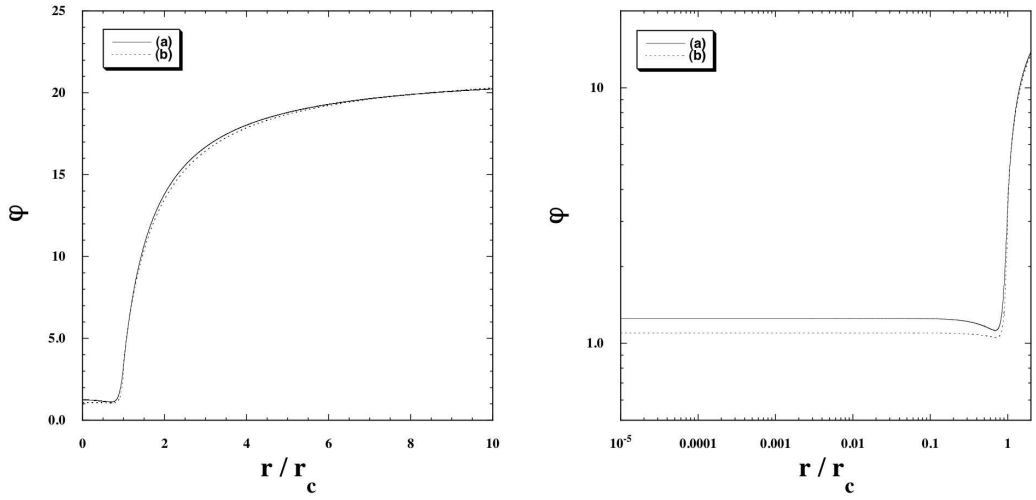

Figure 8.1: Thin shell field profile found by Tsujikawa et. al. for $\Phi_c = 0.2, n = 2, \beta = 1,\ \Delta R = 0.1$ and $m_s R_s = 20.0$, expressed in terms of the dimensionless field $\varphi = \Phi/\Phi_s$ as a function of $x = r/R_s$. The black and dotted lines corresponds to the numerical and analytic solutions respectively where the initial value for the numerical profile is $\varphi_i = 1.2539010$ at $x_i = 10^{-5}$ compared to $\varphi_i = 1.2539010$ for the analytic one.

We will end this thesis by giving our approach to the problem and discuss the results we managed to obtain with our algorithm.

8.2 Our General Relativistic Approach

8.2.1 TOV with Chameleon

Our approach to the problem is to generalize the numerical treatment in section 3.6 by including the chameleon, where we use our prototype model given by equation 6.1. Even though we are not able to study the physical solutions because of the initial value problems already discussed, it seems plausible that the equations are valid and that they might be solvable given a more sophisticated algorithm. Further more the solutions we do find seems to fit well with the intuitive notion of a ball rolling in the potential V_{roll} . In our treatment we use the total density $\rho = \rho_{m\Phi} + \rho_\Phi$ and pressure $p = p_{m\Phi} + p_\Phi$, where we have explicit expressions for the density and pressure of the chameleon given by equation 6.17 and 6.18. This means that for a given central density ρ_c , equation of state and initial values for Φ , we have all the information we need since we can find $\rho_{m\Phi}$ and $p_{m\Phi}$ by subtracting the free chameleon density and pressure from the total ones. We choose to model the coupled fluid using the polytropic approximation given by equation 3.64 and simply denote the coupled densities and pressure $\rho_{m\Phi}$ and $p_{m\Phi}$ by ρ_m and p_m . A more realistic approach would be to take into account the Φ -coupling when choosing an equation of state, so that $p_m = f(\rho_m, \Phi)$, but at this level of approximation our choice should be sufficient.

In section 6.3 we argued that the Einstein equations considered in 3.5 are valid as long as we remember that the density and pressure from the right hand side of Einstein's equations 3.30 comes from the full stress-energy tensor $T^M_{\mu\nu} = T^\Phi_{\mu\nu} + T^m_{\mu\nu}$, and for this reason the TOV equations in the coupled case are simply given by the ordinary TOV equations 3.43 and 3.44 but where ρ and p is now composed of two forms of energy with different equations of state. We already rendered these equations dimensionless in section 3.6 so we still have the dimensionless TOV part

$$\textbf{I} \quad \frac{dp}{dr} = -\frac{(\rho+p)\left[4\pi G p r^3 + Gm\,(r)\right]}{r\left[r - 2Gm\,(r)\right]} \quad , \quad \textbf{II} \quad \frac{dm}{dr} = 4\pi r^2 \rho$$

$$(\rho, p) = P_d(\hat{\rho}, \hat{p}) \qquad m = M_d \hat{m} \qquad r = R_d \hat{r}$$
$$P_d = \rho_c \qquad M_d = \frac{1}{\sqrt{4\pi G^3 P_d}} \qquad R_d = \frac{1}{\sqrt{4\pi G P_d}}$$

$$\Rightarrow \ \textbf{I} \quad \frac{d\hat{p}}{d\hat{r}} = -\frac{(\hat{\rho}+\hat{p})\left[\hat{p}\hat{r}^3 + \hat{m}\right]}{\hat{r}\left[\hat{r} - 2\hat{m}\right]} \quad , \quad \textbf{II} \quad \frac{d\hat{m}}{d\hat{r}} = \hat{r}^2 \hat{\rho}$$

But where the density and pressure now corresponds to the total pressure and density of both chameleon and matter given by different equations of state

$$\hat{\rho} = \hat{\rho}_m + \hat{\rho}_\Phi \quad , \quad \hat{p} = \hat{p}_m + \hat{p}_\Phi$$
$$\hat{p}_\Phi = \hat{\rho}_\Phi - 2V(\hat{\Phi}) \quad , \quad \hat{p}_m = \hat{K}\hat{\rho}_m^{5/3}$$

To see how TOV equation **I** compares to the one obtained by Tsujikawa et. al in [28] we assume $\Phi'', V << p_m$ yielding the right hand side of the equation identical to the uncoupled version. The only contribution from Φ then comes from the the left hand side through the derivative of the chameleon pressure, $\partial_r p_\Phi$, which when neglecting Φ'^2 -terms is approximately given by

$$\frac{dp_\Phi}{dr} = \frac{d}{dr}\left[\frac{1}{2}\left(1 - \frac{2Gm}{r}\right)\Phi'^2 - V(\Phi)\right] \approx \Phi'\left[\left(1 - \frac{2Gm}{r}\right)\Phi'' - \partial_\Phi V\right]$$

By comparing this result with what is found from multiplying the equation of motion by Φ' and neglecting the Φ'^2 -term we find

$$\left(1 - \frac{2Gm}{r}\right)\Phi'\Phi'' \approx \Phi'\partial_\Phi V + \Phi'\frac{\partial_\Phi \Omega}{\Omega}\left(\rho_{m\Phi} - 3p_{m\Phi}\right)$$
$$\Rightarrow \quad \frac{dp_\Phi}{dr} \approx \frac{\partial_\Phi \Omega}{\Omega}\frac{d\Phi}{dr}\left(\rho_{m\Phi} - 3p_{m\Phi}\right) \tag{8.6}$$

which, when moved to the left hand side of the equation, yields the coupling term given in 8.2. Continuing our treatment we need to know how much of the total density and pressure is attributed to the chameleon and how much is attributed to matter, and as such we close the set of equations by adding the chameleon equation of motion in the dimensionless form given by equation 7.21, but with the friction term replaced by the general relativistic one given in 6.12

$$\frac{d^2\hat{\Phi}}{d\hat{r}^2} + \left(\frac{2}{\hat{r}} - \frac{\hat{r}^3\left(\hat{\rho} - \hat{p}\right) - 2\hat{m}}{\hat{r}\left[\hat{r} - 2\hat{m}\right]}\right)\frac{d\hat{\Phi}}{d\hat{r}} = -A\hat{\Phi}^{-(n+1)} + B\left(\hat{\rho}_m - 3\hat{K}\hat{\rho}_m^{5/3}\right)$$
$$A = \frac{nM^{4+n}R_d^2}{\Phi_d^{n+2}} \qquad , \qquad B = \frac{\beta R_d^2 P_d}{M_{Pl}\Phi_d}$$

where we choose $A = B = C_1$ so that the dimensionless chameleon $\hat{\Phi}$ is $\mathcal{O}(1)$ when the chameleon is close to the minimum of the effective potential V_{eff} at $r = 0$

$$A = B = C_1 \quad \Rightarrow \quad \Phi_d = \left(\frac{nM_{Pl}M^{4+n}}{\beta P_d}\right)^{1/(n+1)}$$

we also need the pressure and density of the free chameleon, given by 6.17 and 6.18, which in dimensionless form can be written

$$\hat{\rho}_\Phi = C_2\left(1-\frac{2\hat{m}}{\hat{r}}\right)\left(\frac{d\hat{\Phi}}{d\hat{r}}\right)^2 + C_3\hat{\Phi}^{-n} \quad , \quad p_\Phi = C_2\left(1-\frac{2\hat{m}}{\hat{r}}\right)\left(\frac{d\hat{\Phi}}{d\hat{r}}\right)^2 - C_3\hat{\Phi}^{-n}$$

$$C_2 = \frac{\Phi_d^2}{2R_d^2P_d} \qquad , \qquad C_3 = \frac{M^4}{P_d}\left(\frac{M}{\Phi_d}\right)^n$$

and finally by rewriting the chameleon equation of motion as two coupled first order equations as in chapter 7 and combining all these expressions, we obtain the full set of equations to be solved numerically

I $$\frac{d\hat{p}}{d\hat{r}} = -\frac{(\hat{\rho}+\hat{p})\left[\hat{p}\hat{r}^3+\hat{m}\right]}{\hat{r}\left[\hat{r}-2\hat{m}\right]}$$

II $$\frac{d\hat{m}}{d\hat{r}} = \hat{r}^2\hat{\rho}$$

III $$\frac{d\hat{\lambda}}{d\hat{r}} = -\left(\frac{2}{\hat{r}} - \frac{\hat{r}^3(\hat{\rho}-\hat{p})-2\hat{m}}{\hat{r}\left[\hat{r}-2\hat{m}\right]}\right)\hat{\lambda} + C_1\frac{\hat{\rho}_m - 3\hat{K}\hat{\rho}_m^{5/3} - \hat{\Phi}^{-(n+1)}}{\left(1-\frac{2\hat{m}}{\hat{r}}\right)}$$

IV $$\frac{d\hat{\Phi}}{d\hat{r}} = \hat{\lambda}$$

V Equations of State

$$\hat{\rho} = \hat{\rho}_m + \hat{\rho}_\Phi \quad , \quad \hat{p} = \hat{p}_m + \hat{p}_\Phi$$

$$\hat{\rho}_\Phi = C_2\left(1-\frac{2\hat{m}}{\hat{r}}\right)\hat{\lambda}^2 + C_3\hat{\Phi}^{-n} \quad , \quad \hat{p}_\Phi = C_2\left(1-\frac{2\hat{m}}{\hat{r}}\right)\hat{\lambda}^2 - C_3\hat{\Phi}^{-n}$$

$$\hat{p}_m = \hat{K}\hat{\rho}_m^{5/3}$$

8.2.2 Numerical Solutions

The Full Set of Equations

To get an idea of the order of magnitude of the dimensionless constants that appear in our equation for neutron star densities, we choose $P_d = \rho_c = 10^{35}\ J/m^3$, and look at a model with $n = \beta = 1$ and $M = 10^3\ m^{-1}$ which yields

Dimensionfull Constants		Dimensionless Constants
$R_d = 6.6461$	$[10\ km]$	$C_1 = 1.25 \cdot 10^{40}$
$M_d = 0.9815$	$[M_\odot]$	$C_2 = 6.4 \cdot 10^{-81}$
$\Phi_d = 1.98 \cdot 10^{-6}$	$[m^{-1}]$	$C_3 = 1.6 \cdot 10^{-40}$

We see that by choosing our dimensionless constant so that the dimensionless integration interval, central density and initial value for Φ are all $\mathcal{O}(1)$ we see that C_1 becomes extremely large meaning both that the friction term is negligible throughout most of the star, and that the natural scale of the curvature of the

potential V_{eff} is extremely large compared to the value Φ takes at the center of the star. Alternatively we could have chosen R_d so that $C_1 = 1$ but in this case we would have corresponding large numerical constants in the TOV equation and in the Chameleon equation the curvature of the potential would be of the same order as Φ but the integration interval would be very large instead. We also find that the fine tuning problem is much more severe. The closest we got to the right initial value, using $n = \beta = 1, M = 10^3\ m^{-1}$ and starting integration at $r_0 = 10^{-6}\ m$, was $\Phi_i = 1.11306798573713716$. The resulting profile is not able to stay close the top of the potential and rolls down the right hand side, but by lowering the last digit in Φ_i, the field is not able to stay on the right hand side of the maximum of V_{roll} and drops to zero on scales $r = r_0 + \mathcal{O}(10^{-15}\ m)$. However we see that the fine tuning helps and it seems plausible that if we had infinitely many significant digits then we could fine tune Φ_i so that it neither rolls down on the left or the right but reaches the maximum of V_{roll} in the background as $r \to \infty$. The profile for Φ_i is shown in figure 8.2a, while the effect of fine tuning are shown in figure 8.2b

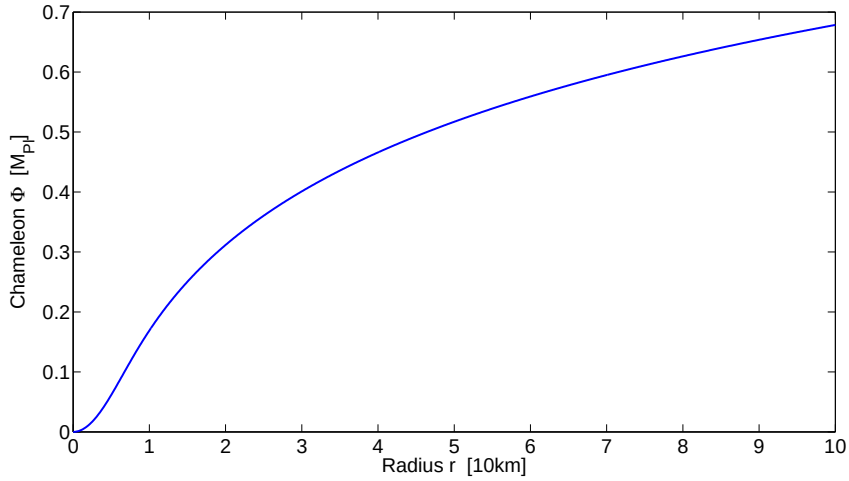

a.)

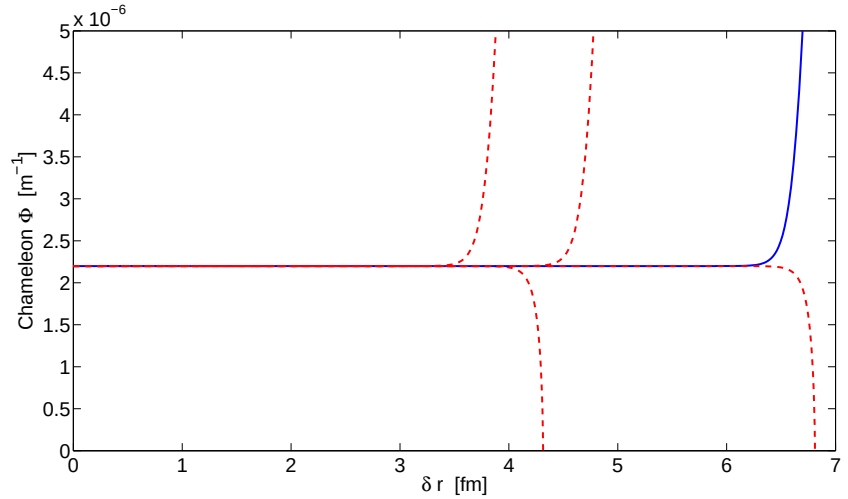

b.)

Figure 8.2: a) Profile for $\Phi(r = 10^{-6}m) = \Phi_i$ for $\rho_c = 10^{35}\ J/m^3, M = 10^3\ m^{-1}$ and $n = \beta = 1$. b) Effect of small variations in the initial value, $\hat{\Phi}(\hat{r}_0) = \Phi_i \pm 2n \cdot 10^{-17}$ for $n = 1, 2$, in the interval $r = r_0 + \delta r$ with $r_0 = 1\mu m$. The blue line corresponds to the Φ_i solution while the red dotted lines corresponds to the variations, larger initial values corresponds to the overshooting solutions, while smaller initial values to the undershooting solutions.

The profile in figure 8.2a was found together with the density, pressure and mass profiles given in figure 8.3

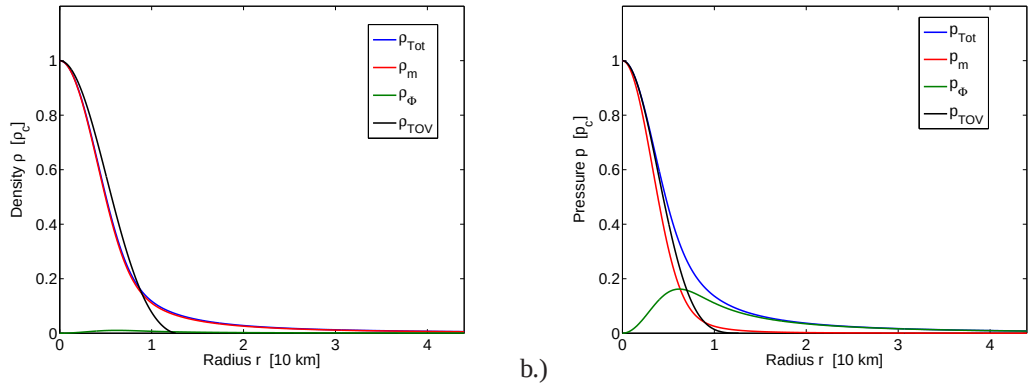

a.) b.)

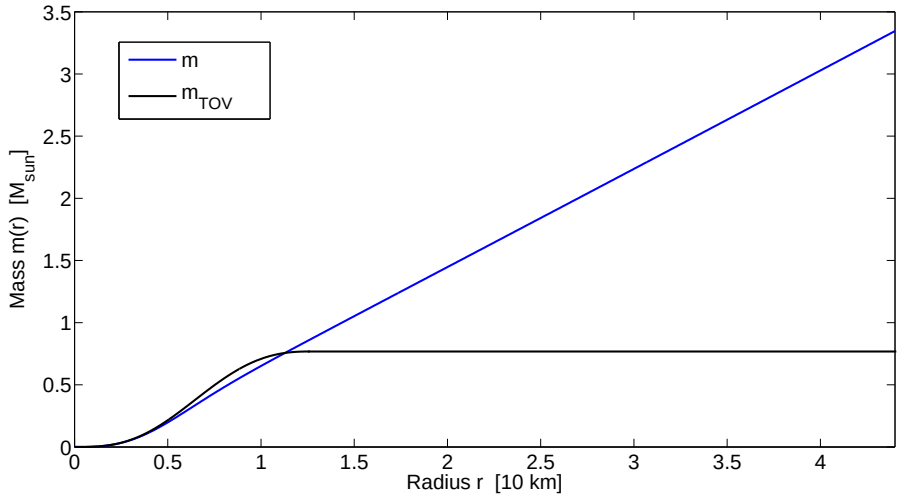

c.)

Figure 8.3: a.) Total density profile together with the individual contributions from chameleon and matter, together with the corresponding profile from the ordinary TOV equations. b.) Similar plot but this time for the pressure. c.) Comparison of the mass profiles with and without Chameleon

We see that when the Chameleon is not able to stay around the maximum of the potential V_{roll} , it quickly starts rolling down on the right hand side, giving rise to considerable contributions to the total pressure and density, and the contributions causes the matter density to decline slower than it would without it. This gives a larger stellar mass and radius than in the ordinary treatment in section 3.6, because the the matter density and pressure no longer tends to zero at $r \approx 8\ km$.

The increase in instability of the thin shell solution can be seen by generalizing the rolling argument from chapter 7 but this time the maximum of the potential V_{roll} depends on the radial coordinate r . To obtain a converging solution we need Φ to change in such a way that it stays on the right hand side of the potential throughout most of the star, but close enough to the maximum to get caught up by the potential as the density reaches the background density ρ_b before it rolls up towards the maximum outside, eventually reaching it as $r \to \infty$. From this point of view the increase in instability of the converging solution, compared to the Beryllium ball example, is mostly due to the field having to balance close to the top of an extremely steep potential for a considerable amount of time. In addition we also have the relativistic effects, which reduces the time dependent friction term due to the negative density correction and also increases the slope of the potential through the mass correction, making the converging solution even more

sensitive to variations in the initial conditions. We also need to consider that the maximum changes with r but this does not seem to make a lot of difference. This can be seen by looking at how the maximum of V_{roll} changes with r. The potential depends inversely on the density and pressure

$$\Phi_{max}(r) \approx \left(\frac{nM^{4+n}M_{Pl}}{\beta(\rho_m(r) - 3p_m(r))} \right)^{1/(n+1)} \tag{8.7}$$

and for the the parameters we have used, $\beta = 1$ and $M = 10^3$, $\Phi_{max} \sim 1$ when $\rho \sim 10^{27}\ J/m^3$. This means that for $\rho > 10^{27}\ J/m^3$, an order of magnitude change in ρ, only induces a change in the leading decimal of Φ_{max}. In the profiles obtained in chapter 3.6 the density drops from $\rho \sim 10^{35}$ to $rho \sim 10^{30}$ from $r = 0$ to $r = 0.99 * R_s$ so that the maximum of the potential is of order one or smaller throughout 99% of the star, before the density drops below $10^{27}\ J/m^3$ in a thin shell just below the surface, where practically all the change in the maxima occurs. In figure 8.4 we have plotted the maximum as a function of r for the original pressure and density profiles together with the original thin shell solution from chapter 7, where we have added a background density $\rho_b = 10^{-5}\ J/m^3$ to the density profile to obtain a background maximum for V_{roll}. This choice of ρ_b roughly corresponds to the density of baryonic gas and dark matter in the Milky Way, [34]

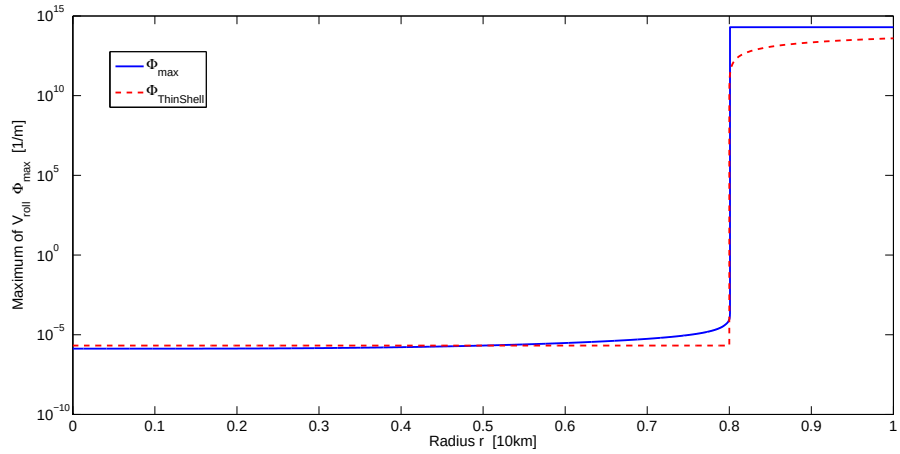

Figure 8.4: The maximum of V_{roll} as a function of radius (blue line) together with the non relativistic thin shell solution (red dotted line)

We see that approximating the density inside the star as constant is a good approximation because most of the change in the maximum occurs when the density is close to the background density. We also see that if we assume that the field stays close to the maximum of V_{roll} then Φ changes very little except for a thin shell close to the surface, and since the corrections to the matter density and pressure profiles from the rapidly changing solution in figure 8.2a were quite small it seems unlikely that the converging Φ -profile , if it exists, would alter the original TOV results significantly.

Chapter 9

Concluding Remarks

We end this thesis by giving a summary of the results we have obtained and how these can be built upon

9.1 Short Summary of Results

Unfortunately our treatment has given us no firm predictions, but we have seen that the physically viable converging solutions are difficult to obtain due to extreme sensitivity to variations in the the value of Φ at the core. These fine tuning issues were so severe that we did not manage to obtain the converging solutions for the maximum mass neutron star using $\beta = 1, n = 1$ and $M = 6 \cdot 10^3 m^{-1}$. These problems where seen to become even more severe when relativistic effects where taken into account.

We also found that the solutions we did obtain fits well with the notion of a ball rolling in a potential V_{roll} , but that the solutions either overshot the top of the exterior potential or got caught up by the maximum of the interior potential causing the field to drop to zero. In fact we found the rolling ball analogy to be a very helpful tool for studying the solutions to the chameleon equations of motion and that both the stability of the solutions and the parameter dependence of the thin shell could be roughly explained using this analogy.

We also looked at the solutions we managed to obtain where the field rapidly rolled towards large values and got significant but not dominating pressure and density contributions from the chameleon in the TOV equation. These contributions caused the matter density to drop to zero much slower than in the ordinary TOV equations and gave both a larger stellar mass M and radius R . However the change in the matter density profiles were not that large, at least not compared to how rapidly the chameleon changed compared to what one naively would expect from a physically viable converging solution. This seems to suggest that a significant change in the stability of a neutron star is unlikely if the chameleon stays close to the maximum of the potential.

9.2 Things For The Future

The obvious next step is to try to develop an algorithm that manages to deal with the stability issues. With such an algorithm at hand we could see whether our rather dubious predictions hold and hopefully also be able to obtain constraints on the values of β and M from the results. Other obvious extensions of the work done in this thesis is to look at more realistic equations of state, where we could take into account the Φ coupling in ρ_m , and to find analytic approximations that could be validated by the numerics and used as a basis for an analytical treatment of the problem. When it comes to how we should go about finding a working algorithm we have no good suggestions, but it seems like a way out of the problem might be to use an algorithm that takes as its starting point the boundary values at both $r = 0$ and $r = \infty$ and uses some kind of predictor-corrector scheme to find the best fit solution. However all this is for the future...

Appendices

Appendix A

Einstein Tensors

In this appendix I'll calculate the components of the Einstein tensor $E_{\mu\nu}$ for the spatially homogeneous and isotropic spacetime used to find the Friedmann equations, and for the spherically symmetric spacetime used to find the TOV equations. I'll do the calculations in coordinate basis where the connection can be written in terms of the metric $g_{\mu\nu}$

$$\Gamma^{\alpha}{}_{\mu\nu} = \frac{1}{2} g^{\alpha\lambda} \left(\partial_\nu g_{\mu\lambda} + \partial_\mu g_{\lambda\nu} - \partial_\lambda g_{\mu\nu} \right)$$

These can be used to find the components of the Riemann tensor $R^{\alpha}{}_{\mu\beta\nu}$, the Ricci tensor $R_{\mu\nu}$, the Ricci scalar R and eventually the Einstein tensor $E_{\mu\nu}$.

$$\begin{aligned}
R^{\alpha}{}_{\mu\beta\nu} &= \partial_\beta \Gamma^{\alpha}{}_{\mu\nu} + \Gamma^{\alpha}{}_{\beta\lambda} \Gamma^{\lambda}{}_{\mu\nu} - \partial_\nu \Gamma^{\alpha}{}_{\mu\beta} - \Gamma^{\alpha}{}_{\nu\lambda} \Gamma^{\lambda}{}_{\mu\beta} \\
R_{\mu\nu} &= \delta^{\beta}{}_{\alpha} R^{\alpha}{}_{\mu\beta\nu} = R^{\alpha}{}_{\mu\alpha\nu} \\
R &= g^{\mu\nu} R_{\mu\nu} = R^{\mu}{}_{\mu} \\
E_{\mu\nu} &= R_{\mu\nu} - \frac{1}{2} R g_{\mu\nu}
\end{aligned}$$

An alternative, and perhaps easier way to find the components of the Einstein tensor is by using the Cartan formalism, see [5], but this requires a coordinate independent formulation of GR.

A.1 Spatially Homogeneous and Isotropic Spacetime

The lineelement ds^2 for a homogeneous and isotropic spacetime in spherical coordinates t, r, θ, ϕ takes the form

$$ds^2 = -dt^2 + a^2(t) \left[\frac{1}{1 - kr^2} dr^2 + r^2 d\theta^2 + r^2 \sin^2\theta d\phi^2 \right]$$

Christoffel Symbols $\Gamma^{\alpha}{}_{\mu\nu}$

This lineelement yields the following non-vanishing Christoffel symbols $\Gamma^{\alpha}{}_{\mu\nu}$, together with the ones related to these by the symmetry of the lower indices $\mu\nu = \nu\mu$. I use the fact that for a diagonal metric the inverse is given by $g^{\mu\nu} = \frac{1}{g_{\mu\nu}}$.

- $\alpha = t$:

$$\Gamma^t{}_{rr} = \frac{1}{2}\partial_t g_{rr} = \left(1-kr^2\right)^{-1} a\partial_t a \tag{A.1}$$

$$\Gamma^t{}_{\theta\theta} = \frac{1}{2}\partial_t g_{\theta\theta} = r^2 a\partial_t a \tag{A.2}$$

$$\Gamma^t{}_{\phi\phi} = \frac{1}{2}\partial_t g_{\phi\phi} = r^2\sin^2\theta a\partial_t a \tag{A.3}$$

- $\alpha = r$:

$$\Gamma^r{}_{tr} = \frac{1}{2}\left(1-kr^2\right)a^{-2}\partial_t g_{rr} = \frac{\partial_t a}{a} \tag{A.4}$$

$$\Gamma^r{}_{rr} = \frac{1}{2}\left(1-kr^2\right)a^{-2}\partial_r g_{rr} = \left(1-kr^2\right)^{-1} kr \tag{A.5}$$

$$\Gamma^r{}_{\theta\theta} = -\frac{1}{2}\left(1-kr^2\right)a^{-2}\partial_r g_{\theta\theta} = -\left(1-kr^2\right) r \tag{A.6}$$

$$\Gamma^r{}_{\phi\phi} = -\frac{1}{2}\left(1-kr^2\right)a^{-2}\partial_r g_{\phi\phi} = -\left(1-kr^2\right) r\sin^2\theta \tag{A.7}$$

$$\tag{A.8}$$

- $\alpha = \theta$:

$$\Gamma^\theta{}_{t\theta} = \frac{1}{2}r^{-2}a^{-2}\partial_t g_{\theta\theta} = \frac{\partial_t a}{a} \tag{A.9}$$

$$\Gamma^\theta{}_{r\theta} = \frac{1}{2}r^{-2}a^{-2}\partial_r g_{\theta\theta} = \frac{1}{r} \tag{A.10}$$

$$\Gamma^\theta{}_{\phi\phi} = -\frac{1}{2}r^{-2}a^{-2}\partial_\theta g_{\phi\phi} = -\sin\theta\cos\theta \tag{A.11}$$

$$\tag{A.12}$$

- $\alpha = \phi$:

$$\Gamma^\phi{}_{t\phi} = \frac{1}{2}r^{-2}\sin^{-2}\theta a^{-2}\partial_t g_{\phi\phi} = \frac{\partial_t a}{a} \tag{A.13}$$

$$\Gamma^\phi{}_{r\phi} = \frac{1}{2}r^{-2}\sin^{-2}\theta a^{-2}\partial_r g_{\phi\phi} = \frac{1}{r} \tag{A.14}$$

$$\Gamma^\phi{}_{\theta\phi} = \frac{1}{2}r^{-2}\sin^{-2}\theta a^{-2}\partial_\theta g_{\phi\phi} = \frac{\cos\theta}{\sin\theta} \tag{A.15}$$

$$\tag{A.16}$$

Riemann Tensor $R^\alpha{}_{\mu\beta\nu}$

Using the Christoffel symbols we can construct the components of the Riemann tensor. I will focus on the components relevant for $R_{\mu\nu}$. The non-vanishing relevant components are

- $\alpha = \beta = t$:

$$
\begin{aligned}
R^{t}{}_{rtr} &= \partial_t \Gamma^{t}{}_{rr} - \Gamma^{t}{}_{rr}\Gamma^{r}{}_{tr} \\
&= \left(1 - kr^2\right)^{-1} a \partial_t^2 a && \text{(A.17)} \\
R^{t}{}_{\theta t\theta} &= \partial_t \Gamma^{t}{}_{\theta\theta} - \Gamma^{t}{}_{\theta\theta}\Gamma^{\theta}{}_{t\theta} \\
&= r^2 a \partial_t^2 a && \text{(A.18)} \\
R^{t}{}_{\phi t\phi} &= \partial_t \Gamma^{t}{}_{\phi\phi} - \Gamma^{t}{}_{\phi\phi}\Gamma^{\phi}{}_{t\phi} \\
&= r^2 \sin^2\theta a \partial_t^2 a && \text{(A.19)}
\end{aligned}
$$

- $\alpha = \beta = r$:

$$
\begin{aligned}
R^{r}{}_{trt} &= -\partial_t \Gamma^{r}{}_{tr} - \Gamma^{r}{}_{tr}\Gamma^{r}{}_{tr} \\
&= -\frac{\partial_t^2 a}{a} && \text{(A.20)} \\
R^{r}{}_{\theta r\theta} &= \partial_r \Gamma^{r}{}_{\theta\theta} + \Gamma^{r}{}_{tr}\Gamma^{t}{}_{\theta\theta} + \Gamma^{r}{}_{rr}\Gamma^{r}{}_{\theta\theta} - \Gamma^{r}{}_{\theta\theta}\Gamma^{\theta}{}_{r\theta} \\
&= r^2 \left[(\partial_t a)^2 + k\right] && \text{(A.21)} \\
R^{r}{}_{\phi r\phi} &= \partial_r \Gamma^{r}{}_{\phi\phi} + \Gamma^{r}{}_{tr}\Gamma^{t}{}_{\phi\phi} + \Gamma^{r}{}_{rr}\Gamma^{r}{}_{\phi\phi} - \partial_\phi \Gamma^{r}{}_{\phi r} - \Gamma^{r}{}_{\phi\phi}\Gamma^{\phi}{}_{r\phi} \\
&= r^2 \sin^2\theta \left[(\partial_t a)^2 + k\right] && \text{(A.22)}
\end{aligned}
$$

- $\alpha = \beta = \theta$:

$$
\begin{aligned}
R^{\theta}{}_{t\theta t} &= -\partial_t \Gamma^{\theta}{}_{t\theta} - \left(\Gamma^{\theta}{}_{t\theta}\right)^2 \\
&= -\frac{\partial_t^2 a}{a} && \text{(A.23)} \\
R^{\theta}{}_{r\theta r} &= \Gamma^{\theta}{}_{t\theta}\Gamma^{t}{}_{rr} + \Gamma^{\theta}{}_{r\theta}\Gamma^{r}{}_{rr} - \partial_r \Gamma^{\theta}{}_{r\theta} - \left(\Gamma^{\theta}{}_{r\theta}\right)^2 \\
&= \left(1 - kr^2\right)^{-1} \left[(\partial_t a)^2 + k\right] && \text{(A.24)} \\
R^{\theta}{}_{\phi\theta\phi} &= \partial_\theta \Gamma^{\theta}{}_{\phi\phi} + \Gamma^{\theta}{}_{t\theta}\Gamma^{t}{}_{\phi\phi} + \Gamma^{\theta}{}_{r\theta}\Gamma^{r}{}_{\phi\phi} - \Gamma^{\phi}{}_{\theta\phi}\Gamma^{\theta}{}_{\phi\phi} \\
&= r^2 \sin^2\theta \left[(\partial_t a)^2 + k\right] && \text{(A.25)}
\end{aligned}
$$

- $\alpha = \beta = \phi$:

$$
\begin{aligned}
R^{\phi}{}_{t\phi t} &= -\partial_t \Gamma^{\phi}{}_{t\phi} - \left(\Gamma^{\phi}{}_{t\phi}\right)^2 \\
&= -\frac{\partial_t^2 a}{a} && \text{(A.26)} \\
R^{\phi}{}_{r\phi r} &= \Gamma^{\phi}{}_{t\phi}\Gamma^{t}{}_{rr} + \Gamma^{\phi}{}_{r\phi}\Gamma^{r}{}_{rr} - \partial_r \Gamma^{\phi}{}_{r\phi} - \left(\Gamma^{\phi}{}_{r\phi}\right)^2 \\
&= \left(1 - kr^2\right)^{-1} \left[(\partial_t a)^2 + k\right] && \text{(A.27)} \\
R^{\phi}{}_{\theta\phi\theta} &= \Gamma^{\phi}{}_{t\phi}\Gamma^{t}{}_{\theta\theta} + \Gamma^{\phi}{}_{r\phi}\Gamma^{r}{}_{\theta\theta} - \partial_\theta \Gamma^{\phi}{}_{\theta\phi} - \left(\Gamma^{\phi}{}_{\theta\phi}\right)^2 \\
&= r^2 \left[(\partial_t a)^2 + k\right] && \text{(A.28)}
\end{aligned}
$$

Ricci Tensor $R_{\mu\nu}$ and Ricci Scalar R

- Ricci Tensor $R_{\mu\nu}$

$$\begin{aligned} R_{tt} &= R^{r}{}_{trt} + R^{\theta}{}_{t\theta t} + R^{\phi}{}_{t\phi t} \\ &= -3\frac{\partial_t^2 a}{a} && \text{(A.29)} \\ R_{rr} &= R^{t}{}_{rtr} + R^{\theta}{}_{r\theta r} + R^{\phi}{}_{r\phi r} \\ &= \left(1-kr^2\right)^{-1}\left[a\partial_t^2 a + 2\left(\partial_t a\right)^2 + 2k\right] && \text{(A.30)} \\ R_{\theta\theta} &= R^{t}{}_{\theta t\theta} + R^{r}{}_{\theta r\theta} + R^{\phi}{}_{\theta\phi\theta} \\ &= r^2\left[a\partial_t^2 a + 2\left(\partial_t a\right)^2 + 2k\right] && \text{(A.31)} \\ R_{\phi\phi} &= R^{t}{}_{\phi t\phi} + R^{r}{}_{\phi r\phi} + R^{\theta}{}_{\phi\theta\phi} \\ &= r^2\sin^2\theta\left[a\partial_t^2 a + 2\left(\partial_t a\right)^2 + 2k\right] && \text{(A.32)} \end{aligned}$$

- Ricci Scalar R

$$R = g^{tt}R_{tt} + g^{rr}R_{rr} + g^{\theta\theta}R_{\theta\theta} + g^{\phi\phi}R_{\phi\phi} = 6\left[\frac{a\partial_t^2 a + \left(\partial_t a\right)^2 + k}{a^2}\right] \qquad \text{(A.33)}$$

Einstein Tensor $E_{\mu\nu}$

$$\begin{aligned} E_{tt} &= R_{tt} - \frac{1}{2}g_{tt}R = \frac{3}{a^2}\left[\left(\partial_t a\right)^2 + k\right] && \text{(A.34)} \\ E_{rr} &= R_{rr} - \frac{1}{2}g_{rr}R = \left(1-kr^2\right)^{-1}\left[-2a\partial_t^2 a - \left(\partial_t a\right)^2 - k\right] && \text{(A.35)} \\ E_{\theta\theta} &= R_{\theta\theta} - \frac{1}{2}g_{\theta\theta}R = r^2\left[-2a\partial_t^2 a - \left(\partial_t a\right)^2 - k\right] && \text{(A.36)} \\ E_{\phi\phi} &= R_{\phi\phi} - \frac{1}{2}g_{\phi\phi}R = r^2\sin^2\theta\left[-2a\partial_t^2 a - \left(\partial_t a\right)^2 - k\right] && \text{(A.37)} \\ & && \text{(A.38)} \end{aligned}$$

A.2 Static Spherically Symmetric Spacetime

The lineelement for a spherically symmetric spacetime in spherical coordinates t, r, θ, ϕ takes the form

$$ds^2 = -e^{2\alpha(r)}dt^2 + e^{2\beta(r)}dr^2 + r^2 d\theta^2 + r^2\sin^2\theta d\phi^2$$

Christoffel Symbols $\Gamma^{\alpha}{}_{\mu\nu}$

This lineelement yields the following non-vanishing Christoffel symbols, together with the ones related to these by the symmetry of the lower indices $\mu\nu = \nu\mu$. I use the fact that for a diagonal metric the inverse is given by $g^{\mu\nu} = \frac{1}{g_{\mu\nu}}$.

- $\alpha = t$:

$$\Gamma^{t}{}_{tr} = -\frac{1}{2}e^{-2\alpha(r)}\partial_r g_{tt} = \partial_r\alpha$$

- $\alpha = r$:

$$\Gamma^{r}_{\ tt} = -\frac{1}{2}e^{-2\beta(r)}\partial_r g_{tt} = \partial_r \alpha e^{2(\alpha-\beta)} \tag{A.39}$$

$$\Gamma^{r}_{\ rr} = \frac{1}{2}e^{-2\beta(r)}\partial_r g_{rr} = \partial_r \beta \tag{A.40}$$

$$\Gamma^{r}_{\ \theta\theta} = -\frac{1}{2}e^{-2\beta(r)}\partial_r g_{\theta\theta} = -re^{-2\beta} \tag{A.41}$$

$$\Gamma^{r}_{\ \phi\phi} = -\frac{1}{2}e^{-2\beta(r)}\partial_r g_{\phi\phi} = -r\sin^2\theta e^{-2\beta} \tag{A.42}$$

- $\alpha = \theta$:

$$\Gamma^{\theta}_{\ r\theta} = \frac{1}{2}r^{-2}\partial_r g_{\theta\theta} = \frac{1}{r} \tag{A.43}$$

$$\Gamma^{\theta}_{\ \phi\phi} = -\frac{1}{2}r^{-2}\partial_\theta g_{\phi\phi} = -\sin\theta\cos\theta \tag{A.44}$$

- $\alpha = \phi$:

$$\Gamma^{\phi}_{\ r\phi} = \frac{1}{2}r^{-2}\sin^{-2}\theta\partial_r g_{\phi\phi} = \frac{1}{r} \tag{A.45}$$

$$\Gamma^{\phi}_{\ \theta\phi} = \frac{1}{2}r^{-2}\sin^{-2}\theta\partial_\theta g_{\phi\phi} = \frac{\cos\theta}{\sin\theta} \tag{A.46}$$

Riemann Tensor $R^{\alpha}_{\ \mu\beta\nu}$

$$R^{\alpha}_{\ \mu\beta\nu} = \partial_\beta\Gamma^{\alpha}_{\ \mu\nu} + \Gamma^{\alpha}_{\ \beta\lambda}\Gamma^{\lambda}_{\ \mu\nu} - \partial_\nu\Gamma^{\alpha}_{\ \mu\beta} - \Gamma^{\alpha}_{\ \nu\lambda}\Gamma^{\lambda}_{\ \mu\beta}$$

- $\alpha = \beta = t$:

$$\begin{aligned} R^{t}_{\ rtr} &= \Gamma^{t}_{\ rt}\Gamma^{r}_{\ rr} - \partial_r\Gamma^{t}_{\ rt} - \left(\Gamma^{t}_{\ rt}\right)^2 \\ &= \partial_r\alpha\partial_r\beta - \partial_r^2\alpha - (\partial_r\alpha)^2 \end{aligned} \tag{A.47}$$

$$\begin{aligned} R^{t}_{\ \theta t\theta} &= \Gamma^{t}_{\ rt}\Gamma^{r}_{\ \theta\theta} \\ &= -r\partial_r\alpha e^{-2\beta} \end{aligned} \tag{A.48}$$

$$\begin{aligned} R^{t}_{\ \phi t\phi} &= \Gamma^{t}_{\ rt}\Gamma^{r}_{\ \phi\phi} \\ &= -r\sin^2\theta\partial_r\alpha e^{-2\beta} \end{aligned} \tag{A.49}$$

- $\alpha = \beta = r$:

$$\begin{aligned} R^{r}_{\ trt} &= \partial_r\Gamma^{r}_{\ tt} + \Gamma^{r}_{\ rr}\Gamma^{r}_{\ tt} - \Gamma^{r}_{\ tt}\Gamma^{t}_{\ rt} \\ &= \left[\partial_r^2\alpha + (\partial_r\alpha)^2 - \partial_r\alpha\partial_r\beta\right]e^{2(\alpha-\beta)} \end{aligned} \tag{A.50}$$

$$\begin{aligned} R^{r}_{\ \theta r\theta} &= \partial_r\Gamma^{r}_{\ \theta\theta} - \Gamma^{r}_{\ \theta\theta}\Gamma^{\theta}_{\ \theta r} \\ &= +2r\partial_r\beta e^{-2\beta} \end{aligned} \tag{A.51}$$

$$\begin{aligned} R^{r}_{\ \phi r\phi} &= \partial_r\Gamma^{r}_{\ \phi\phi} + \Gamma^{r}_{\ rr}\Gamma^{r}_{\ \phi\phi} - \Gamma^{r}_{\ \phi\phi}\Gamma^{\phi}_{\ r\phi} \\ &= r\sin^2\theta\partial_r\beta e^{-2\beta} \end{aligned} \tag{A.52}$$

- $\alpha = \beta = \theta$:

$$\begin{aligned} R^{\theta}{}_{t\theta t} &= \Gamma^{\theta}{}_{r\theta}\Gamma^{r}{}_{tt} \\ &= \frac{1}{r}\partial_r \alpha e^{2(\alpha-\beta)} \end{aligned} \tag{A.53}$$

$$\begin{aligned} R^{\theta}{}_{r\theta r} &= \Gamma^{\theta}{}_{r\theta}\Gamma^{r}{}_{rr} - \partial_r \Gamma^{\theta}{}_{r\theta} - \left(\Gamma^{\theta}{}_{r\theta}\right)^2 \\ &= \frac{1}{r}\partial_r \beta \end{aligned} \tag{A.54}$$

$$\begin{aligned} R^{\theta}{}_{\phi\theta\phi} &= \partial_\theta \Gamma^{\theta}{}_{\phi\phi} + \Gamma^{\theta}{}_{r\theta}\Gamma^{r}{}_{\phi\phi} - \Gamma^{\theta}{}_{\phi\phi}\Gamma^{\phi}{}_{\theta\phi} \\ &= \sin^2\theta\left(1 - e^{-2\beta}\right) \end{aligned} \tag{A.55}$$

- $\alpha = \beta = \phi$:

$$\begin{aligned} R^{\phi}{}_{t\phi t} &= \Gamma^{\phi}{}_{r\phi}\Gamma^{r}{}_{tt} \\ &= \frac{1}{r}\partial_r \alpha e^{2(\alpha-\beta)} \end{aligned} \tag{A.56}$$

$$\begin{aligned} R^{\phi}{}_{r\phi r} &= \Gamma^{\phi}{}_{r\phi}\Gamma^{r}{}_{rr} - \partial_r \Gamma^{\phi}{}_{r\phi} - \left(\Gamma^{\phi}{}_{r\phi}\right)^2 \\ &= \frac{1}{r}\partial_r \beta \end{aligned} \tag{A.57}$$

$$\begin{aligned} R^{\phi}{}_{\theta\phi\theta} &= \partial_\phi \Gamma^{\phi}{}_{\theta\theta} + \Gamma^{\phi}{}_{r\phi}\Gamma^{r}{}_{\theta\theta} - \partial_\theta \Gamma^{\phi}{}_{\theta\phi} - \left(\Gamma^{\phi}{}_{\theta\phi}\right)^2 \\ &= 1 - e^{-2\beta} \end{aligned} \tag{A.58}$$

Ricci Tensor $R_{\mu\nu}$ and Ricci Scalar R

- Ricci Tensor $R_{\mu\nu}$

$$\begin{aligned} R_{tt} &= R^{r}{}_{trt} + R^{\theta}{}_{t\theta t} + R^{\phi}{}_{t\phi t} \\ &= \left[\partial_r^2 \alpha + (\partial_r \alpha)^2 + \frac{2}{r}\partial_r \alpha - \partial_r \alpha \partial_r \beta\right] e^{2(\alpha-\beta)} \end{aligned} \tag{A.59}$$

$$\begin{aligned} R_{rr} &= R^{t}{}_{rtr} + R^{\theta}{}_{r\theta r} + R^{\phi}{}_{r\phi r} \\ &= \partial_r \alpha \partial_r \beta - \partial_r^2 \alpha - (\partial_r \alpha)^2 + \frac{2}{r}\partial_r \beta \end{aligned} \tag{A.60}$$

$$\begin{aligned} R_{\theta\theta} &= R^{t}{}_{\theta t\theta} + R^{r}{}_{\theta r\theta} + R^{\phi}{}_{\theta\phi\theta} \\ &= \left[r\left(\partial_r \beta - \partial_r \alpha\right) - 1\right] e^{-2\beta} + 1 \end{aligned} \tag{A.61}$$

$$\begin{aligned} R_{\phi\phi} &= R^{t}{}_{\phi t\phi} + R^{r}{}_{\phi r\phi} + R^{\theta}{}_{\phi\theta\phi} \\ &= \sin^2\theta\left(\left[r\left(\partial_r \beta - \partial_r \alpha\right) - 1\right] e^{-2\beta} + 1\right) \end{aligned} \tag{A.62}$$

- Ricci Scalar R

$$\begin{aligned} R &= g^{tt}R_{tt} + g^{rr}R_{rr} + g^{\theta\theta}R_{\theta\theta} + g^{\phi\phi}R_{\phi\phi} \\ &= -2\left[\partial_r^2 \alpha + (\partial_r \alpha)^2 + \frac{2}{r}\left(\partial_r \alpha - \partial_r \beta\right) - \partial_r \alpha \partial_r \beta + \frac{1}{r^2}\left(1 - e^{2\beta}\right)\right] e^{-2\beta} \end{aligned} \tag{A.63}$$

Einstein Tensor $E_{\mu\nu}$

$$E_{tt} = R_{tt} - \frac{1}{2} g_{tt} R = \frac{1}{r^2} \left[2r\partial_r \beta + e^{2\beta} - 1 \right] e^{2(\alpha-\beta)} \tag{A.64}$$

$$E_{rr} = R_{rr} - \frac{1}{2} g_{rr} R = \frac{1}{r^2} \left[2r\partial_r \alpha - e^{2\beta} + 1 \right] \tag{A.65}$$

$$E_{\theta\theta} = R_{\theta\theta} - \frac{1}{2} g_{\theta\theta} R = r^2 \left[\partial_r^2 \alpha + (\partial_r \alpha)^2 + \frac{1}{r} (\partial_r \alpha - \partial_r \beta) - \partial_r \alpha \partial_r \beta \right] e^{-2\beta} \tag{A.66}$$

$$E_{\phi\phi} = R_{\phi\phi} - \frac{1}{2} g_{\phi\phi} R = r^2 \sin^2\theta \left[\partial_r^2 \alpha + (\partial_r \alpha)^2 + \frac{1}{r} (\partial_r \alpha - \partial_r \beta) - \partial_r \alpha \partial_r \beta \right] e^{-2\beta} \tag{A.67}$$

Appendix B

Matlab Code

B.1 Codes for Chapter 3

This is the algorithm used to for the neutron star example in section 3.6

Main Program

```
%TOV SOLVER USING MATLABS ODE SUIT
%BEGIN PROGRAM*************************************************************
%CONSTANTS
c=2.9979*10^8;%Lightspeed [m/s]
G=6.6726*10^(-11);%Newtons constant [Nm^2/kg^2]
M_sol=1.9891*10^(30);%Solar mass in [kg]
mil=1*10^4;%10km [m]
K=2.9837*10^(-25);%Polytropic Constant [J/m^3]
n=5/3;%Non-rel polytropic index

%CENTRAL DENSITY PARAMETERS
J=10;%Number of central densities used
pow_min=30;%Min density order of magnitude rho_min~10^(pow_min)
pow_max=35;%Max density order of magnitude rho_max~10^(pow_max)
pow=(pow_min:(pow_max-pow_min)/(J-1):pow_max);%Magnitude array
rho_c=10.^(pow);%Central density vector
p_c=K*rho_c.^n;%Central pressure vector
M=zeros(1,J);%Initializing stellar mass M(rho_c)
R=zeros(1,J);%Initializing stellar radius R(rho_c)


%Central density loop
for j=1:J
%Dimensionless Constants
P_d=rho_c(j);%Pressure and density dimensions (J/m^3)
K_d=P_d^(-2/3);%Dimensionfull polytropic constant [(J/m^3)^(-2/3)]
R_d=c^2/(mil*sqrt(4*pi*G*P_d));%radius dimensions in 10km
M_d=c^4/(M_sol*sqrt(4*pi*G^3*P_d));%mass dimensions in solar masses

%Spatial Parameters
N_r=1000;
r_max=100/R_d;%Upper limit for the radial coordinate r
r_min=0.0001/R_d;%Lower limit for the radial coordinate r
```

```
r_span=[r_min r_max];%Radius

C=[K/K_d n];
m_c=(r_min)^3*(rho_c/P_d)/3;%mass of initial sphere with radius r_min
Init=[p_c(j)/P_d m_c(j)];%m_c(j)/M_d

%Matlab ODE solver
options=odeset('RelTol',1e-10,'Events',@p_zero);%'OutputFcn',@odeplot,'NonNegative',1
Sol=ode23tb(@TOVfun,r_span,Init,options,C);
r_max=Sol.xe;
r=linspace(r_min,r_max,N_r);
p=P_d*deval(Sol,r,1);
rho=(p/K).^(1/n);
m=M_d*deval(Sol,r,2);
r=R_d*r;

%Additional functions
[M(j),i]=max(m);%Stellar mass M(rho_c) and its radial index
R(j)=r(i);%Stellar radius
end

%Interpolation for smoothness
x=1:J;
PolyP_R=polyfit(x,R,3);
R_p=polyval(PolyP_R,x);
%PolyP_M=polyfit(x,M,10);
%M_p=polyval(PolyP_M,x);

%Maximum quantities
[MaxMass,J_max]=max(M);%Maximum stellar mass and its density index
MaxR=max(R);%Upper radial axis limit
MinR=min(R);%Lower radial axis limit

%Print Maxmass and corresponding radius and density
fprintf('\n Maximum Mass=%4f solar masses\n',MaxMass)
fprintf('\n Radius=%4f *10km\n',R(J_max))
fprintf('\n Central Density=%4e J/m^3\n',rho_c(J_max))

%clear x r_max r_min options drho Sol i j J

%END PROGRAM*****************************************************************
```

TOV Function and Event Locator

```
%TOV FUNCTION
function df=TOVfun(r,x,C)
K=C(1);
n=C(2);

df=zeros(2,1);
rho=(x(1)/K)^(1/n);%Polytropic EOS

df(1)=-(rho+x(1))*(x(1)*r^3+x(2))/(r^2-2*x(2)*r);%TOV1
df(2)=rho*r^2;%TOV2
```

```
if(x(1)<=0)
  x(1)=0;
  df(1)=0;
  df(2)=0;
end

end

%EVENT LOCATOR
function [value,isterminal,direction]=p_zero(r,x,C)
value = x(1);     % Detect p=0
isterminal = 1;   % Stop the integration
direction = -1;   % Negative direction only
```

B.2 Codes for Chapter 7

The Code used to reproduce the results of Khoury and Weltman is a simplfied version of the code used for chapter 12. Instead of using the two modified TOV equations to determine the matter part of the potential this is approximated by a step function.

Main Program

```
%CHAMELEON EOM SOLVER
%This solver employs a two step density profile and uses matlabs ode solver
%on the functions SEOS1 and SEOS2. We express everything in units [1/m]

%NATURAL CONSTANTS
c=2.9979*10^8;%Lightspeed [m/s]
G=6.6726*10^(-11);%Newtons constant [Nm^2/kg^2]
hbar=1.054589*10^(-34);%Planck constant [Js]
M_Pl=sqrt(hbar*c^5/(8*pi*G))/(hbar*c);%Planck mass [1/m]

%THEOTY PARAMETERS
M_phi=6*10^(3);%Potential mass scale [1/m]
n=1;%Potential power
beta=1;%Chameleon coupling

%RADIUS
R_s=40/M_phi;%40/M_phi;

%REGION I*************************************************************
%DENSITY
rho_s=10^3*(c/hbar);%10^3*(c/hbar);%Inside density in units [1/m^4];

%MINIMA Phi_c (Assuming (beta*Phi_c/M_Pl<<1)
Phi_s=(M_phi^(4+n)*M_Pl/rho_s)^(1/(n+1));

%DIMENSIONS
P_d1=rho_s;%Pressure and density dimensions (J/m^3)
Phi_d1=Phi_s;
R_d1=M_phi^(-1)*(Phi_s/M_phi)^(1+n/2);%Phi_d^(n+2)/(n*M_phi^(n+4));
C1=beta*Phi_s/M_Pl;
```

```
%SPATIAL PARAMETERS
N_r=10000;%Number of point in output funct
r_max1=R_s/R_d1;%Upper limit for the radial coordinate r
r_min1=0.2*R_s/R_d1;%0.000001/R_d;%Lower limit for the radial coordinate r
r_span1=[r_min1 r_max1];%Radius

Const1=[C1 n beta];
Phi_i1=1+0.1;%+0.1*10^(-17);%199999
L_i1=0;
Init1=[Phi_i1 L_i1];

%Matlab ODE solver
Options=odeset('RelTol',1e-10,'InitialStep', 1e-4);%'NonNegative',1,'OutputFcn',@odep
Sol_1=ode113(@EOM,r_span1,Init1,Options,Const1);%,Options);
r_1=linspace(r_min1,r_max1,N_r);
Phi_1=Phi_d1*deval(Sol_1,r_1,1);
L_1=Phi_d1*deval(Sol_1,r_1,2)/R_d1;
r_1=R_d1*r_1;

%REGION II*********************************************************************
%DENSITY
rho_b=10^(-1)*(c/hbar);%Outside density in units [1/m^4];

%MINIMA Phi_c (Assuming (beta*Phi_c/M_Pl<<1)
Phi_b=(M_phi^(4+n)*M_Pl/rho_b)^(1/(n+1));

%DIMESNIONS
P_d2=rho_b;%Pressure and density dimensions (J/m^3)
Phi_d2=Phi_b;
R_d2=M_phi^(-1)*(Phi_b/M_phi)^(1+n/2);%Phi_d^(n+2)/(n*M_phi^(n+4));
C2=beta*Phi_b/M_Pl;

%SPATIAL PARAMETERS
r_max2=3*R_s/R_d2;%Upper limit for the radial coordinate r
r_min2=R_s/R_d2;%0.000001/R_d;%Lower limit for the radial coordinate r
r_span2=[r_min2 r_max2];%Radius

Const2=[C2 n beta];
Phi_i2=Phi_1(N_r)/Phi_d2;
L_i2=R_d2*L_1(N_r)/(Phi_d2);

Init2=[Phi_i2 L_i2];

%Matlab ODE solver[r_2,x_2]
Sol_2=ode113(@EOM,r_span2,Init2,Options,Const2);%,Options);
r_max2=max(Sol_2.x);
r_2=linspace(r_min2,r_max2,N_r);
Phi_2=Phi_d2*deval(Sol_2,r_2,1);
L_2=Phi_d2*deval(Sol_2,r_2,2)/R_d1;
r_2=R_d2*r_2;
%*********************************************************************

%Chameleon Masses
```

```
m_b=sqrt(n*(n+1)*M_phi^(4+n)*Phi_b^(-(n+2))+beta^2/(M_Pl^2)*exp(C1)*rho_b);%[1/m]
m_s=sqrt(n*(n+1)*M_phi^(4+n)*Phi_s^(-(n+2))+beta^2/(M_Pl^2)*exp(C2)*rho_s);%[1/m]

%Full Chameleon and Gradient Profiles
L=[L_1 L_2];%[1/m^2]
Phi=[Phi_1 Phi_2]/M_phi;%[1/m]
r=[r_1 r_2]/R_s;%*M_phi;%[m]

%Clearing Workspace
clear r_span1 r_span2 r_min1 r_min2 r_max1 r_max2 R_d1 R_d2 N_r
clear Phi_d1 Phi_d2 P_d1 P_d2 f_b f_ns C1 C2 Phi_i1 Phi_i2 L_i1 L_i2
clear Const1 Const2 Init1 Init2 Sol_1 Sol_2 Options
clear Phi_1 Phi_2 L_1 L_2 r_1 r_2
clear hbar c G M_Pl M_phi n beta R_ns
```

EOM Function

```
%EOM
function df=EOM1(r,x,Const)

df=zeros(2,1);%x(1)=Phi,x(2)=dPhi
C=Const(1);
n=Const(2);
beta=Const(3);

%dPhi=Lambda
df(1)=x(2);
%dLambda=-2/r*Lambda+V,Phi
df(2)=-(2/r)*x(2)-n*x(1)^(-n-1)+beta*exp(C*x(1));

end
```

B.3 Codes for Chapter 8

Main Program

This algorithm calls matlab's built in ode solver to solve the four coupled equations for hydrostatic equilibrium encoded in the function CTOV

```
%CTOV SOLVER USING MATLABS ODE SUIT
%BEGIN PROGRAM************************************************************
%CONSTANTS
c=2.9979*10^8;%Lightspeed [m/s]
G=6.6726*10^(-11);%Newtons constant [Nm^2/kg^2]
hbar=1.054589*10^(-34);%Planck constant
M_Pl=sqrt(hbar*c^5/(8*pi*G));%Planck mass [J]
M_phi=10^(3);%Potential mass scale [1/m]
M_sol=1.9891*10^(30);%Solar mass in [kg]
mil=1*10^4;%10km [m]
K=2.9837*10^(-25);%Polytropic Constant [J/m^3]
N=5/3;%Non-rel polytropic index
```

```
beta=1;%Coupling constant
n=1;%Potential Power

%CENTRAL MATTER DENSITY
rho_mc=1*10^(35);%Central Matter Density [J/m^3]
p_mc=K*rho_mc^(N);%Central Matter Pressure [J/m^3]

%DIMESNIONS
P_d=rho_mc;%Pressure and density dimensions (J/m^3)
K_d=P_d^(-2/3);%Polytropic dimensions
Phi_d=((n*M_Pl*M_phi^(4+n))/(beta*P_d))^(1/(n+1));
R_d=c^2/(sqrt(4*pi*G*P_d));%radius dimensions in m
M_d=c^4/(sqrt(4*pi*G^3*P_d));%mass dimensions in kg

%SPATIAL PARAMETERS
N_r=1000;%Number of steps in output
r_max=10^(6)/R_d;%Upper limit for the radial coordinate r
r_min=10^(-6)/R_d;%0.000001/R_d;%Lower limit for the radial coordinate r
r_span=[r_min r_max];%Radius

%DIMENSIONLESS CONSTANTS
C_1=beta*R_d^2*P_d/(M_Pl*Phi_d);%Chameleon equation constant
C_2=Phi_d^2*(hbar*c)/(2*R_d^2*P_d);%Kinetic constant
C_3=hbar*c*M_phi^4/P_d*(M_phi/Phi_d)^n;%Potential constant

Phi_i=1+1.1306798573713716*10^(-1);%Initial value for Phi
rho_Phic=C_3*Phi_i^(-n);%Chameleon initial density
p_Phic=-C_3*Phi_i^(-n);%Chameleon initial pressure
rho_c=(rho_mc/P_d)+rho_Phic;%Total central density
p_c=(p_mc/P_d)+p_Phic;%Total central pressure
m_c=(r_min^3/3)*rho_c;%Core mass

%SOLVER INPUT
C=[C_1 C_2 C_3 K/K_d N n];%Input constants
Init=[p_c m_c Phi_i 0];%Initial conditions

%Matlab ODE solver
Options=odeset('RelTol',1e-6,'Events',@p_zeroC);
%,'OutputFcn',@odeplot ,'OutputSel',[3 4], 'NormControl',10^(-10)), 'NonNegative',1
Sol=ode45(@CTOV,r_span,Init,Options,C);
r_max=max(Sol.x);

%Results
r=linspace(r_min,r_max,N_r);
dr=linspace(0,r_max-r_min,N_r);
p=deval(Sol,r,1);
m=deval(Sol,r,2);
Phi=deval(Sol,r,3);
Lambda=deval(Sol,r,4);
p_Phi=C_2*(1-2*m./r).*Lambda.^2-C_3*Phi.^(-n);
rho_Phi=C_2*(1-2*m./r).*Lambda.^2+C_3*Phi.^(-n);
p_m=p-p_Phi;
rho_m=(p_m*K_d/K).^(1/N);
rho=rho_m+rho_Phi;
```

```
%Maximum values
M=max(m);
Phi_max=max(Phi);
Lambda=deval(Sol,r,4);
Lambda_max=max(Lambda);
rho_Phi=C_2*(1-2*m./r).*Lambda.^2+C_3*Phi.^(-n);
p_Phi=C_2*(1-2*m./r).*Lambda.^2-C_3*Phi.^(-n);
p_m=p-p_Phi;
rho_m=(p_m*K_d/K).^(1/N);
rho=rho_m+rho_Phi;

%DIMENSIONFULL QUANTITIES
%Densities in [J/m^3]
Phi=Phi_d*Phi;%Field [J]
Lambda=Phi_d*Lambda/R_d;%
p_Phi=P_d*p_Phi;
rho_phi=P_d*rho_Phi;
p_m=P_d*p_m;%Matter density [J]
rho_m=P_d*rho_m;
p=P_d*p;%Pressure in
rho=P_d*rho;%Density in [J/m^3]
r=R_d*r/mil;%Radius in 10km
m=M_d*m/M_sol;%Mass in solar masses
```

CTOV Function and Event Locator

This is the function supplied to the solver

```
%CTOV FUNCTION
function df=CTOV(r,x,C)

C_1=C(1);
C_2=C(2);
C_3=C(3);
K=C(4);
N=C(5);
n=C(6);

df=zeros(4,1);

rho_phi=C_2*(1-2*x(2)/r)*x(4)^2+C_3*x(3)^(-n);
p_phi=C_2*(1-2*x(2)/r)*x(4)^2-C_3*x(3)^(-n);

p_m=(x(1)-p_phi);
rho_m=(p_m/K)^(1/N);%EOS
rho=rho_m+rho_phi;

A=-(2/r-(r^3*(rho-x(1))-2*x(2))/(r*(r-2*x(2))))*x(4);
B=C_1*(rho_m-3*p_m-x(3)^(-(n+1)))/(1-2*x(2)/r);

df(1)=-(rho+x(1))*(x(1)*r^3+x(2))/(r^2-2*x(2)*r);
df(2)=rho*r^2;
df(3)=x(4);
```

```
df(4)=A+B;

end

%EVENT LOCATOR
function [value,isterminal,direction]=p_zeroC(r,x,C)

value =x(1)-C(2)*(1-2*x(2)/r)*x(4)^2+C(3)*x(3)^(-C(6));% Detect p_m=0
isterminal = 1;   % Stop the integration
direction = -1;   % Negative direction only
```

Bibliography

[1] H. Goldstein, C. Pool, and J. Safko, *Classical Mechanics* (Addison Wesley, 2002).

[2] I. J. R. Aitchison and A. J. G. Hey, *Gauge Theories in Particle Physics Vol. 1: From Relativistic Quantum Mechanics to QED* (Taylor & Francis, New York, U.S.A., 2003).

[3] A. Zee, *Quantum Field Theory in a Nutshell* (Princeton University Press, 2003).

[4] S. Carroll, *Spacetime and Geometry: An Introduction to General Relativity* (Addison Wesley, 2004).

[5] Øyvind Grøn and S. Hervik, *Einstein's General Theory of Relativity With Modern Applications in Cosmology* (Springer, 2007).

[6] B. F. Schutz, *A First Course in General Relativity* (Cambridge University Press, 1985).

[7] R. M. Wald, *General Relativity* (University Of Chicago Press, 1984).

[8] Wikipedia, Jacobian — wikipedia, the free encyclopedia, 2009, [Online; accessed 2-April-2009].

[9] K. B. Petersen and M. S. Pedersen, The matrix cookbook, 2008, Version 20081110.

[10] D. V. Schroeder, *An Introduction to Thermal Physics* (Addison Wesley, 2000).

[11] Øystein Elgarøy, Lecture notes ast4220: Cosmology 1.

[12] N. K. Glenndenning, *Compact Stars, Second Edition* (Springer, 2000).

[13] S. L. Shapiro and S. A. Teukolsky, *Black Holes, White Dwarfs, and Neutron Stars, The Physics of Compact Objects* (Wiley, 1983).

[14] M. Hjort-Jensen, Computational physics, 2008.

[15] J. Frieman, M. Turner, and D. Huterer, Ann. Rev. Astron. Astrophys. **46**, 385 (2008), 0803.0982.

[16] S. Weinberg, *Cosmology* (Oxford University Press, 2008).

[17] S. Dodelson, *Modern Cosmology* (Academic Press, 2003).

[18] J. Loveday, G. Efstathiou, B. A. Peterson, and S. J. Maddox, Astrophysical Journal, Part 2 - Letters **400**, L43 (1992).

[19] M. Bucher and N. Turok, Open inflation with an arbitrary false vacuum mass, 1995.

[20] D. Pogosian and A. A. Starobinsky, (1994), astro-ph/9502019.

[21] B. P. Schmidt, Bulletin of the Astronomical Society of India **32**, 269 (2004).

[22] MaxiBoom, J. R. Bond *et al.*, Cmb analysis of boomerang & maxima & the cosmic parameters $\{\Omega_{tot}, \Omega_b h^2, \Omega_{cdm} h^2, \Omega_\Lambda, n_s\}$, 2000, astro-ph/0011378.

[23] M. Kowalski *et al.*, Improved cosmological constraints from new, old and combined supernova datasets, 2008, 0804.4142.

[24] S. M. Carroll, Living Rev. Rel. **4**, 1 (2001), astro-ph/0004075.

[25] Y. Fujii and K.-I. Maeda, *The Scalar-Tensor Theory of Gravitation* (Cambridge University Press, 2007).

[26] H. Alnes, M. Amarzguioui, and O. Gron, Phys. Rev. **D73**, 083519 (2006), astro-ph/0512006.

[27] R. R. Caldwell and M. Kamionkowski, ArXiv e-prints (2009), 0903.0866.

[28] S. Tsujikawa, T. Tamaki, and R. Tavakol, ArXiv e-prints (2009), 0901.3226.

[29] T. Tamaki and S. Tsujikawa, Physical Review D **78**, 084028 (2008).

[30] V. Faraoni, E. Gunzig, and P. Nardone, Fund. Cosmic Phys. **20**, 121 (1999), gr-qc/9811047.

[31] E. E. Flanagan, CLASS.QUANT.GRAV **3817** (2004).

[32] T. P. Waterhouse, (2006), astro-ph/0611816.

[33] D. F. Mota and D. J. Shaw, Physical Review D **75**, 063501 (2007).

[34] J. Khoury and A. Weltman, Physical Review Letters **93**, 171104 (2004).

[35] J. Khoury and A. Weltman, Physical Review D **69**, 044026 (2004).